THE USE OF FLUOROCARBON TRACERS TO MONITOR THE MOVEMENT OF WATER IN UNSATURATED POROUS MEDIA: COLUMN STUDY AND COMPUTER MODEL

by

Mary Elizabeth Roberts

A Thesis Submitted to the Faculty of the

DEPARTMENT OF HYDROLOGY AND WATER RESOURCES ADMINISTRATION

In Partial Fulfillment of the Repuirements
For the Degree of

MASTER OF SCIENCE
WITH A MAJOR IN HYDROLOGY

In the Graduate College

THE UNIVERSITY OF ARIZONA

1 9 8 6

STATEMENT BY AUTHOR

This thesis has been submitted in partial fulfillment of requirements for an advanced degree at The University of Arizona and is depositied in the University Library to be made available to borrowers under rules of the Library.

Brief quotations from this thesis are allowable without special permission, provided that accurate acknowledgement of source is made. Requests for permission for extended quotation from or reproduction of this manuscript in whole or in part may be granted by the head of the major department or the Dean of the Graduate College when in his or her judgment the proposed use of the material is in th interests of scholarship. In all other instances, however, permision must be obtained from the author.

SIGNED: Mary E Roberts

APPROVAL BY THESIS DIRECTOR

This thesis has been approved on the date shown below:

D.D. Evans
Professor of Hydrology and ater Resources

Sept. 16 1986
Date

ACKNOWLEDGMENTS

I would like to express my gratitude to my thesis director, Dr. D.D. Evans who suggested the thesis topic and patiently guided me to its completion. I gratefully acknowledge Todd Rassmussen, Jim Szecscody, Rick Seidemann, Ingrid Anderson, Mark Worthington, and Derrik Williams, who helped me in various capacities to complete this thesis.

This thesis was supported by the Nuclear Regulatory Commission under contract number NRC-04-81-224.

TABLE OF CONTENTS

TABLE OF CONTENTS -- Continued

LIST OF FIGURES

LIST OF FIGURES -- Continued

LIST OF FIGURES -- Continued

LIST OF FIGURES -- Continued

LIST OF FIGURES -- Continued

LIST OF FIGURES -- Continued

LIST OF TABLES

LIST OF TABLES -- Continued

ABSTRACT

A major problem associated with monitoring the velocity of water in unsaturated porous media is the difficulty of removing samples of the pore water at different times for analysis. A possible solution to this problem is to use volatile fluorocarbon tracers which are transported in a soluble form, yet can be measured in a gaseous state, thus eliminating the difficult process of extracting liquid samples from soils with high matric suction. The three fluorocarbon tracers used to investigate the suitability of a volatile tracer method were bromochlorodifluoromethane, chlorodifluoroethane and sulfur hexafluoride.

Five laboratory column experiments were conducted to determine under what conditions volatile tracers would give reliable estimates of water flow rates. The Discrete State Compartment computer model was used to interpret the laboratory data, thereby allowing a more accurate estimate of water travel times in unsaturated media.

CHAPTER 1

INTRODUCTION

A volatile tracer method to measure the travel time for water in unsaturated soils is presented in this thesis. Volatile tracer concentration in the gas phase is used to indicate the presence of that tracer in the liquid phase. The volatile tracer method would be advantageous under conditions of high matric suction. A volatile tracer can be transported in the soluble phase and sampled in the gaseous phase, thereby eliminating the difficult process of extracting a liquid sample from soils with high matric suctions.

Laboratory column experiments were conducted to determine under what conditions volatile tracers would give reliable estimates of water flow rates. The column tests consisted of introducing water, along with a volatile fluorocarbon compound, into a soil column. As the water percolated down the soil column, the fluorocarbon tracer volatilized into the soil atmosphere where the gaseous tracer could be easily sampled. Several column tests were run at various water application rates to determine the range of water flow rates where the volatile tracer method would accurately estimate the travel time of the water.

Results of the laboratory soil column tests indicated that several overlapping processes are involved in the transport of a volatile tracer. The most important processes are: (1) advection of

tracer in the soluble phase, (2) movement of tracer in the gaseous phase, and (3) sorption of tracer onto the soil.

Computer modeling was used to help interpret the data from the column test, thus allowing a more accurate prediction of water travel times rates in unsaturated media.

Fluorocarbon compounds were selected as tracers for this study because of their advantageous physical properties and the previous field work done using these compounds in both saturated and unsaturated porous media.

Physical Properties of Fluorocarbon Tracers

Fluorocarbons are man-made compounds which were first produced in the late-1930's and are now widely used as propellants, refrigerants, and solvents. Several physical properties of fluorocarbons make them suitable for use as hydrologic tracers. The first important advantage is that they are generally considered to have very low toxicities (Davis et al., 1980). Secondly, among all organic compounds, fluorocarbons have the lowest known surface energies and are therefore not likely to adsorb onto solid particles (Shafrin and Zisman, 1960). Field tests using fluorocarbons and bromide, the latter being a commonly used tracer, indicate that there is little difference in sorption between the conservative bromide ion tracer and the fluorocarbon tracers tested (Davis et al., 1980). The third major advantage of fluorocarbons is their high affinity for electrons, which makes them suitable for analysis using a gas chromatograph equipped with an electron capture

detector. Detection limits of as low as one part per trillion can be achieved using gas chromatography (Lovelock et al., 1973).

Properties of interest in the selection of a tracer for this study were primarily: natural abundance in the environment, boiling temperature, critical temperature, solubility in water, toxicity and availability. The natural abundance of a tracer in the hydrologic system must be low for it to be used effectively as a tracer. Dichlorodifluoromethane (F-12) and trichlorofluoromethane (F-11) are the two most abundant fluorocarbon compounds found in the environment. F-12 and F-11 are found in the atmosphere in concentrations of up to 300 and 173 parts per trillion by volume, respectively (Weeks et al., 1982). The relatively high concentration of these two fluorocarbons in the environment rule out their use as hydrologic tracers. The boiling temperature of a volatile tracer must be below the ambient temperature in order for the compound to exist as a gas in the soil atmosphere. A critical temperature of greater than $50^{o}C$ is generally needed to construct a permeation device to store and release most fluorocarbons. The permeation device is needed if the technique is used in the field but it was not needed in the laboratory experiment.

A summary of the significant properties of the most common fluorocarbon compounds is presented in Table 1.1. Table 1.2 defines the toxicity classification used in Table 1.1. From this list, five possible tracers can be shown to fill the requirements needed for the column test: BCF, F-22, F-13B1, SF_6, and F-114. Of the five tracers, three (BCF, F-22, and SF_6) were selected for initial testing because of their availability and their previous use by other investigators.

Table 1.1 Properties of fluorocarbon tracers considered for use in the column tests. (From the Handbook of Chemistry and Physics, Chemical Rubber Company, 1979-80, and E.I. Du Pont De Nemours & Company),

Tracer	Formula	Boiling Temp `C	Critical Temp `C	Solubility by Wt. %	Toxicity *
F-11	CCl_3F	23.82	198	.011	5a
F-12	CCl_2F_2	-29.79	112	.028	6
F-13	$CClF_3$	-81.4	28.9	.009	Prob. 6
F13B-1	$CBrF_3$	-57.75	67	.03	6
F-14	CF_4	-127.96	-45.67	.0015	Prob. 6
F-21	$CHCl_2F$	8.92	178.5	.95	4-5
F-22	$CHClF_2$	-40.75	96	.30	5a
F-23	CHF_3	-82.03	25.9	.10	Prob. 6
F-112	C_2Cl_4F2	92.8	278	.12	4-5
F-113	$C_2Cl_3F_3$	47.57	214	.017	4-5
F-114	$C_2Cl_2F_4$	3.77	145.7	.013	6
F-114B2	$C_2Br_2F_4$	47.26	214.5	---	5a
F-115	C_2ClF_5	-38.7	80	.006	6
F-116	C_2F_6	-78.2	19.7	---	Prob. 6
12B1 (BCF)	$CClBrF_2$	-3.98	153.9	---	Non Toxic

* Underwriters Classification (see Table 1.2)

- -

Table 1.2 Underwriters' laboratories' classification of comparative life hazard of gases and vapors. (From Handbook of Chemistry and Physics, Chemical Rubber Company, 1979-80)

Group	Definition
1	Gases or vapors which in concentrations of the order of 1/2 to 1 percent for duration of exposure of the order of 5 minutes are lethal or produce serious injury. Example: Sulfur dioxide
2	Gases or vapors which in concentrations of the order of 1/2 to 1 percent for durations of exposure of the order of 1/2 hour are lethal or produce serious injury. Examples: Ammonia, Methylbromide
3	Gases or vapors which in concentrations of the order of 2 to 2-1/2 percent for durations of exposure of the order of 1 hour are lethal or produce serious injury. Examples: Carbon tetrachloride, Chloroform
4	Gases or vapors which in concentrations of the order of 2 to 2-1/2 percent for durations of exposure of the order of 2 hours are lethal or produce serious injury. Examples: Dichloroethylene, Methylchloride, Ethylbromide
4-5	Appear to classify as somewhat less toxic than Group 4. Example: Methylene chloride
5a	Gases or vapors much less toxic than Group 4 but more toxic than Group 6. Example: Carbon dioxide
5b	Gases or vapors which available data indicate would classify as either Group 5a or Group 6. Examples: Ethane, Propane
6	Gases or vapors which in concentrations up to at least about 20 percent by volume for durations of exposure of the order of 2 hours do not appear produce injury. Example: Many Refrigerants

History of Fluorocarbon Tracers in Hydrology

One of the major reasons fluorocarbon compounds were selected for this study is that these compounds have been successfully used as environmental tracers by numerous investigators. Investigations and results of other researchers may give an indication of how successful fluorocarbons will be in monitoring water movement in unsaturated porous media.

One of the first reported uses of a fluorocarbon compound as a hydrologic tracer was by Thompson et al. (1974). Thompson et al. used perfluoro-1 3-dimethylcyclohexane for measuring stream discharge and for determining the direction of ground-water flow in the saturated zone. Field tracer tests conducted by Thompson and Hayes (1979) demonstrated the use of trichlorofluoromethane (F-11) concentration in ground water to indicate the age of ground water.

In a review of ground-water tracers, Davis et al. (1980) discussed the use of fluorocarbon compounds as potential hydrologic tracers. Field tests, under saturated conditions, using fluorocarbon tracers were conducted in Aurora, Nebraska by Davis et al. (1980). By using a sequence of fluorocarbon tracers, Davis et al. (1980) were able to simultaneously run multiple tracer tests. Each water sample taken in the Nebraska test was analyzed simultaneously for 4 different tracers, CCL_2F_2, $CClBrF_2$, CBr_2F_2, and $CBrF_2$-$CBrF_2$. Another advantage in using fluorocarbon tracers was that only a small amount of fluorocarbon was needed to run the test because of the low tracer concentrations detectable using gas chromatography.

The use of fluorocarbon compounds as tracers in saturated porous media was investigated by Brown (1980) using column tests. He determined that fluorocarbon tracers traveled slightly slower than the average water velocity.

Six fluorocarbon compounds were evaluated by Thompson and Stiles (1981) for use as ground-water tracers under saturated conditions. The six fluorocarbons studied were F-12, F-11, BCF, DDM, F-113, and F-114B2. Partition coefficients were determined, and stream tracer tests were conducted using the six tracers. Also, analytical techniques for measuring fluorocarbon concentrations were outlined by Thompson and Stiles.

In 1981, the United States Geological Survey conducted artificial recharge experiments in Texas using several tracers, including fluorocarbon compounds. Injection tests were run using F-12, F-11, BCF, and DDM (Bassett et al., 1981). One of the major objectives of the tracer injection test was to test the water-sampling apparatus and monitoring equipment. Problems with pressure fluctuations in the injection of fluorocarbon tracers resulted in large variations in the input tracer concentration during the tracer test.

The retention characteristics of fluorocarbon tracers in ground-water flow were investigated by Stiles (1982). Stiles concluded that fluorocarbon compounds make favorable tracers but that their sorption characteristics in the field can be highly variable. Fluorocarbons were also found to be useless as tracers in aquifers with high organic content because of high adsorption onto organic materials.

Field tests were performed by Kreamer (1982) using BCF and SF_6 to measure gaseous diffusion parameters and effective porosity of soils in the unsaturated zone.

Further work by Kreamer (1983) extended his tracer work of 1982 to a gaseous diffusion experiment at the Nevada Test Site. Gaseous diffusion tests using fluorocarbon tracers were proposed to evaluate the potential of deep alluvial sediments for disposal of low level radioactive waste.

F-11 and F-12 concentrations in soil gas were used by Weeks et al. (1982) to determine gaseous diffusion parameters in the unsaturated zone. Results from the field tests confirmed that the traditional theoretical and laboratory methods of measuring tortuosity are useful in predicting tortuosity values in the field.

Enrichment mechanisms for F-11 and F-12 in ground water were studied by Russell and Thompson (1983) in an attempt to explain why fluorocarbon concentrations in recharge areas are often higher than concentrations in water at equilibrium with the atmosphere. Their laboratory experiments indicated that sorption and desorption of fluorocarbons from soil particles as soil moisture content fluctuates may account for the enhanced concentrations in recharge areas.

The brief summary of research presented in this section show that fluorocarbon compounds have been used successfully as hydrologic tracers for various applications. These applications include: (1)measurement of tracer travel times and retention characteristics of fluorocarbons in the saturated zone (Davis et al., 1980; Bassett et al., 1981; and Stiles, 1982), (2) investigation of the retention

characteristics of fluorocarbons under saturated conditions using laboratory column studies (Stiles 1982, and Brown 1980), (3) field experiments to determine gaseous diffusion coefficients in the unsaturated zone (Kreamer 1982, Kreamer 1983, and Weeks et al. 1982), and (4) mechanisms for fluorocarbon enrichment in recharge areas (Russell and Thompson 1983).

Expanding the role of fluorcarbon compounds to monitor water movement in the vadose zone is the objective of this study. Presented in this thesis are the results from the laboratory soil column tests and computer simulations performed to study the behavior of fluorocarbon tracers and to test their suitability for measuring water flow rates in unsaturated porous media.

CHAPTER 2

PHYSICAL PROPERTIES INVOLVED WITH TRANSPORT OF A VOLATILE TRACER IN UNSATURATED POROUS MEDIA

The primary objective of the column study and the computer simulation was to gain a better understanding of the processes involved in the movement of a volatile compound under unsaturated conditions. To interpret water flow rates using a volatile tracer technique, the following processes must be understood: (1) flow of water in the unsaturated zone, (2) dispersion of a tracer as it moves through porous media, (3) movement of a tracer in the gaseous phase, and (4) retardation of a tracer by sorption onto soil particles.

Flow of Water in the Unsaturated Zone

Flow of water in the unsaturated zone is governed by Darcy's equation (equation 2.1 Hillel, 1982):

$$q = -K(\Psi)\ \nabla H \qquad (2.1)$$

where

q = flux, volume of water flowing through a unit cross sectional area per unit time,

$K(\Psi)$ = hydraulic conductivity is a function of matric suction (Ψ), and

H = hydraulic head.

To obtain the equation for non-steady state flow the continuity equation (2.2):

$$\delta\theta/\delta t = -\nabla \cdot q \qquad (2.2)$$

where

$\emptyset$ = water content, and
t = time;

is combined with Darcy's law (Hillel, 1982).

The resulting general non-steady state flow equation for unsaturated flow in porous media is presented in equation 2.3 (Hillel, 1982).

$$\delta\emptyset/\delta t = \nabla [K(\Psi)\nabla H] \qquad (2.3)$$

The general flow equation can be expanded (equation 2.4) by representing the hydraulic head as the sum of the suction head (Ψ), and the gravitational head (z), and replacing ∇ z with zero for horizontal flow and unity for vertical flow (Hillel, 1982):

$$\delta\emptyset/\delta t = -\delta(K(\Psi)/\delta x)/\delta x - \delta(K(\Psi)/\delta y)/\delta y - \delta(K(\Psi)/\delta z)/\delta z + \delta K(\Psi)/\delta z \qquad (2.4)$$

Equation 2.4 is complex due to heterogeneities in the soil and the variances in $K(\Psi)$ with changes in matric suction. To determine actual field values for the parameters in the flow equation tracer studies are commonly performed.

Many types of tracers have been used to measure soil properties, the most common of these tracers are chloride, nitrate, bromide and deuterated and tritiated water (Bowman, 1984). Chloride was used in this thesis as a known conservative tracer to compare the movement of water in soils to that of selected fluorocarbons tracers.

Dispersion

Experimental studies have shown that solutes/tracers are dispersed, while moving through porous media, to a greater extent than is predicted by advection alone.

Mathematically, the process of dispersion is generally combined with the advection equation to describe solute movement in porous media. The combined advection-dispersion equation for one-dimensional liquid flow in unsaturated porous media is (Van Genuchten et al, 1982):

$$\delta c/\delta t = [D_m \delta C/\delta x]/ x - v/\emptyset[\delta C/\delta x] + S \qquad (2.5)$$

where

C = concentration of solute,
t = time,
D_m = dispersion coefficient,
x = distance,
v = vertical flow velocity,
$\emptyset$ = water content, and
S = source/sink term.

The dispersion coefficient is made up of 2 components: the coefficient of mechanical dispersion and the coefficient of molecular diffusion. The dispersion coefficient is generally on the order of 10^{-6} cm^2/sec (Anderson, 1984). Except for extremely slow flow velocities, the component of molecular diffusion is orders of magnitude smaller than the coefficient of mechanical dispersion.

Mechanical dispersion arises due to solute molecules traveling along different flow paths than the average water molecule. Microscopically, a solute particle which moves in the center of a pore space travels at a higher velocity than a solute particle which travels near the pore wall. Macroscopically, differences in flow paths can

occur due to either large or small scale heterogeneities encountered as the solute travels through porous media.

Dispersion of a solute can also be generated by molecular diffusion, which is related to the Brownian motion of the solute molecules.

According to Freeze and Cherry (1979), dispersion of solutes is small for relatively homogeneous sandy materials, such as those used in the column studies. Dispersion becomes increasingly important as the heterogeneity of the porous media increases.

Equation 2.5 is analogous to the Fickian equation used to describe gaseous diffusion. The validity of assuming that dispersion is a Fickian process has been discussed by Anderson (1984). Anderson concludes that dispersion is non-Fickian at short distances away from a solute source, but that at large distances from a solute source dispersion can be represented by an analogous Fickian equation such as equation 2.5. The distance at which the Fickian equation can be applied is on the order of 10's or 100's of meters (Anderson, 1984).

Dispersion was not incorporated into the analysis of the column study because there was not enough information to quantify the contribution of dispersion to tracer movement. However, the amount of tracer dispersion occurring during the column test was probably small, considering there were no large scale heterogeneities within the column.

Movement of Tracer in the Gaseous Phase

Movement of a tracer in the gas phase is governed by both convective and diffusive processes. Convection is the movement of gas

as a direct result of differences in total gas pressure, while diffusive transport occurs because of differences in partial pressures.

Convection

The primary processes which produce convective movement of gas in the soil are: (1) water table fluctuations forcing air in and out of the soil pores as water content changes, (2) recharge water pushing antecedent soil gases ahead of the front, and (3) barometric fluctuations creating pressure differentials between air-filled pores near the surface and those at depth.

During the column test, the water table did not fluctuate, a recharge front was not generated, and barometric fluctuations were considered insignificant; therefore, the transport of a gaseous tracer by convective forces was not incorporated into the computer model used.

However, if this method is applied to a field situation, convective transport may become important. Convective flow is created by a total pressure gradient and is composed of both viscous flow and slip flow (Green, 1986). Figure 2.1 illustrates the differences between the two types of convective flow.

Slip flow becomes prominent when the Knudsen number (Kn) is close to unity (Green, 1986). Kn is defined as the distance between molecular collisions (mean path length) divided by the distance between pore walls.

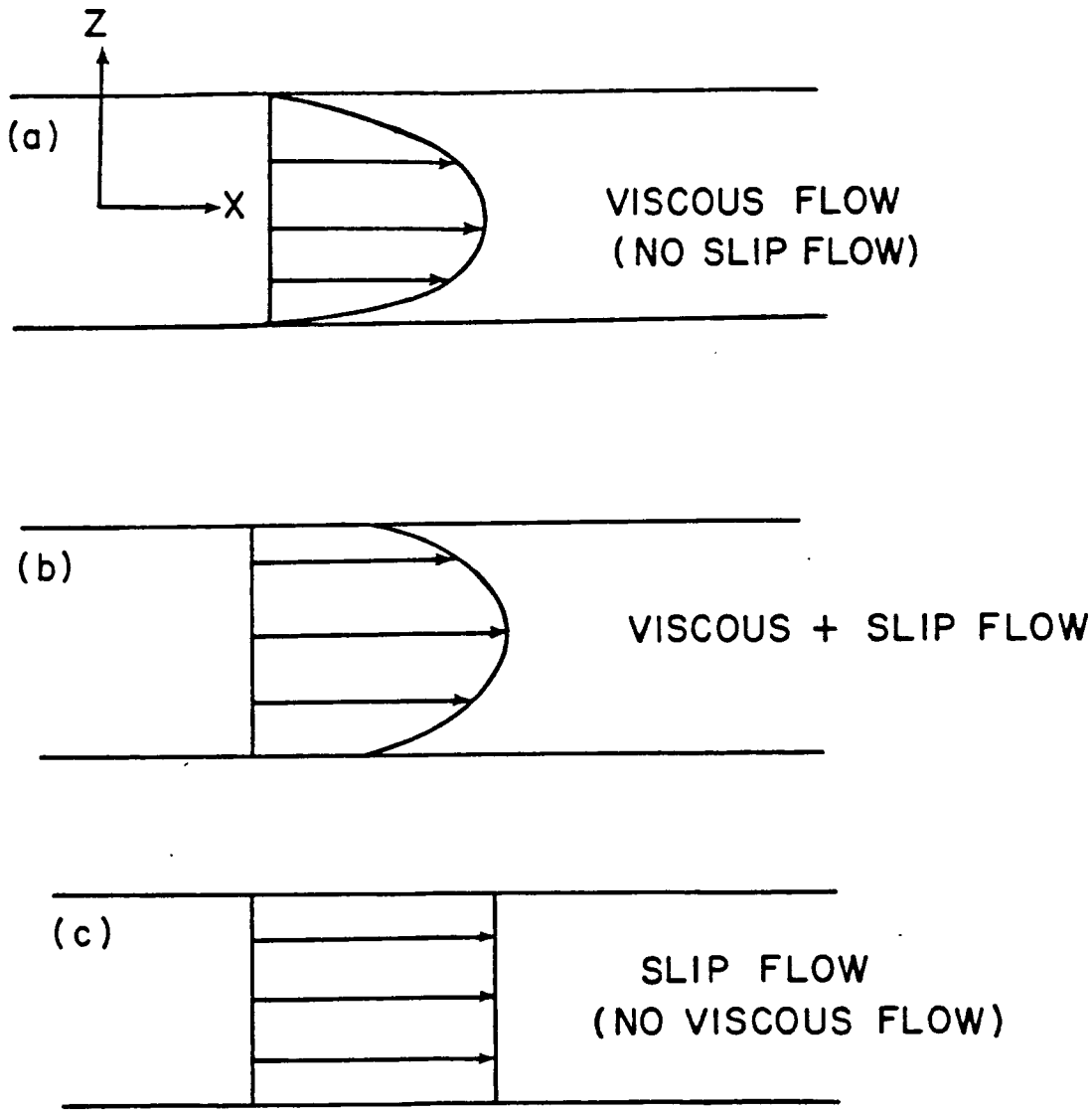

Figure 2.1 The two components of convective flow a)viscous flow, b)pressure flow and slip flow, and c)slip flow only. (From Green, 1986)

The one dimesional equation governing gaseous flow due to convection (Equation 2.6) is analogous to Darcy's equation used for the flow of water.

$$q_m = - (\rho k/n)(\delta P/\delta x) \qquad (2.6)$$

where

q_m = mass convective flux,
ρ = density of soil air,
k = permeability of the air-filled pores,
n = viscosity of soil air,
P = pressure gradient.

The continuity equation for a compressible liquid (Hillel, 1982):

$$\delta\rho/\delta t = -\delta q_m/\delta x \qquad (2.7)$$

is combined with Darcy's law to account for non-steady state flow (Hillel, 1982):

$$\delta\rho/\delta t = \delta[(\rho k/n)(\delta P/\delta x)]/\delta x \qquad (2.8)$$

The ideal gas law (equation 2.9) is used to relate air density (ρ), to pressure(P), temperature(T), molecular weight(m), and volume (V) of the gas (Hillel, 1982).

$$\rho = mP/RT \qquad (2.9)$$

where

R = universal gas constant.

Substituting the ideal gas law into equation 2.8 the general equation for transient convective flow (equation 2.10) is obtained (Hillel, 1982):

$$\delta P/\delta t = a\delta^2 P/\delta x^2 \qquad (2.10)$$

where

$$a = RTk/m$$

In deriving equation 2.10 it is assumed that pressure gradients in the air-filled pores is small and flow is laminar.

Diffusion

Diffusive transport occurs even under uniform total pressure. Several types of diffusion are known to occur in soils, the most important being ordinary gaseous diffusion, driven by concentration gradients; thermal diffusion, caused by fluctuations in the soil temperature; counterdiffusion, caused by evapotranspiration; (Weeks et al. 1982).

According to Evans (1965) ordinary gaseous diffussion is the dominant process governing gaseous transfer at shallow depths in the vadose zone. Ordinary diffusion is composed of four separate processes (Green, 1986): (1) Knudsen diffusion, resulting from collisions between gas molecules and pore walls; (2) self diffusion, resulting from collisions between like gas molecules; (3) surface diffusion, resulting from diffusion of gas molecules along the layer of molecules adsorbed onto the pore wall; and (4) binary diffusion, in response to the respective concentration gradients of the gas molecules.

Knudsen diffusion becomes more important at large Kn values where pressures are low and/or where the flow path aperature is small. When the Knudsen number is below unity self diffusion becomes prominent. Self diffusion and binary diffusion were the only two types of diffusion considered for this study.

Fick's first law which describes steady-state ordinary diffusion in one dimension (Jaynes and Rogowski, 1983) is:

$$q_A = D_{AB}\ \delta C_A/\delta z \qquad (2.11)$$

where

q_A = mass transfer rate of component A per unit area,
D_{AB} = Fickian diffusion coefficient for gas A into gas B,
C_A = concentration of a, and
z = distance.

To account for non-steady state diffusion, Fick's second law (equation 2.12) is applied (Weeks et al., 1982):

$$D_{AB}\ \delta^2 C_A/\delta x^2 = \delta C_A/\delta t \qquad (2.12)$$

where

D_{AB} = molecular diffusion coefficient for diffusion of gas A into gas B,

C_A = concentration of gas A,

x = dimension in the direction of diffusion, and

t = time.

The molecular diffusion coefficient can be calculated using either simplified kinetic theory or rigorous kinetic theory. Simplified kinetic theory assumes gas molecules behave like billard balls. Molecules are assumed to be rigid, non-attracting spheres which travel at the arithmetic mean velocity, parallel to one of the three cartesian axes (Green, 1986). Rigorous kinetic theory, also known as Chapman-Enskog theory, uses a distribution function to describe molecular behavior. Because the parameters needed to use rigorous kinetic theory were not available the simplified kinetic theory was used in calculating the diffusion coefficient.

The binary and self diffusion coefficient for non-polar gases into air is calculated using equation 2.12 derived by Slattery and Bird (1958).

$$D_{AB} = \frac{(P_{CA}P_{CB})^{1/3}(T_{CA}T_{CB})^{5/12}(1/M_B+1/M_A)^{1/2}}{P} \times a[T/(T_{CA}T_{CB})^{1/2}]^b \qquad (2.12)$$

where

P_c = critical pressure for the designated gas (atm),

T_C = the critical temperature for the designated gas (Kelvin),

M = molecular weight of the designated gas (gm/mole),

P = prevailing pressure (atm),

T = prevailing temperature (Kelvin),

A = designated gas A,

B = designated gas B,

a = 2.745E-04, and

b = 1.823.

Penman (1940) applied Fick's second law to diffusion in soils by taking into account the tortuosity of the soil and the effect of porosity:

$$t'\emptyset_d \, D_{AB} \, \delta C_A/\delta x^2 = \delta C_A/\delta t \qquad (2.13)$$

where

t' = tortuosity, and
$\emptyset_d$ = drained porosity.

In the literature, the parameters on the left-hand side of equation 2.13 are commonly condensed into one parameter called the effective diffusion coefficient (D') as shown in equation 2.14.

$$D' = t' \, \emptyset_d \, D_{AB} \tag{2.14}$$

Penman estimated the tortuosity factor to be 0.66. Several other investigators have also sought out an expression for tortuosity. Weeks et al (1982) compiled an incomplete listing of some of the published equations for determining the tortuosity factor. This list is presented in Table 2.1.

Weeks et al. (1982) concluded that the estimation of tortuosity using only drained or air filled porosity was inadequate and the inclusion of pore size distribution, pore geometry, and pore interconnections was necessary to define the parameter. The equations of Marshall (1959) and Millington (1959) are the only two equations in Table 2.1 that incorporate theoretical pore size distributions.

The diffusion equation was altered to include sorption of the gas onto soil particles and the dissolution of the gas into the liquid phase by Weeks et al. (1982). Weeks et al. used the same Fickian equation as Penman (1940) but redefined the effective diffusion coefficient (Weeks et al., 1982):

$$D' = t' \, \emptyset_d \, D_{AB} / [\emptyset_d + (\emptyset - \emptyset_d \, \rho_w \, K_w \quad (1-\emptyset_d) \rho_s \, K_s] \tag{2.15}$$

where

K_w = liquid-gas partitioning coefficient,

K_s = gas-liquid-solid distribution coefficient,

ρ_s = particle density of soil matrix, and

ρ_w = density of water.

A field estimate for the effective diffusion coefficient was determined by Weeks et al. (1982) using concentrations of F-11 and F-12, along with a computer program. Results indicated that the theoretical and laboratory methods for estimating tortuosity agree with the tortuosity values found in the field.

Table 2.1 Partial list of published expressions relating tortuosity to air-filled and total porosity (Weeks et al., 1982).

Table 5.2 Partial list of published expressions relating tortuosity to air-filled and total porosity (Weeks et. al., 1982).

Investigator	Date	Tortuosity Factor[1] dry	wet
Buckingham	1904	θ_t	θ_d
Penman	1940	0.66	0.66
van Bavel	1951	0.6	0.6
Marshall	1959	$(\theta_d)^{0.5}$	-
Millington	1959	$(\theta_d)^{0.333}$	$(\theta_d)^{.033}\ (\theta_d/\theta_t)^2$
Wesseling	1962	-	$0.9\theta_d - 0.1$
Grable and Siemer	1968	-	$5.25(\theta_d)^{2.36}$
Currie	1970	-	$(\theta_t)^{0.5}\ (\theta_d/\theta_t)^4$
de Jong and Schappert	1972	-	$0.31 - 0.59(\theta_t - \theta_d)$
Lai et al.	1976	-	$(\theta_d)^{4/3}$
Albertson	1979	-	$0.777\ (\theta_d/\theta_t) - 0.274$

[1] θ_d is drained porosity; and
θ_t is total porosity.

Sorption

Sorption of fluorocarbons onto soil must be understood before fluorocarbon tracer tests can be used to estimate water travel times in the vadose zone. The most important function of sorption is to retard the rate of solute movement in relation to the overall movement of water. The perfect tracer would never sorb onto the soil but this ideal is impossible to attain.

For organic compounds such as fluorocarbons, the magnitude and kinetics of the sorption/desorption processes are controlled by the following factors (Miller and Weber, 1984):

- Physical and chemical characteristics of the soil;
- Physical and chemical characteristics of the solute;
- Presences of competing solutes;and
- Levels and types of background organic matter in solution.

A commonly used first approximation of the sorption process is to assume instantaneous equilibrium between the solute in solution and the sorbate on the solid and to assume the solid phase concentration at equilibrium (Cs) is linear with respect to the solution phase concentration (Cw). This assumption allows the sorption/desorption process to be represented by a partition coefficient called K_d for porous media, where:

$$K_d = Cs / Cw \qquad (2.16)$$

In unsaturated media, the presence of the gaseous phase must be incorporated into the partitioning of solutes. Three separate partition coefficients are used to express the distribution of solutes between the three phases:

K_s = gas-liquid-solid distribution product and expresses the relationship of the moles of the gas sorbed on the solid phase per unit mass of solid phase to the gas in the soil atmosphere (cm^3 gas / gm solid);

K_d = solid-liquid distribution coefficient which describes the ratio of the mass concentration of solute sorbed on the solid phase divided by the concentration of the solute in the water (moles/gm solid / moles/gm water); and

K_w = liquid - gas partitioning coefficient and relates K_d to K_s. K_w describes the ratio of the concentration of the gas in solution to its concentration in the overlying gas phase under equilibrium conditions (moles/gm solid / moles/cc gas).

where: $K_s = K_w \times K_d$

Models of sorption/desorption processes can be divided into two categories on the basis of which of the two following assumptions is relaxed:

- o Instantaneous equilibrium occurs, and
- o The partition coefficient represents an equilibrium condition. In other words, at equilibrium the solid phase concentration is a linear function of the solution phase concentration.

Sorption kinetics relaxes the assumption that instantaneous equilibrium and deals with the rate at which equilibrium is attained. Sorption equilibria describes the nature of equilibria and deals with the relationship between Cs and Cw at equilibrium.

Sorption Kinetics

For many tracers, the sorption process does not occur instantaneously, thus the assumption of immediate equilibrium can not be applied. Several different types of kinetic models, each requiring the

validity of various assumptions, have been used to describe the process of noninstantaneous adsorption and desorption.

The most simple of these models uses a first-order linear differential equation to simulate sorption. In this case, the rate of sorption is dependent on the gradient between the concentration of the ion on the particle and the concentration of the ion in the solution (Rasmussen, 1982). The relationship is expressed mathematically by Equations 2.17 and 2.18 (Rasmussen, 1982).

$$dCw/dt = -1/K_+(Cw - Cs / K_d) \quad (2.17)$$

for $Cs < K_d \times Cw$ (sorption process)

$$dCw/dt = 1/K_-(Cw - Cs / K_d) \quad (2.18)$$

for $Cs > K_d \times Cw$ (desorption process)

where

Cw = concentration of solute in solution (M/L^3),

Cs = concentration of solute (M^0),

K_d = partition coefficient between liquid and solid (L^3/M),

K_+ = sorption rate coefficient (t), and

K_- = desorption rate coefficient (t).

This linear sorption rate equation is the one employed in the Discrete State Compartment model (DSC) to simulate sorption in the laboratory column tests.

Miller and Weber (1984) summarized a number of different sorption kinetic models and these models and their inherent assumptions are briefly described in Table 2.2.

Table 2.2 Brief summary of kinetic sorption models (from Miller, 1984)

Source	Model Assumptions
Oddson et al. (1970)	First order reversible rate model for sorption of nonionic surfactants.
Cameron and Klute (1977)	A rate model based on the assumption that a portion of the sorption process is governed by a rapidly achieved local equilibrium (linear) and the remainder by an independent reversible rate process (first-order function).
Karickhoff (1980)	Two-step relationship in which a linear equilibrium controlled process and a first-order rate process are coupled. Also assumed is that sorption and desorption rates are equal.
Miller and Weber (1983)	Two-resistance rate model. One equation governs diffusive transport of solute from solution to the external surface of the solid phase across a hydrodynamic boundary layer (film transport). The other equation is coupled and governs subsequent diffusion of solute within the solid phase (intraparticle transport).

Linear and Nonlinear Sorption Equilibria

Linear sorption is expressed by the equilibrium partition coefficient equation;

$$K_d = Cw/Cs \qquad (2.19)$$

Figure 2.2a illustrates the linear sorption equation. The DSC model utilizes this equation when simulating the column test. Plotting solute concentration in the solid phase versus concentration in

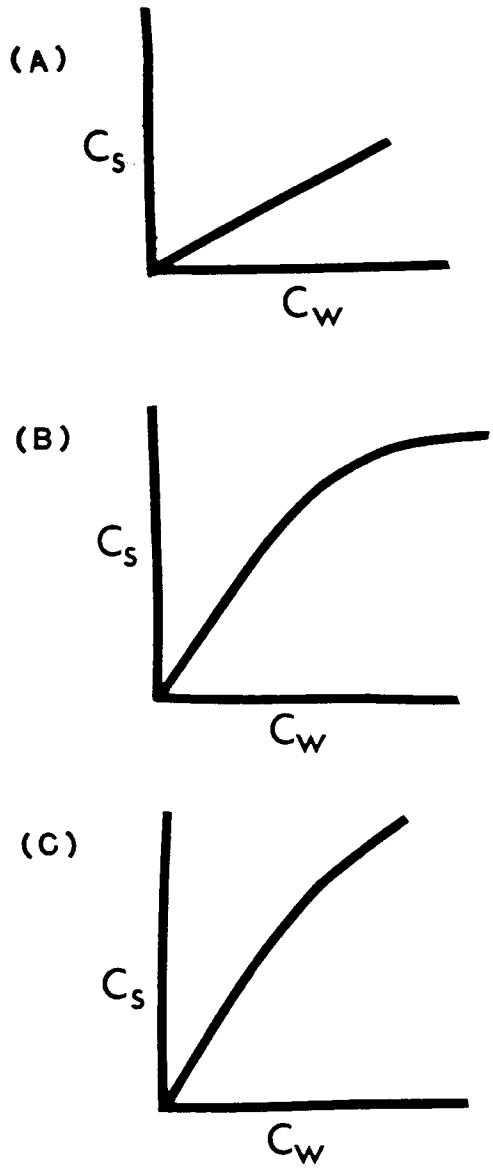

Figure 2.2 Sorption equilibrium equations: a)Linear, b) Langmuir and c) Freundlich. Where Cs is the equilibrium solute concentration on the solid and Cw is the equilibrium solute concentration in solution (From Miller and Weber, 1984).

the liquid phase results in a straight line with a slope equal to Kd. This curve describing the conditions at equilibrium is called the sorption isotherm. According to Miller and Weber (1984), the linear sorption isotherm can only adequately describe the sorption process over narrow concentration ranges.

When data do not support the use of a linear sorption model, two of the most commonly used equations are the Langmuir and the Freundlich equations. The Langmuir equation assumes that there is a limit to the amount of tracer that can be sorbed, thus causing a flattening out of the isotherm as concentration of solute increases. The Freundlich equation is similar to the Langmuir except that in the Freundlich the energy required to sorb onto a soil particle varies with the amount of solute sorbed. Both of these equations were derived using thermodynamics. Graphs of these two isotherm equations are shown in Figure 2.2b and 2.2c.

Specific data on fluorocarbon sorption were determined by Kreamer (1982). Kreamer measured Ks values for BCF and SF_6 under various solute concentrations and water contents. Two significant trends can by obtained from his data. First, that sorption increases significantly with decreasing water content, and second, changes in solute concentration only slightly affected the partition coefficient.

Brown (1982) stated that fluorocarbon tracers are almost totally sorbed onto soils with high organic content.

Under field conditions, Stiles (1982) found the sorption characteristics of the fluorocarbons to be highly variable, and in general, they do not perform as well as anionic tracers. He also

stated that although fluorocarbon compounds are retarded in saturated porous media the sorption is of the same magnitude as other tracers commercially available. Even though the fluorocarbon tracers exhibit some negative sorption characteristics, Stiles concluded his analysis of tracers by stating: "Fluorocarbons as a class are attractive for use as ground-water tracers primarily in situations where their non-toxicity, large dilution potential and negligible natural background are highly desirable."

Kreamer (1982), Thompson et al. (1974), Thompson and Hayes (1979), and Weeks (1982) all used fluorocarbon compounds to answer various hydrologic questions with some degree of success. Although fluorocarbons are affected by sorption, they still may be used effectively as environmental tracers in situations where few organic materials are present.

CHAPTER 3

COLUMN TEST PROCEDURE

Column experiments were the main focus of this study to investigate the movement of volatile tracers under unsaturated conditions. Water mixed with a volatile tracer and a chloride tracer was introduced into the top of a sand column where the tracer solution then moved downward through the column. The fluorocarbon tracer volatilized out of the water as the solution traveled down the sand column.

Measurements of the gaseous fluorocarbon concentration, as well as the qualitative measurement of the chloride concentration in the liquid phase, were made at three fixed points through time. Using the resulting breakthrough curves of the gaseous and liquid phase, the feasibility of estimating liquid velocity by sampling only the gaseous phase was evaluated.

Column tests were run for the three tracers; BCF, SF_6, and F-22, at several different flow rates to evaluate the behavior of each gas and to determine the effects of gaseous diffusion and sorption at different water displacement velocities. A diagram of the soil column test apparatus is shown in Figure 3.1. Three sampling ports were used and each port was equipped to sample resisitivity and fluorocarbon concentration. The volatile tracer and chloride ion solution were

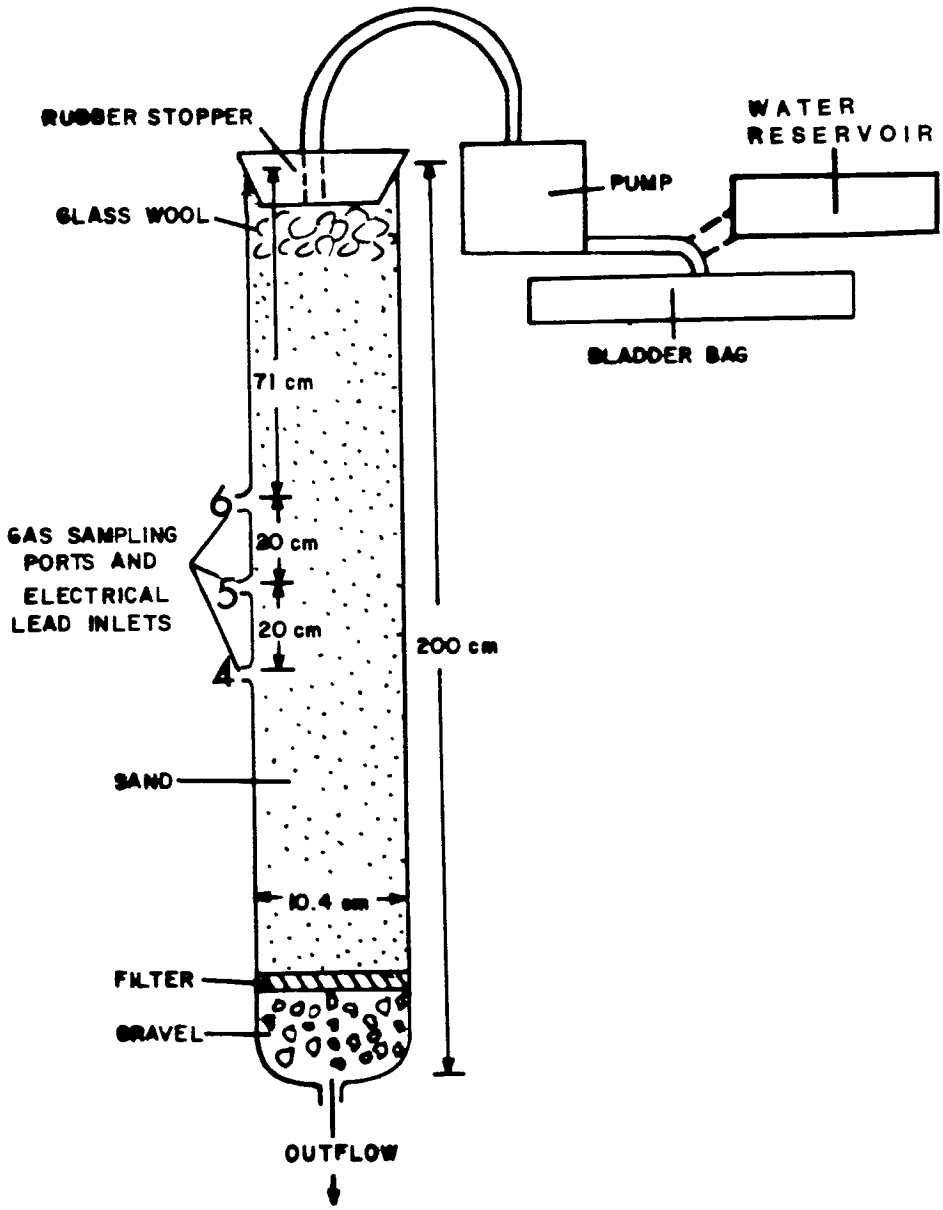

Figure 3.1 Diagram of the soil column test appartatus.

introduced into the system using a teflon bladder bag which collapsed as water was pumped out of the bag, thus keeping the system fluorocarbon leakproof. The top of the column was sealed using a large stopper to prevent the escape of fluorocarbon tracer to the atmosphere. Switching the flow system from tap water to tracer solution was accomplished by detaching the water delivery tube from the jug of tap water and attaching it to the bladder bag. Tracer solution was applied in a pulse which lasted from 45 to 322 minutes, depending on the water application rate. At the end of the pulse the water delivery tube was switched back to the jug of tap water.

Outlined below is the procedure followed for the sand column test:

- o Turn on peristaltic pump and measure outflow at bottom of column;
- o Let tap water flow through the column until the outflow rate of water at the bottom of the column becomes constant;
- o Prepare tracer standards;
- o Calibrate standards on gas chromatograph;
- o Take gas samples from each of the three ports on the column to obtain the initial concentration of tracer before test starts;
- o Take resistivity/conductivity measurement to get background values for chloride concentration;
- o Substitute tap water with fluorocarbon and chloride tracers into the column system;
- o Take sample of tracer solution just before tracer water flows into column to establish initial concentration of fluorocarbon tracer (Co);
- o Take resistivity/conductivity measurements to obtain chloride concentration at regular intervals; and

- o Take periodic gas samples from column using a syringe to obtain fluorocarbon concentration and inject into gas chromatograph.
- o When the tracer solution is empty switch the water delivery tube back the tap water.

Details of the important components of the column tests are presented in the following sections. These sections summarize the column set-up, the analytical procedure to determine chloride ion concentration, fluorocarbon standard preparation, and the use of gas chromatography to determine fluorocarbon gas concentration.

Column Set-Up

The column used for the volatile tracer study was 200 cm in length, 10.4 cm in diameter, and made out of glass. A glass column was necessary to reduce sorption along the column walls. Because fluorocarbon compounds readily adsorb onto teflon and other plastics, these materials were avoided during the test.

Highland Wash sand was used to fill the column. The sand was passed through a Number 5 screen and then funneled into the glass column using a tremy tube. The tremy tube was used to avoid layering of the sand during packing. This technique was only partially successful, because a small amount of layering could not be eliminated. The sand was primarily a medium- to fine-grained sand. A sieve analysis of the soil is presented in Table 3.1.

Table 3.1 Sieve analysis for the Highland Wash sand used in column study.

Sieve Number	Sieve Aperature (mm)	Amount Passing
5	4.	100%
10	2.	86%
14	1.4	74%
30	0.6	29%
60	0.25	3%
120	0.125	0.3%
200	0.075	0.0%

Three sampling ports at distances of 70, 90, and 110 cm from the top of the column were used to extract gas samples. These ports were also used to take conductance measurements needed to obtain chloride ion measurements.

Chloride Measurement

Monitoring the movement of water was done with a chloride tracer. The chloride was used as a conservative tracer to compare breakthrough characteristics of chloride to those of the fluorocarbon tracers. Chloride was chosen as a tracer in the liquid phase because it is easy to measure and it has been shown to be a conservative tracer

Relative chloride concentration was determined by placing two very closely spaced electrodes in the same sampling port and measuring the electrical conductance between them. The electrodes were made of silver wire wrap wire. At high flow water application rates a digital resistivity meter was used to measure conductance, but flow the slower water application rates a conductivity bridge was used instead the resistivity meter.

Changes in conductance relate to changes in chloride concentration. This technique has been used successfully several times for saturated flow problems (see Silliman, 1981). However, under unsaturated conditions, the high variability of the conductance readings became a problem. Column studies run at high flow rates gave reliable conductance readings. Chloride pulses could easily be distinguished, but due to erratic fluctuations of the conductance meter it was impossible to place actual concentrations values to the readings.

The most probable explanation for this phenomenon is that there was not always a saturated environment around the electrode to maintain a reliable electrical connection. Any fluctuations in water content around the electrode would cause the conductivity reading to also fluctuate. As the chloride tracer moved past the electrode the conductivity reading increased but continued to fluctuate. As the flow rate and water content decreased the fluctuation of conductivity readings increased making chloride breakthrough curves more difficult to obtain. Frequently, whole tests had to be rerun because chloride breakthrough curves were impossible to determine. At the lower flow rates a conductivity bridge was substituted for the resistivity meter to measure chloride concentration. The conductivity bridge was better able to measure the chloride concentration at lower flow rates than the conductivity meter. Figure 3.2 shows a sample chloride breakthrough curve for the three sampling ports used in the study. The curve was obtained during a test run at a water application rate of 4ml/min.

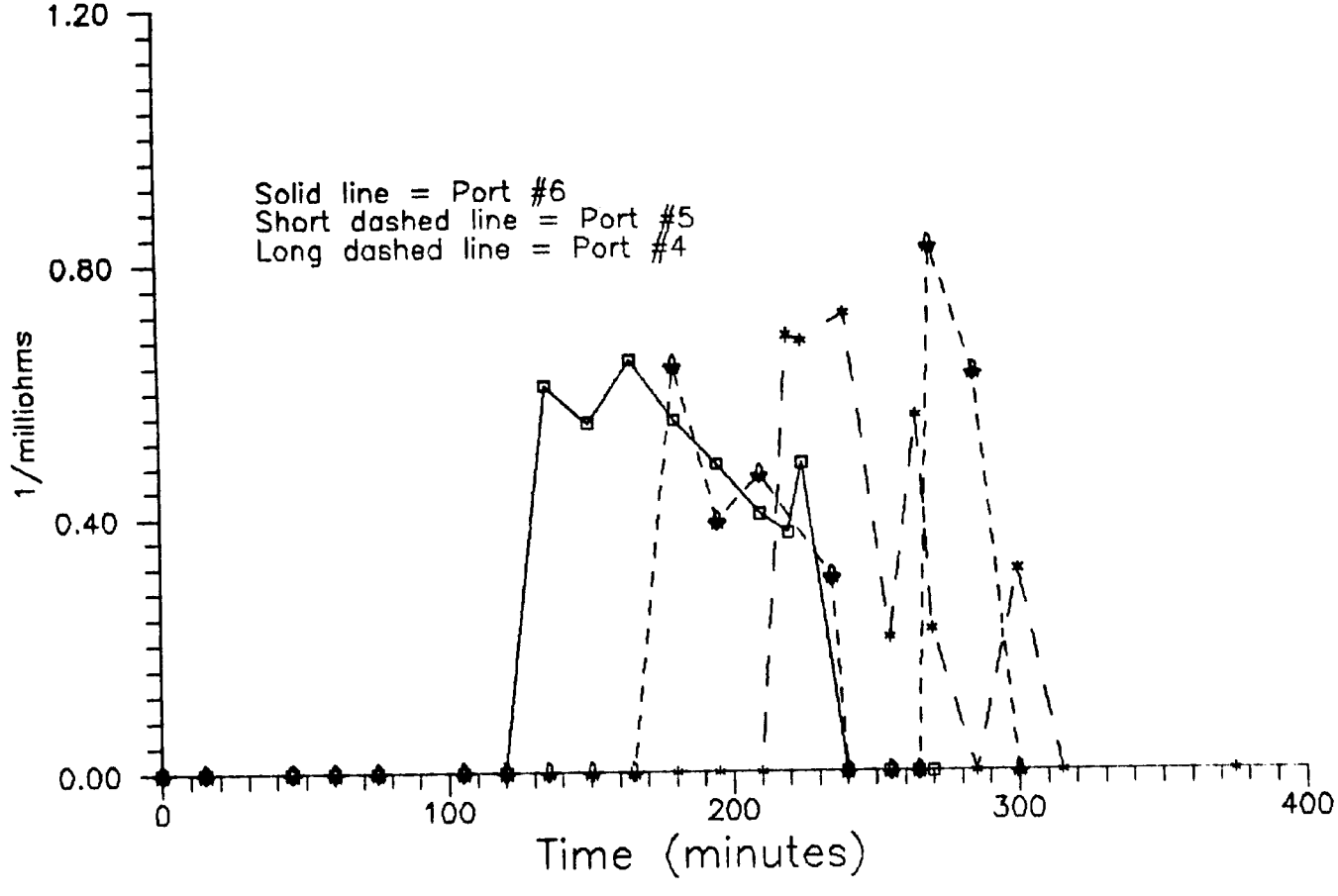

Figure 3.2 Examples of salt breakthrough curves for a water application rate of 4 ml/min.

Fluorocarbon Standard Preparation

Gas chromatography measures the concentration of a chemical compound relative to a standard concentration of that compound. Tracer standards are necessary to calculate concentrations of the fluorocarbon samples taken during the column tests.

Tracer standards were prepared differently for each fluorocarbon gas. BCF standards were prepared by Matheson Gas Company (8800 Utica Ave., Cucamonga, CA) at a concentration of 1 ppm. This standard was injected directly into the gas chromatograph. No pre-made standards were available for F-22 and SF_6.

Standards for F-22 were made by following EPA standard method 601 (Environmental Protection Agency, 1982). This method requires that a 10 ml flask be filled with approximately 9.8 ml of methanol and weighed. After weighing, pure F-22 gas is slowly syringe injected into the methanol, the syringe needle being held just above the methanol surface. The flask is re-weighed to determine the amount of F-22 in the sample. Finally, the flask is filled to the 10 ml line with methanol, shaken lightly and transfered to an air-tight vial. The methanol solution is then syringe injected into the gas chromatograph.

SF_6 standards could not be prepared in the manner described for F-22. Instead, 250 ml air-tight glass canisters with septums were used to prepare SF_6 standards. The canisters were cleaned and nitrogen purged while being oven dried. One microliter of pure gas was injected into the sealed canisters. After eight hours syringe samples of standard were extracted through the septum and injected into the gas chromatograph.

Fluorocarbon Tracer Preparation

A tracer solution was prepared depending on the type of tracer used. BCF tracer solution was made by bubbling a 1 ppm standard through a covered vial of methanol for at least eight hours. The methanol concentrated the volatile gas in a soluble phase more effectively than water. This achieved higher concentrations in the initial tracer solution. F-22, and SF_6 tracer solutions were prepared by bubbling pure gas into 10 ml of methanol. All tracers that were concentrated in the methanol were then diluted with water. Some methanol was left in the tracer solution, but in such dilute concentrations that it did not show up in any of the samples taken during the column test.

Gas Chromatography

Critical to the use of fluorocarbon tracers is the development of an analytical procedure for determining fluorocarbon concentrations using a gas chromatograph. For this study, a Hewlett-Packard 5700A Series gas chromatograph was used with a Carbopack 1% SP1000 column. Because SF_6 has a very fast elution time, a low column temperature was used. The low temperature, however, retarded the late eluting peaks, requiring an increased time interval between sampling, thereby decreasing the sampling frequency. A sample chromatogram is presented in Figure 3.2.

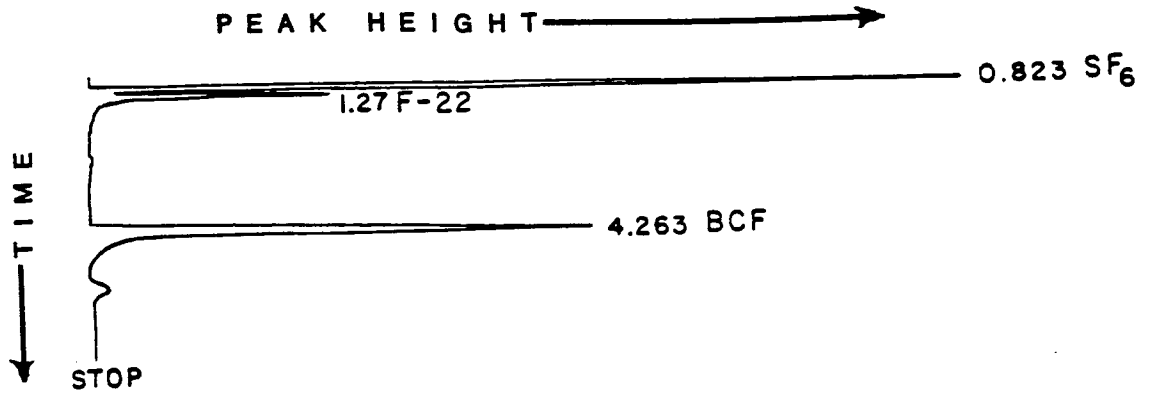

Figure 3.3 Sample chromatogram showing the three fluorocarbon tracers used in study. Analyses were performed using a Hewlett Packard 5700A series gas chromatograph with a Carbopack, 1% SP1000 column at 60°C.

Each tracer must be calibrated to assure that there is a linear relationship between area counts on the chromatogram and the concentration of the tracer. Calibrations must also be made every time the chromatograph is used because changes in electron capture detector sensitivity and column sensitivity can occur. Each test requires that five-point calibrations be made. In addition, a correlation coefficient (which describes the degree of linear relation between two variables) between area counts and concentration must exceed 0.98. Usually, this value was not difficult to attain but occasionally several calibrations had to be made in order to achieve a reasonable value for correlation coefficient. A sample calibration curve is shown in Figure 3.3.

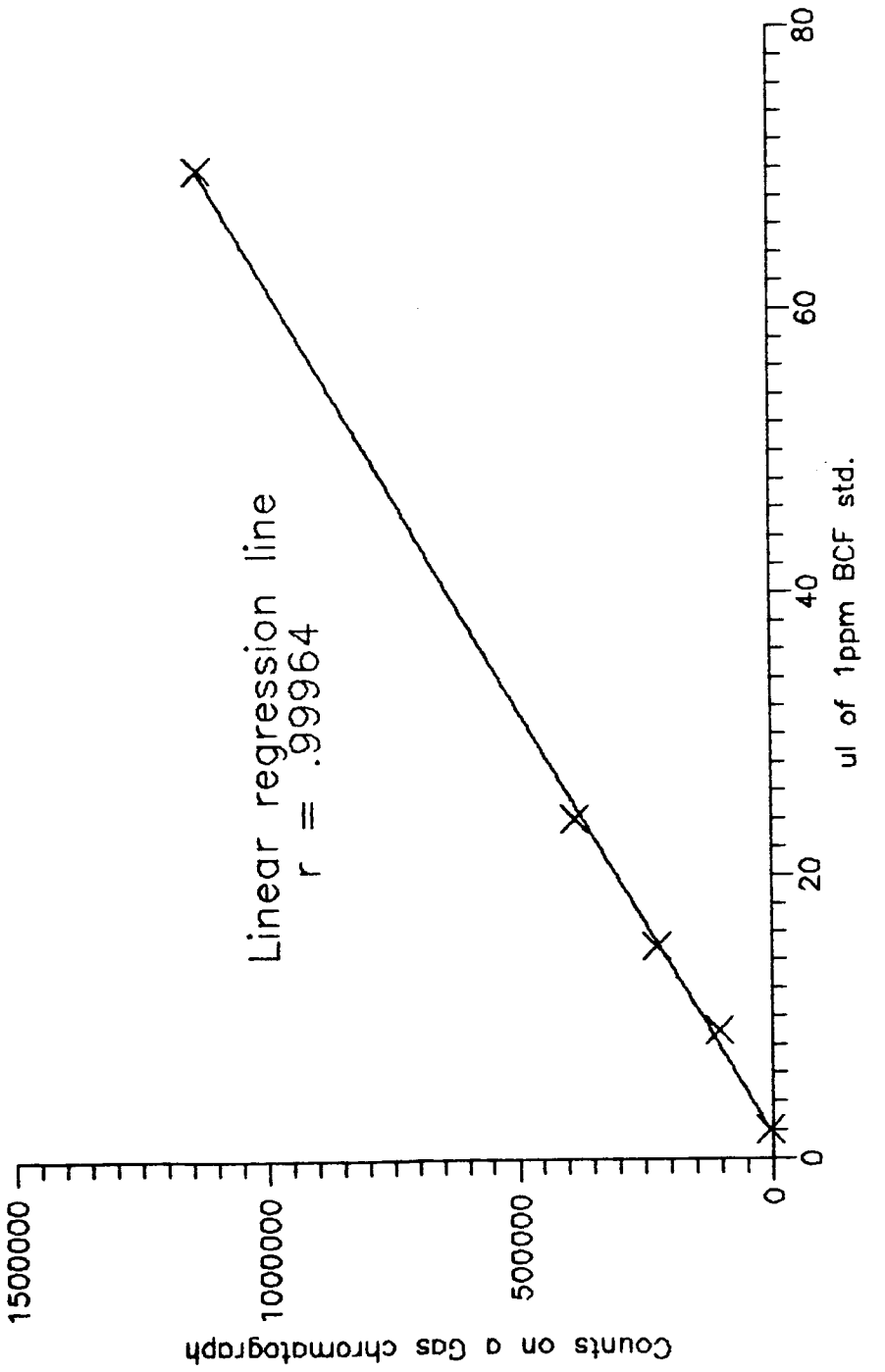

Figure 3.4 Five point calibration curve for 1 ppm std. of BCF.

CHAPTER 4

RESULTS OF COLUMN TESTS

A total of five successful column tests were completed. The type of tracer tests performed are summarized in Table 4.1.

Table 4.1 Summary of Fluorocarbon Tests.

Test #	Date	Water Application Rate	Displacement velocity*	Tracers Used
1	8-12-85	4 ml/min	0.661 cm/min	F-22
2	8-19-85	5 ml/min	0.661 cm/min	BCF
3	9-02-85	1 ml/min	0.155 cm/min	F-22, SF6
4	9-28-85	.286 ml/min	0.050 cm/min	SF6
5	10-10-85	.083 ml/min	0.015 cm/min	F-22, BCF, SF6

* calculated by dividing the water application rate by the water content and by the surface area of the column.

Analysis of Soil Column Tests

Figures 4.1 through 4.6 are graphs depicting breakthrough curves for five of the column tests. All graphs show the time since the start of a test versus the dimensionless concentration C/C_0, where C is the concentration of tracer in the soil gas and C_0 is the concentration of tracer initially dissolved in the water phase. C/C_0, as defined in this paper, is different from the common terminology. The reason the parameter C/C_0 is used to indicate the amount of fluorocarbon needed in the initial tracer solution to obtain measurable concentrations of fluorocarbons in the gas at the sampling port. C/C_0 is defined in this paper in such a way that the parameter will never reach unity. The

vertical line on the graph indicates the beginning of the chloride tracer breakthrough front in the water phase.

Test #1

The breakthrough curves obtained from Test #1 are presented in Figure 4.1. The column test was run at a fairly high water application rate of 4 ml/min with a tracer pulse of 45 minutes.

Fluorocarbon gas and chloride ion broke through at approximately the same time. The first appearance of tracer in the gas signifies the breakthrough of the liquid. Therefore, the volatile gas does a reasonably good job of predicting fast water flow rates. However, the breakthrough results from the other sampling ports show an unexpected decrease in concentration of fluorocarbon tracer as the water moves down the column and reaches port #4.

The drastic reduction in concentration is too large to be explained by dispersion of the tracer front as it moves down the column. This decrease is more likely due to problems with the laboratory technique. During the test, gas samples of 0.5 cc were withdrawn to obtain concentration data. This sampling seems to have affected the concentration of the tracer in the soil atmosphere. The sample size was relatively small compared to the air volume in the column; therefore, it is unlikely that the size of the gas sample affected the test results. However, the process of pulling the air in the column into the syringe could have created a suction force causing laboratory

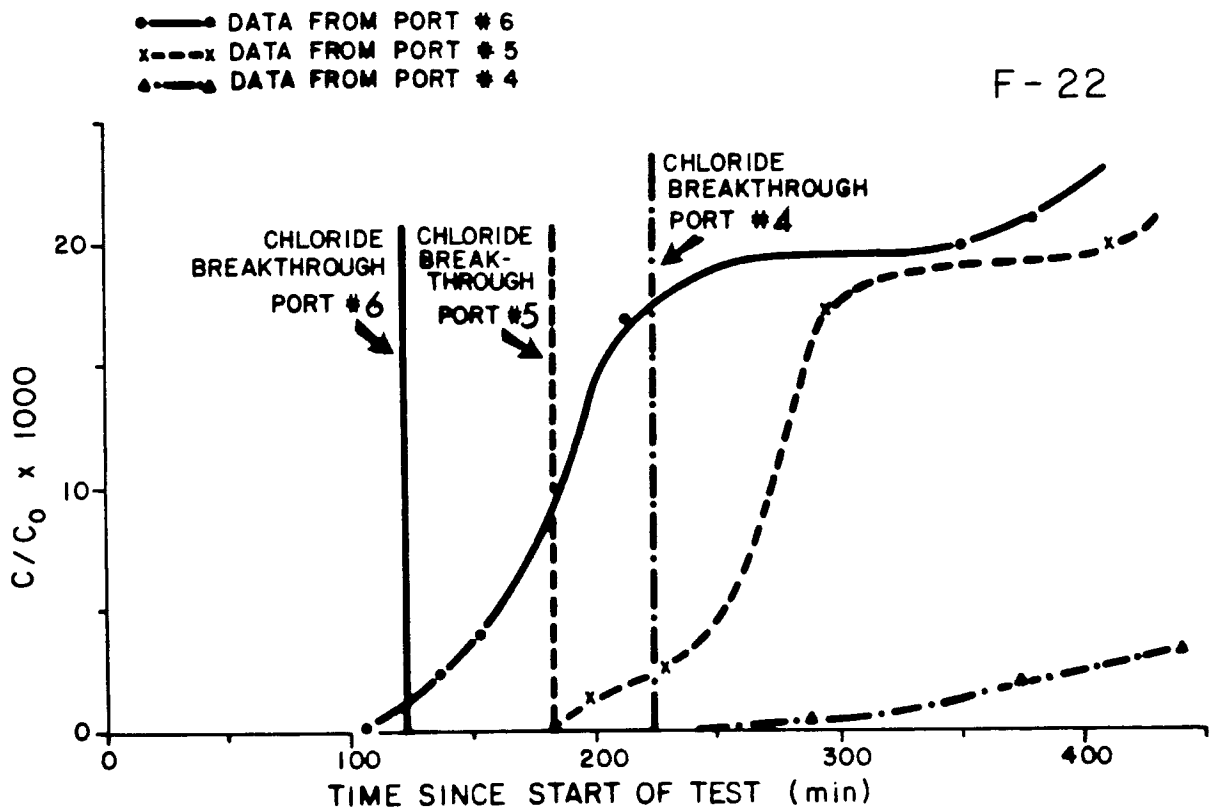

Figure 4.1 Breakthrough curves for Freon-22 test rat at a water application rate of 4ml/min.

air to flow into the column through the sampling port, thus diluting the tracer concentration near the sampling port.

A test of this hypothesis was conducted at the end of the tracer test when there was a large concentration of tracer left in the column. Three gas samples were withdrawn at five-minute intervals, then sampling was stopped for fifteen minutes, and the concentration of tracer was allowed to recover. The results of this test showed that the size of the tracer peak on the gas chromatograph decreased by approximately one-half. After recovering for 15 minutes the concentration of the tracer was essentially the same as at the beginning of the test. These results suggested that air surrounding the column was pulled into the column when the gas sample was being withdrawn, thus creating a dilution effect due to sampling. To standardize the data and make interpretation easier, it became evident that the sampling frequency and sample size should be kept to a minimum and sampling should be done at equal time intervals.

The water displacement velocity measured by the chloride ion breakthrough was 0.609 cm/min. The displacement rate measured by the chloride ion breakthrough is much faster than that measured by calculating the velocity from the water inflow divided by the area of the column and the water content. The same relationship between the two displacements velocities occurred in every test. Table 4.2 summarizes the values of displacement velocities for each test.

Table 4.2 Summary of water displacement velocitys calculated from the water inflow into the column and the displacement velocity derived from chloride ion measurements.

Test	Water Application Rate	Displacement vel. using water inflow rate into column	Displacement vel. using chloride tracer measurements
1	4 ml/min	.528 cm/min	.609 cm/min
2	5 ml/min	.661 cm/min	.875 cm/min
3	1 ml/min	.155 cm/min	.339 cm/min
4	.286 ml/min	.050 cm/min	.200 cm/min
5	.083 ml/min	.015 cm/min	.149 cm/min

The difference between the two displacement velocities is not excessive for the first three tests. However, the tests run at the slower application rates show large differences between the calculated and the measured displacement velocity. The difference in magnitude between the two displacement velocities means that, for small application rates, a significant portion of the chloride tracer travels through the faster, large pore systems in the sand column. However, a significant amount of water is retained in the smaller slow-velocity pore systems. When the water in the small pore systems, which does not contribute significantly to flow, is incorporated into the water content value used to calculate the water displacement velocity, the measured displacement velocity will always be higher than the calculated rate.

Test #2

Figure 4.2 illustrates the breakthrough curve for BCF at a flow rate of 5 ml/min with a tracer pulse of 45 minutes. Here again, the first appearance of volatile fluorocarbon tracer roughly corresponds to the appearance of the chloride tracer. Data from the other two ports

were unavailable because the BCF concentration was too low at these ports to be measured.

The behavior of BCF could not be adequately studied because a concentrated source of the compound was not available. Fluorocarbon concentration in the initial tracer solution needed to be greater than those concentrations used by other investigators. Unlike most tests where fluorocarbons were introduced in one phase and measured in that same phase, this study introduced the tracer in one phase (liquid) and measured the presence of that compound in another phase (gas). The volatile tracer technique requires that there be enough fluorocarbon tracer in the initial liquid phase so that, despite continuous volatilization, when the tracer pulse reaches the sampling port there is still enough tracer left in the liquid phase to volatize out in measurable amounts.

Typical concentrations for the tracer in the gas phase were between 100 to 10,000 times less than the initial concentration of the fluorocarbon-traced water. In other words, C/C_0 values for most tests ranged between 10^{-2} to 10^{-4}. The small C/C_0 values requires that a high concentration of fluorocarbon be used in the initial traced water.

Several attempts were made at concentrating BCF. Unfortunately, the 1 ppm standard could not be concentrated enough so that complete breakthrough curves for slower displacement velocities could be measured.

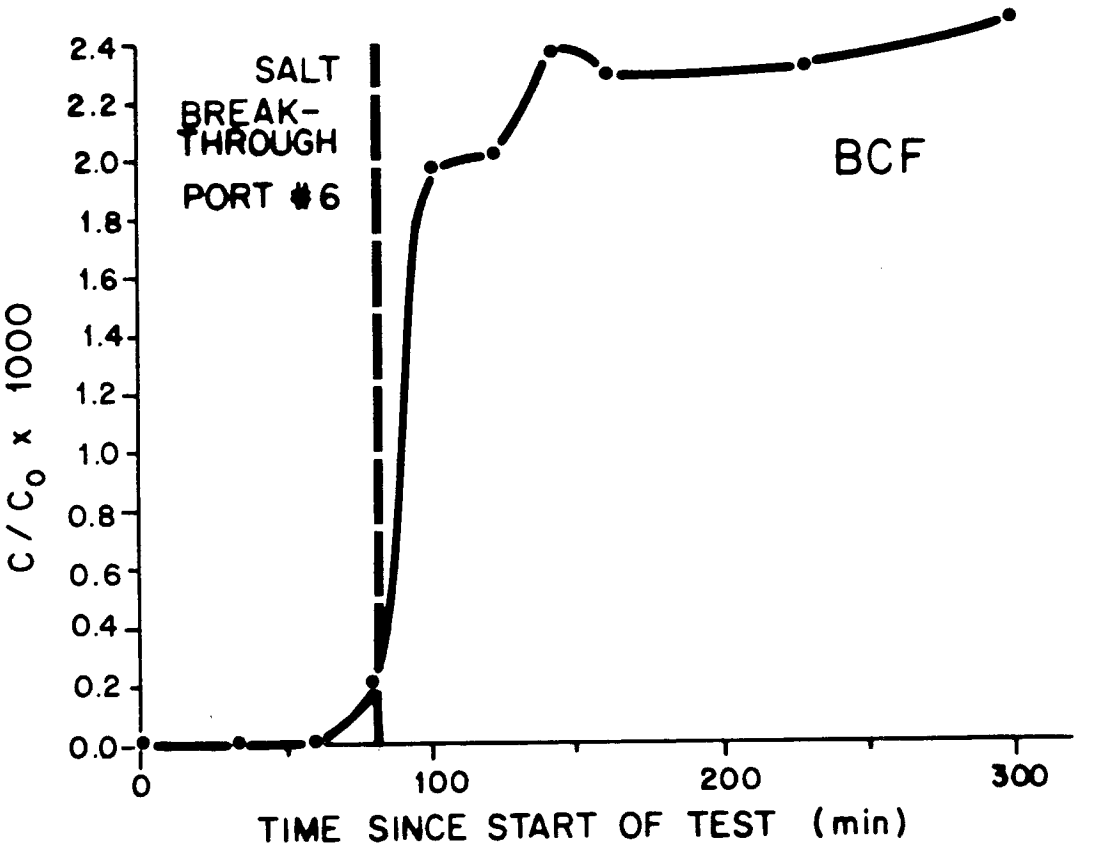

Figure 4.2 Laboratory gaseous breakthrough curve, water application rate equals 5 ml/min

Test #3

The water application rate was decreased to 1 ml/min for test #3. F-22 and SF6 were introduced into the column as a pulse lasting 150 minutes. F-22 tracer from test #1 could not be purged from the column, demonstrating one of the most important problems with the use of F-22 as a hydrologic tracer. The tracer does not readily desorb from soil particles, implying that the use of this tracer in the field might result in long term contamination. Gaseous breakthrough curves for this test are presented for F-22 in Figure 4.3.

SF6 breakthrough curves are presented in Figure 4.4. The gaseous breakthrough curve only slightly preceded the chloride breakthrough curve. The slight lead of SF6 in the breakthrough curve hints at the possibility of diffusion becoming important. Graphs of SF6 breakthrough for ports 5 and 6 were not presented because of problems with the resistivity meter made the detection of the chloride tracer impossible.

Test #4

Test #4 breakthrough curves for SF6 are presented in Figure 4.5. The water application rate for test #4 was 0.286 ml/min and the tracers were administered for a period of 322 minutes. Results from all three ports exhibited large diffusion effects. The fluorocarbon gas precedes the chloride ion in arrival time at the first sampling point by well over one hour. The breakthrough curves show a continuous increase in gaseous tracer concentration with time. Once again the resitivity

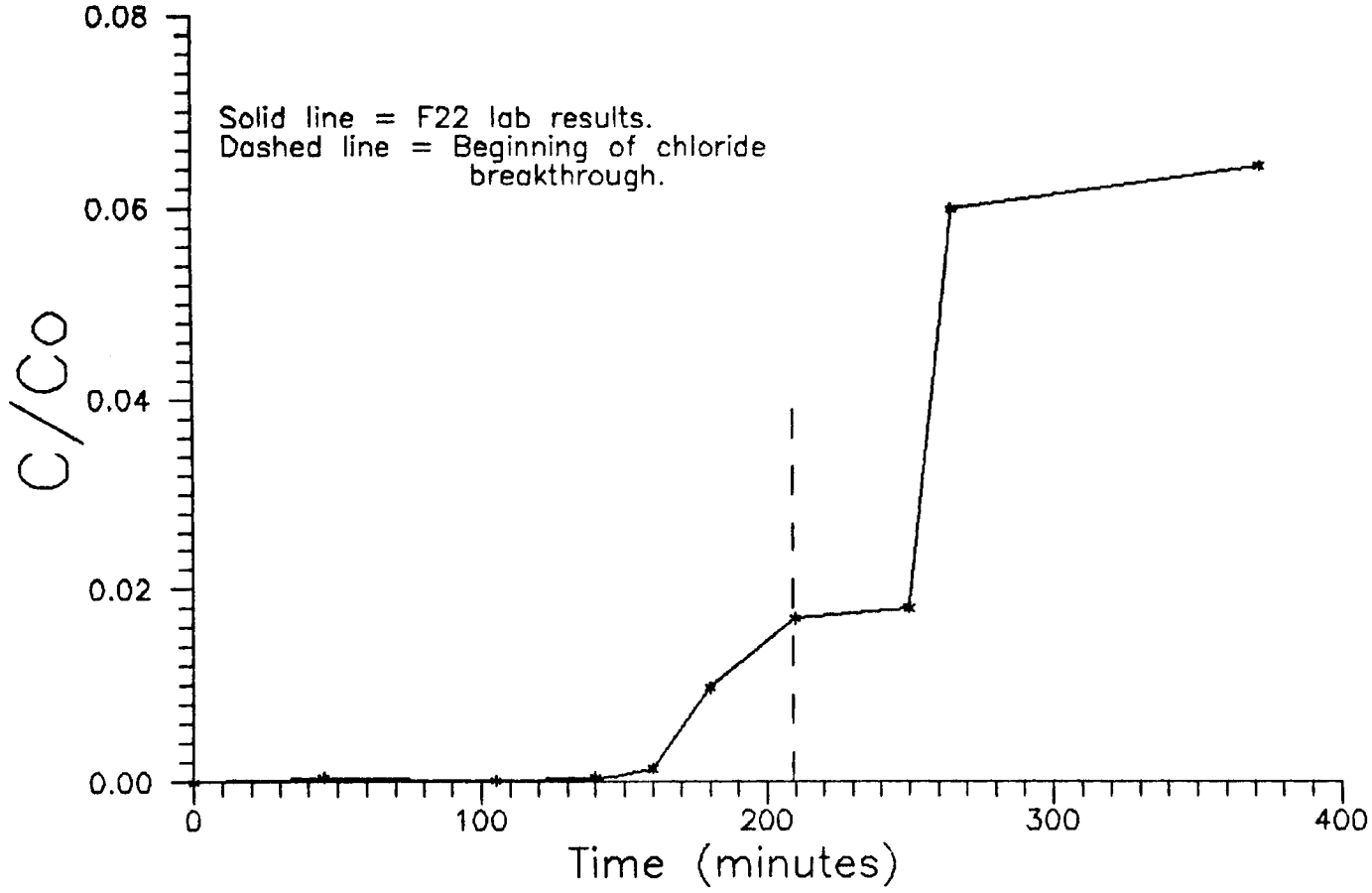

Figure 4.3 F-22 laboratory gas breakthrough curve for a water application rate of 1 ml/min.

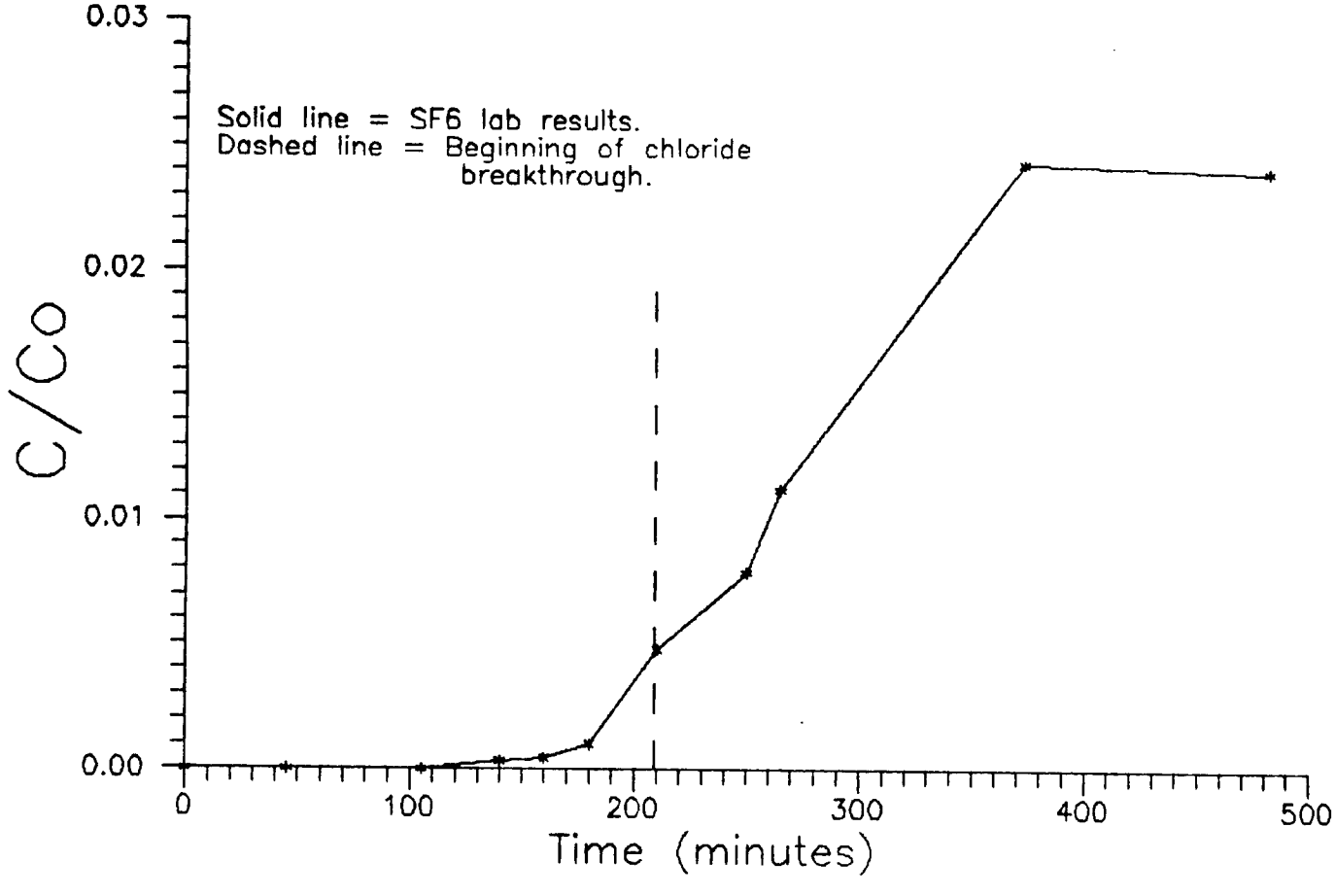

Figure 4.4 SF6 laboratory gas breakthrough curves for a water application rate of 1 ml/min.

measurements for ports 5 and 4 were uninterpretable, therefore the gaseous breakthrough curves could not be used to estimate average water velocity.

The graph for port #6 can be divided into 2 sections. The first section seems to show the early arrival of gas due to gaseous diffusion. The first portion of the graph is characterized by a uniform increase in concentration . The second portion of the graph is recognized by a steeper uniform increase in gas concentration which indicates the beginning of the tracer pulse. The break in slope can be used to estimate water displacement velocitys if two distinct slopes can be separated in the breakthrough curve.

Test #5

The water application rate was further decreased to 0.083 ml/min and three tracers were applied for a period of 300 minutes. Water percolated through the column for several weeks to let the water outflow rate achieve a steady state. The slower flow rate was used to increase the effects of gaseous diffusion. Breakthrough curves for the three tracers are shown in Figure 4.6(a), 4.6(b), and 4.6(c). In all three cases the fluorocarbon tracers appeared in the soil gas significantly ahead of the chloride.

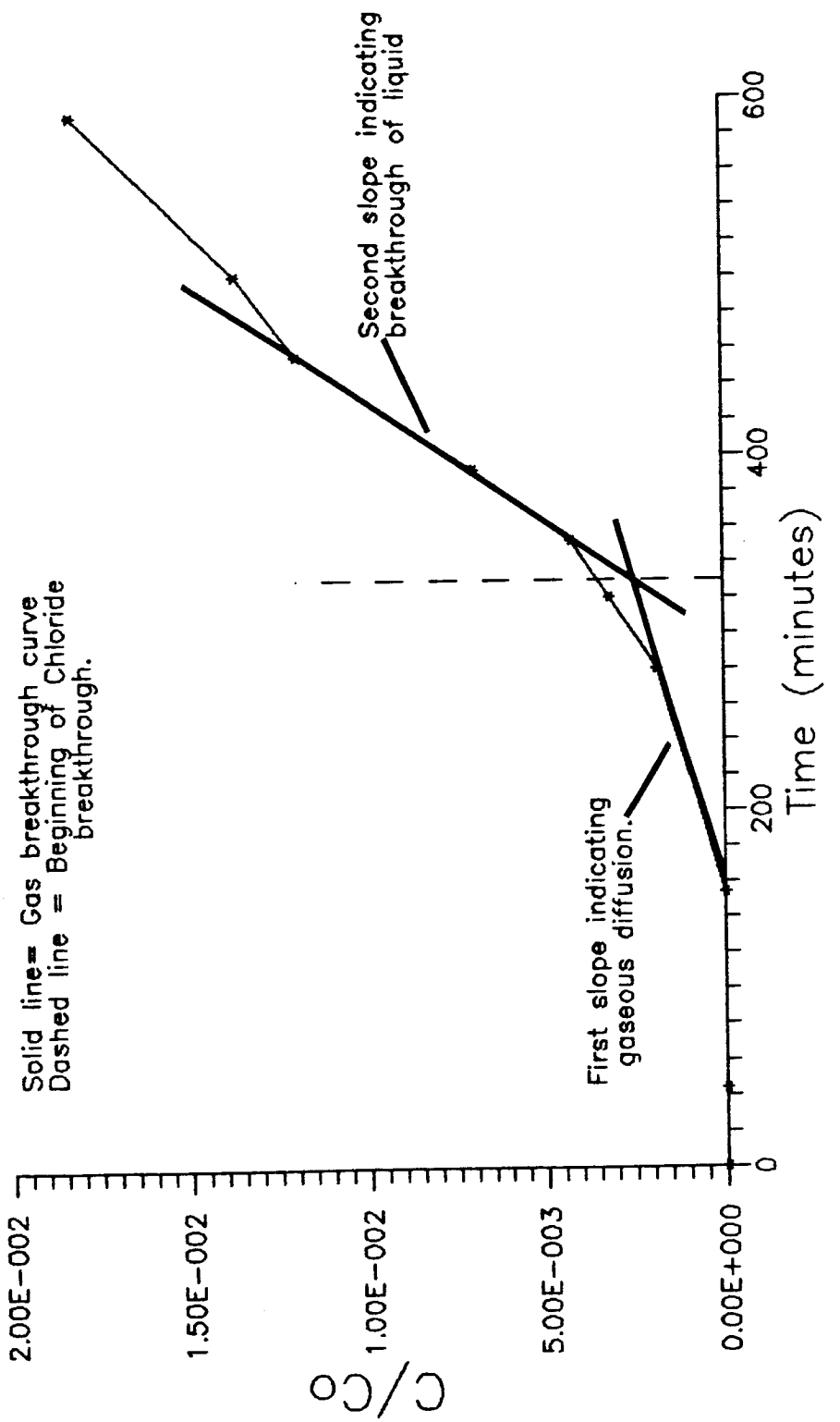

Figure 4.5 Gaseous breakthrough curve for the SF6 test #4 which was run at a water application rate of 0.285 ml/min.

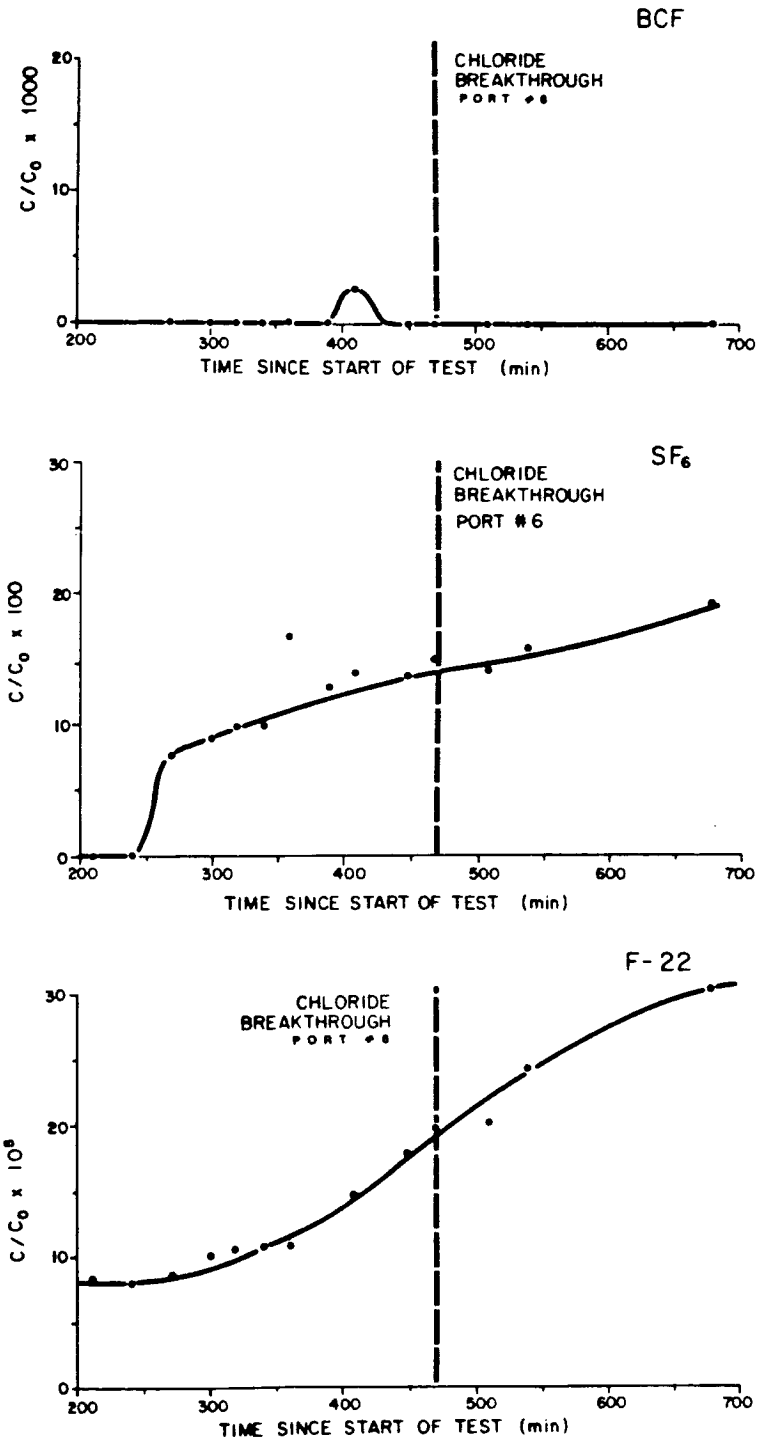

Figure 4.6 Port #6 gaseous breakthrough curves for BCF (a), SF6(b),and F-22(c) for a tracer test run at a water application rate of 0.083 ml/min.

Summary of Column Test Results

Several conclusions on the behavior of the three fluorocarbons tracers can be drawn from the six column tests:

- o If the gaseous breakthrough front is steep and is shaped like a traditional tracer breakthrough curve then the water travel times can be estimated assuming the first sign of gaseous tracer indicates the liquid breakthrough;
- o At low flow rates gaseous diffusion became an important transport process for volatile tracers;
- o At low flow rates the gaseous breakthroug curves can not be used to estimate the travel time of water. Computer modeling of the laboratory data is necessary to separate out the processes of diffusion and advection;
- o BCF was hard to concentrate; therefore, its potential as a tracer was not adequately evaluated;
- o Desorption of F-22 from the Highland Wash soil was extremely slow, so that any field work with the tracer might contaminate the soil for a long time;
- o SF6 was the most mobile of the three tracers in the gaseous phase. SF6 would consistently breakthrough faster than F-22 or BCF in the column tests; and
- o Sampling size and frequency affected the magnitude of the breakthrough curves for ports 4 and 5.

Column tests showed that at low flow rates the gaseous breakthrough curves could not be used to predict water travel times because of the increased effects of gaseous diffusion. For the Highland Wash sand tests, the measured water displacement velocity must be greater than 0.35 cm/min for the volatile tracer method to accurately predict the travel time of water. By using the computer to analyze the effect of diffusion, it may be possible to predict water travel times for the slower flow rates. The next two chapters will detail how computer

modeling can help separate out the different processes involved with transport of a volatile tracer.

CHAPTER 5

APPLICATION OF THE DSC COMPUTER MODEL TO THE STUDY OF VOLATILE TRACERS

Computer modeling is needed to determine when the influence of gaseous diffusion becomes a significant transport process affecting concentration of fluorocarbon tracer in the soil gas.

The Discrete State Compartment (DSC) model was applied to this problem because of its simplicity and the ability to run the model on a microcomputer. A copy of the program is presented in Appendix B. Dr Eugene S. Simpson, of the University of Arizona, originally proposed the DSC model. The original computer code was written by Campana (1975) and expanded on by Rasmusssen (1982). The model was rewritten in FORTRAN 77 by Rasmussen (1986) for use on a microcomputer.

The DSC model uses a series of cells or compartments to represent a hydrologic system. By mixing the contents of adjacent cells in such a way as to conform to the physical laws governing the movement of water, the complexities of a hydrologic system can be simulated.

An iterative equation (Equation 5.1) is used to combine cell inputs, sources and sinks, with a mass balance equation in order to generate a flow system.

$$S(n) = S(n-1) + [BRV(n) * BRC(n)] - [BDV(n) * BDC(n)] +/- R \quad (5.1)$$

where

S = mass, or amount, of tracer in the cell,

BRV = boundary recharge volume, or input volume, of water in the cell,

BRC = boundary recharge concentration, or input concentration, of tracer in the cell,

BDV = boundary discharge volume, or output volume, of water from the cell,

R = source/sink term within the cell, and

n = iteration number.

The DSC model estimates solute transport in both the liquid and vapor phases by using different cells to represent the liquid, solid, and gas phases. That is, for each liquid cell there is a corresponding solid and gas cell. Interactions between the phases are modeled as exchanges between these cells. For example, the process by which a tracer volatilizes out of the liquid phase and into the gas phase is modeled by an exchange between the cells representing the liquid and gas components.

Physical processes occurring within the soil during a tracer test, which must be addressed by the computer simulation, consist primarily of advection, sorption onto the soil particles, partitioning of the volatile tracer into the soil gas, and finally, diffusion of the tracer in the gas phase. Adapting the DSC model to include all of these processes and expressing the mathematical equations was done by Rasmussen (1982, 1985).

Advection

Advection is simulated using a mixing cell algorithm. The DSC model allows for two types of mixing, the first being the Simple Mixing Cell (SMC) approach. At each time step in the SMC method, water output from the preceding cell completely mixes with the contents of the current cell. Incoming water to the cell is accommodated by expanding the cell walls. After complete mixing the walls contract and discharge a volume equal to the volume which entered. Essentially, the algorithm consists of input-mix-output where the boundary discharge concentration equals (Rasmussen, 1982) :

$$BDC(n) = [S(n-1) + \{BRC(n) \times BRV(n)\}]/[VOL + BRV(n)] \qquad (5.2)$$

where

VOL = volume of the cell.

The second scheme used by the DSC model to treat advection is called the Modified Mixing Cell (MMC). The MMC algorithm assumes that at each iteration, incoming water displaces an equal cell volume of water and the incoming cell water mixes with the remaining water in the cell. Boundary discharge concentrations are calculated using Equation 5.3.

$$BRD(n) = S(n-1)/VOL \qquad (5.3)$$

The MMC algorithm produces less numerical dispersion and, therefore, creates a sharper tracer front than with the SMC. The choice of algorithm depends on the shape of the tracer front being simulated.

Figure 5.1 from Rasmussen (1982) shows the differences between the SMC and MMC advection models.

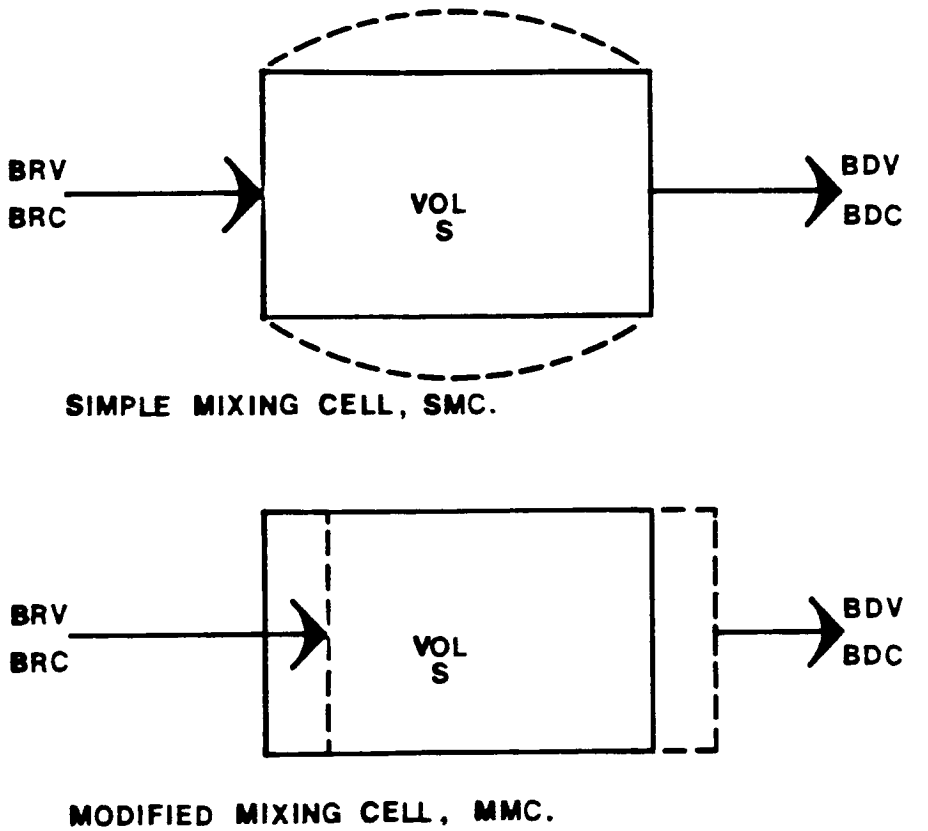

Figure 5.1 Stepwise operation of two advection algorithms by DSC model. (Rasmussen, 1982)

Sorption

Sorption onto the soil particles is incorporated into the model by changing the solid cell volume in such a way as to assure that after mixing, the tracer is distributed proportionally between a cell representing the solid phase and a cell representing the liquid phase as dictated by the distribution coefficient, K_d. The relationship between cell volumes is:

$$VOL_s = K_d \times \rho_b/\emptyset \times VOL_w \qquad (5.4)$$

where

VOL_s = equivalent cell volume of the solid,

K_d = distribution coefficient between solid and liquid,

ρ_b = bulk density of soil,

$\emptyset$ = volumetric water content of the soil, and

VOL_w = equivalent cell volume of the liquid.

Sorption kinetics are incorporated in to the DSC model by the use of the exchange volume. The simplest approach is to use a linear model which assumes the rate of sorption onto the solid is related to the gradient between the concentration tracer in solution and the tracer sorbed on to the solid (See equations 2.8 and 2.9).

Rasmussen (1982) used equations 2.8 and 2.9 to solve for the exchange volume in terms of the parameters K_+ (See equation 5.5). A separate desorption coefficient, K_+, is not used in the simulation of the laboratory results. Therefore, the rate of adsorption equals the rate of desorption in all the computer simulations.

$$\text{Exchange volume} = \frac{\rho/\theta \times K_d \times \text{delt}}{(\rho/\theta \times K_d \times K_+ - \text{delt})} \qquad (5.5)$$

where

delt = time step.

In order to model sorption, the distribution coefficient, K_d, the bulk density, the water content and the rate constant must be known. For this study, partition coefficients describing the sorptive properties of the soil were determined from batch tests for F-22. Details of the procedure are presented in Appendix C. The K_s for F-22 was found to vary from 0.356 to 0.659 cc gas/gm solid as water content varied between 10% and 0%. Averaging the K_s values and dividing by K_w the average K_d used to calculate the volume of the solid cell was 2.3 gms water/ gm solid.

K_d values for SF6 and BCF were reported by Kreamer (1982) and ranged from 3.33 to 0.07 cm^3/g, for soils with low moisture contents. Thompson and Stiles determined a K_d for BCF of 0.05 for pure silica sand under saturated conditions. Because K_d increases sharply with decreasing water content the K_d determined by Thompson and Stiles was not used in the computer model. Instead, the volume of the solid cell for the BCF simulations were estimated to be 150 cm^3. Using 150 cm^3 as the solid cell volume, K_d varied from 2.78 to 0.346 cm^3/g, well within the K_d range measured by Kreamer (1982). The K_d values for SF6 found by Kreamer were approximately the same as those found for BCF; therefore, the same solid cell volume was used for SF6 as for BCF.

A bulk density measurement for the soil is also needed to calculate the volume of the solid cell. This parameter was obtained by dividing the weight of the dry sand in the column by the volume of the soil in the column. The weight of the dry sand was obtained by weighing the glass column empty and again after it was filled with sand. The bulk density of the sand was found to be 1.54 g/cm^3.

Gamma ray measurements were conducted to find the relation between water application rate and water content. The results of the gamma ray measurements are presented in Figure 5.1. The technique and calculations involved in obtaining the graph are detailed in Appendix D.

The last parameter needed to model sorption was the rate constant, K_+. The rate constant is unknown, so exchange volumes had to be estimated and a trial and error method was used to match the column test data to the computer simulation.

Partitioning Between the Liquid and Gas Phases

Partitioning between the liquid and gas phases can be represented in much the same way as partitioning between the liquid and solid phases. Equation 5.6 mathematically expresses the relationship between the gas and liquid phases.

$$VOL_g = 1/K_w \times V_g \times 1/M_w \times VOL_w \qquad (5.6)$$

where

VOL_g = equivalent cell volume of the gas,

V_g = actual volume of gas in an equivalent cell volume, and

M_w = actual mass of water in a cell volume.

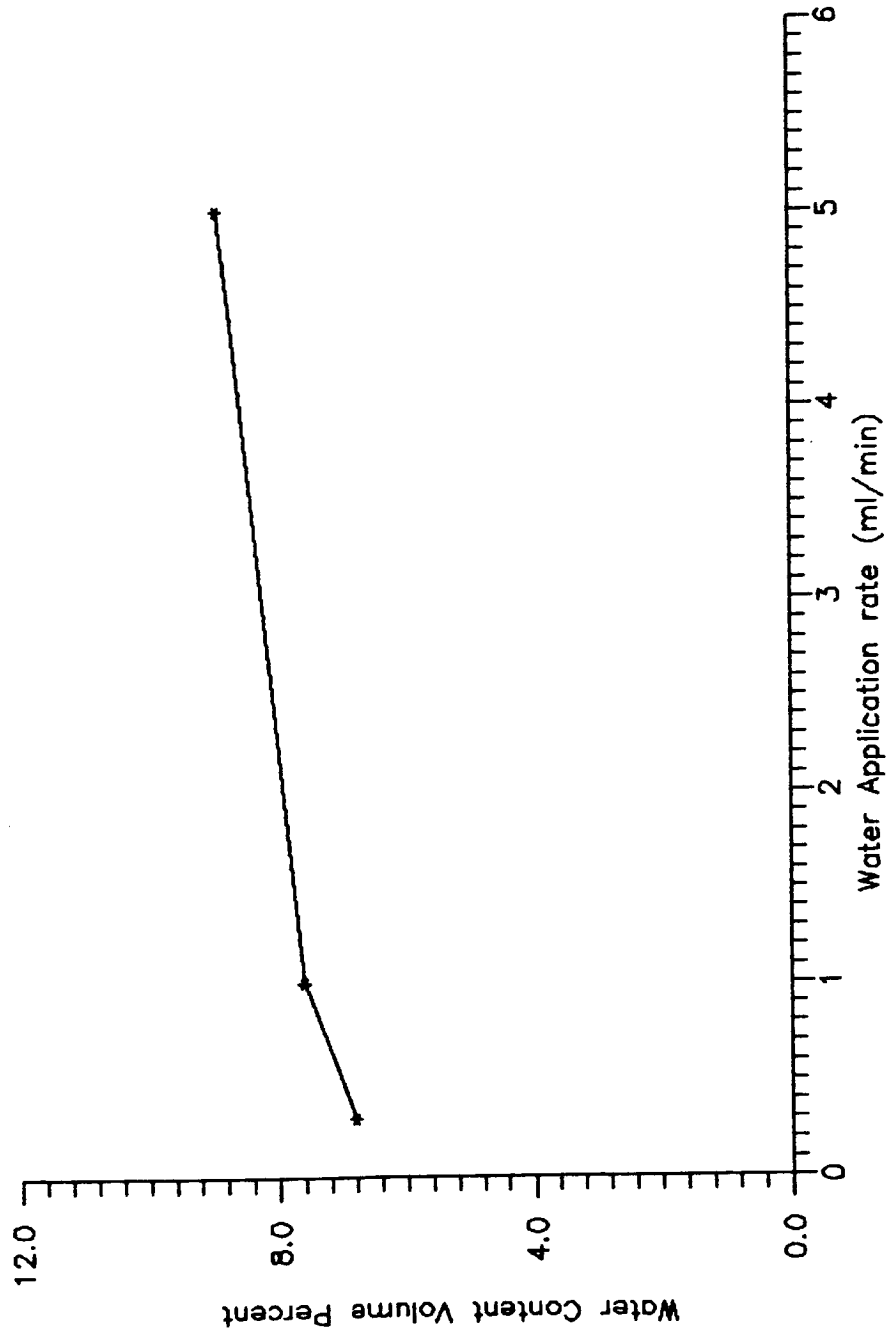

Figure 5.2 Water application rate versus water content derived from gamma ray measurements.

The partitioning rate of solute between the gas and liquid phases was simulated exactly the same way as it is handled in the case of sorption. The exchange volume is calculated using the following general equation which governs the rate process:

$$\text{Exchange Volume} = \frac{\rho/\emptyset \times K_w \times \text{delt}}{(\rho/\emptyset \times K_w \times K_+ - \text{delt})} \qquad (5.7)$$

The partition coefficient, K_w, was obtained from the literature. Kreamer (1982) stated the K_w's for SF6 and BCF to be 0.00806 cm^3/g and 0.22 cm^3/g, respectively. No data were available for F-22, so a value of 0.22 cm^3/g was assumed because, C/Co values for F-22 tests were not as high as the C/Co values found for SF6 even though comparable initial tracer concentrations were used.

As with the sorption process, the rate constant K_+ is unknown and the exchange volume must be found by a trial and error process of matching the computer simulation to the laboratory data.

Diffusion

In Rasmussen (1982), the process of matrix diffusion is incorporated into the DSC model. The term, matrix diffusion is used to describe the process by which water or solutes diffuse into the rock matrix. Matrix diffusion commonly occurs in fractured rock flow systems where water or solutes, flowing along a fracture, diffuse into the fracture walls. The process by which water or solutes diffuse into the rock matrix is governed by the same general equation (i.e., Fick's

second law) as gaseous diffusion. Therefore, gaseous diffusion can be handled by the model in much the same way as matrix diffusion.

Gaseous diffusion is incorporated into the DSC model by using an exchange process between neighboring gas cells. The simple mixing cell approach is used to model the exchange between the gas cells. The DSC model is linked to diffusion by use of the exchange volume and is mathematically expressed by Equation 5.8.

$$\underset{\text{Volume}}{\text{Exchange}} = D' \times \text{delt} \;/\; (\text{delx})^2 \qquad (5.8)$$

where

D' = effective diffusion coefficient,

delt = time step, and

delx = distance across unit cell.

For this study a simplified value for effective diffusion coefficient was employed (equation. 5.9).

$$D' = D_{ab}\, t'\, \emptyset_d \qquad (5.9)$$

where

D_{ab} = diffusion coefficient for the tracer into air,

t' = tortuosity factor, and

$\emptyset_d$ = drained porosity.

The diffusion coefficient for the solute into air is calculated using the equation derived by Slattery and Bird (1958) (see Chapter 2 pg 19).

Free-air diffusion coefficients calculated for the three tracers are presented in Table 5.1.

Table 5.1 Summary of free-air diffusion coefficients for the tracers used in the column tracer tests.

TRACER	$D_{ab}(cm^2/sec)$
BCF	0.092
SF6	0.107
F-22	0.089

The tortuosity factor was calculated by averaging the values obtained using the equations listed in Table 2.1 for wetted soils. A value of .33 was obtained using this method.

Drained porosity was calculated using the results of the gamma ray technique. Table 5.2 summarizes the drained porosity values for each water application rate.

Table 5.2 Summary of drained porosity values obtained using the gamma ray technique.

Water Application Rate	Water Content	Drained Porosity
5 ml/min	8.9%	33.3%
1 ml/min	7.6%	34.6%
0.206 ml/min	6.5%	35.7%
0.083 ml/min	6.3%	35.9%

With values for all the necessary parameters, computer modeling of the volatile tracer tests would be straight forward. The parameters needed for modeling are: water content, porosity, gaseous diffusion coefficient, volatilization coefficient, volatilization rate constant, sorption coefficient, and sorption rate constant. Unfortunately, there is never complete knowledge of all the necessary parameters. Therefore, if values for certain parameters are unknown, these variables must be estimated and re-estimated until the computer simulation results match the lab data.

CHAPTER 6

COMPUTER MODELING RESULTS

Computer simulations were performed for several of the column tests. Table 6.1 summarizes the tests that were modeled. Only results from the first sampling port (port 6) could be successfully simulated because the process of sampling affected the flow of tracer down the column. Therefore, the data acquired from ports 4 and 5 were not used.

Table 6.1 Summary of the column tests which were simulated using the DSC model.

Simulation #	Percolation Rate	Tracer
1	5 ml/min	BCF
2	1 ml/min	SF6
3	0.286 ml/min	SF6
4	0.083 ml/min	BCF
5	0.083 ml/min	F-22

Input parameters used in the DSC model are:

- o volume of water cell,
- o volume of gas cell,
- o volume of solid cell,
- o exchange volume (RI) between gas-liquid,
- o RI between solid - liquid,
- o RI for gaseous diffusion,
- o initial tracer concentration of the liquid,
- o water application rate, and
- o water displacemnt velocity.

The parameters used in each test are presented in Table 6.2.

Table 6.2 Summary of the input parameters used in the 5 DSC simulations performed in this study.

	Simulation Number				
	1	2	3	4	5
Tracer	BCF	SF6	SF6	BCF	F-22
Volume of water cell(cc)	25.	13.1	6.27	2.41	2.41
Volume of gas cell(cc)	610.	16300.	16300.	15.3	15.2
Volume of solid cell(cc)	150.	150.	150.	150.	140.
RI gas-liquid	0.00151	0.041	0.1	0.9	0.08
RI solid-liquid	0.001	0.0001	0.01	0.88	0.35
RI diffusion	0.33	1.12	2.14	2.50	1.00
Initial tracer Conc. (ng/ul)	248.	206.68	175.	0.022	130.
Water application rate (ml/min)	5	1	.286	.083	.083
Measured water displacement velocity (cm/min)	.875	.339	.200	.149	.149
time step (min)	5	13.1	22	29.4	29

Analysis of Each Computer Simulation

Simulation Number 1

The first computer simulation presented is for the BCF test run at a fairly high application rate of 5 ml/min. In this experiment, the transport of BCF was dominated by advection. Results of the DSC model are shown in figures 6.1 and 6.2. Figure 6.1 shows the computer generated breakthrough curves for the BCF tracer in the liquid compared to the breakthrough curve for an idealized BCF tracer where there is no sorption or volatilzation. This idealized tracer represents the chloride ion breakthrough curve, which is the curve used to estimate the water displacement velocity. The only difference between these two

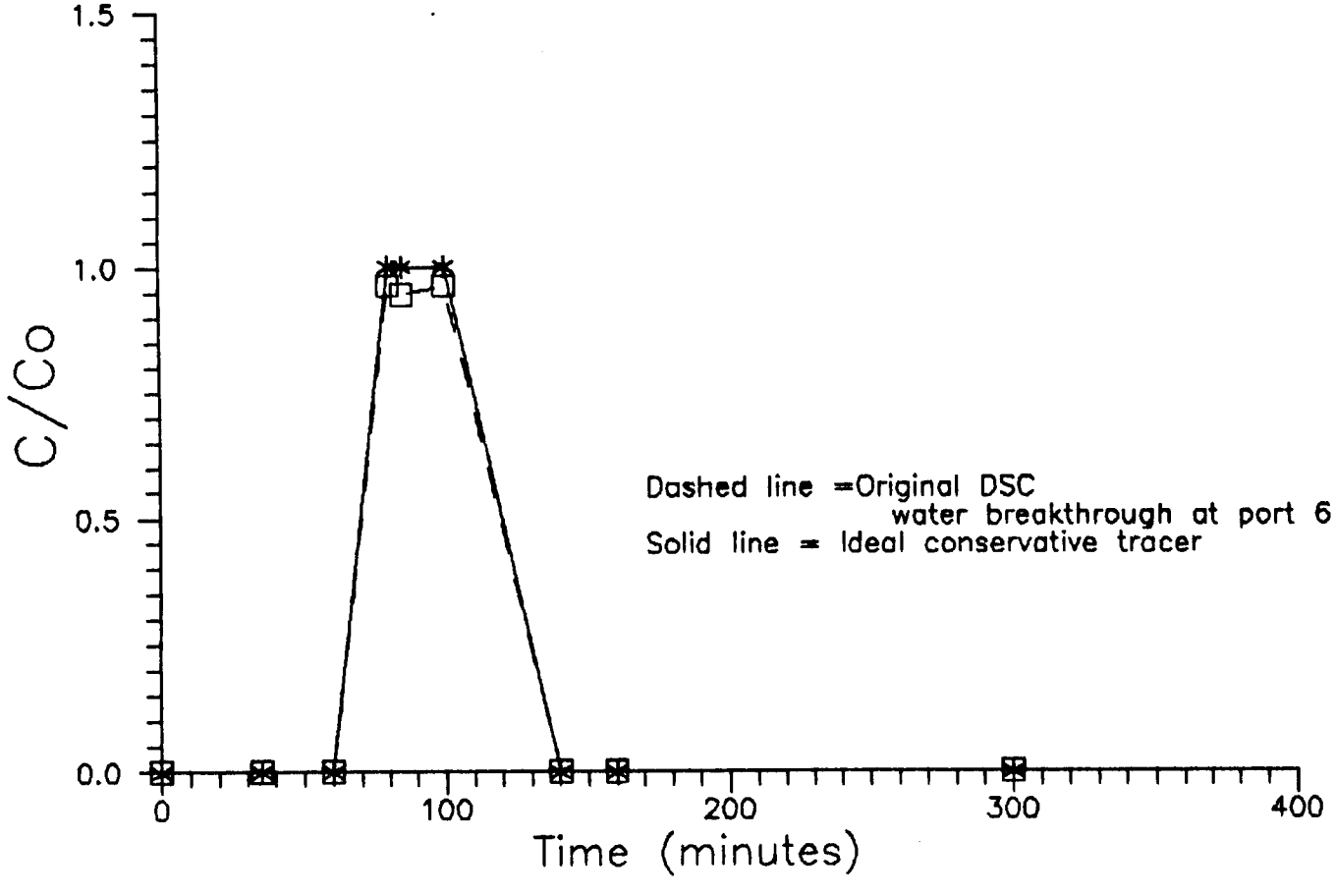

Figure 6.1 Computer simulated comparison of the BCF breakthrough curves for the original DSC test and the water breakthrough curve of an ideal conservative tracer.

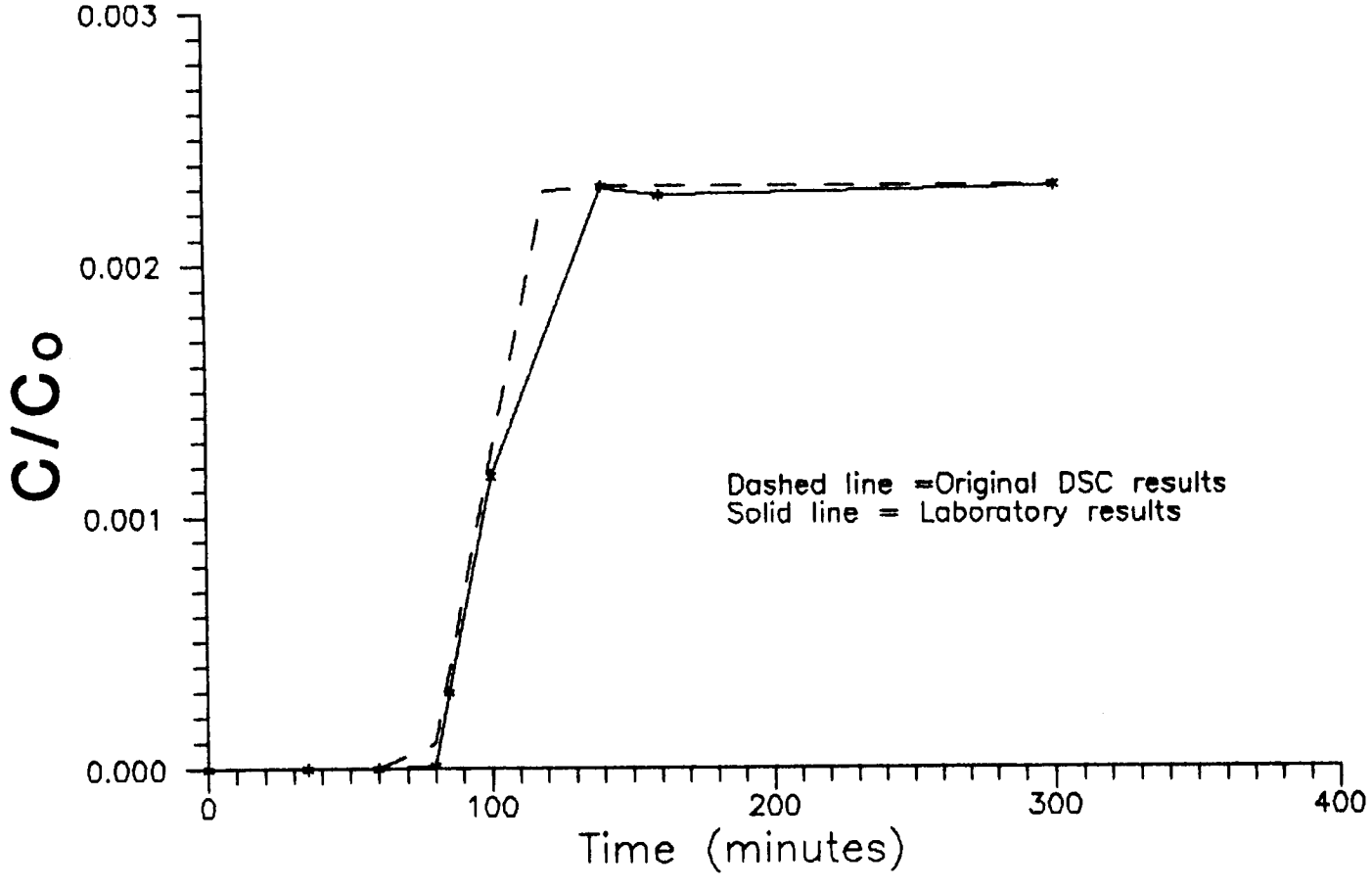

Figure 6.2 Gaseous breakthrough curves comparing the DSC results to that of the laboratory results for the BCF test run at a water application rate of 5 ml/min.

curves is a slight decrease in BCF concentration due to sorption and volatilization of the BCF tracer.

Figure 6.2 compares the computer generated breakthrough curve for BCF in the gas phase to the laboratory data. The two curves agree well, except that the laboratory data show a slightly steeper tracer front than the DSC results. Very steep tracer fronts are hard to simulate using the DSC because of numerical limitations. The tracer front generated by the computer model probably could have been steepened by decreasing the time step and increasing the number of cells used in the model.

The small values for the exchange volume (RI) imply that equilibrium is far from instantaneous. The rate constant calculated from Equation 5.5 is 5000 minutes for sorption and 3330 minutes for partitioning into the gas phase. From the very low RI value between the solid cell and the liquid cell it can be assumed that sorption is not a significant process in this test.

The influence of RI values on the breakthrough characteristics is shown in figure 6.3 through 6.8. In figure 6.3, the RI representing sorption was decreased by a factor of 100. This reduction did not change the DSC results. However, increasing the RI value by 100 (figure 6.4) drastically reduced the amount of tracer in the gas and flattened out the tracer front. Obviously, if a tracer sorbs very slowly onto the soil, little effect on the gaseous breakthrough curve will be noticed if the sorption rate is further decreased. But, if the sorption rate is increased on a very slow process, the effect on the breakthrough curve may be significant.

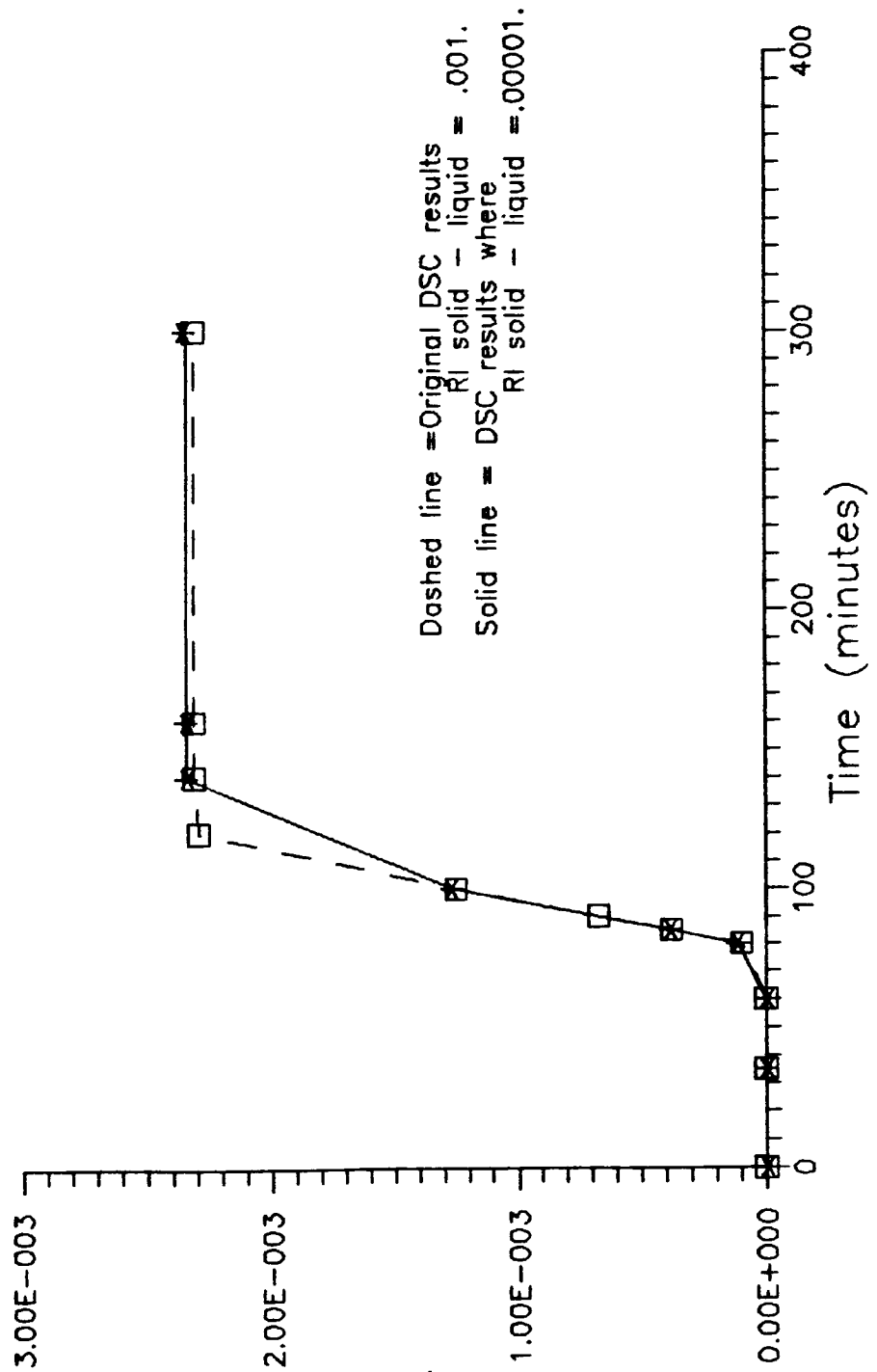

Figure 6.3 Comparison of the original DSC model which simulates the BCF test ran at a water application rate of 5 ml/min to the same DSC model with the RI between the solid and liquid cells decreased by a factor of 100 to 0.00001.

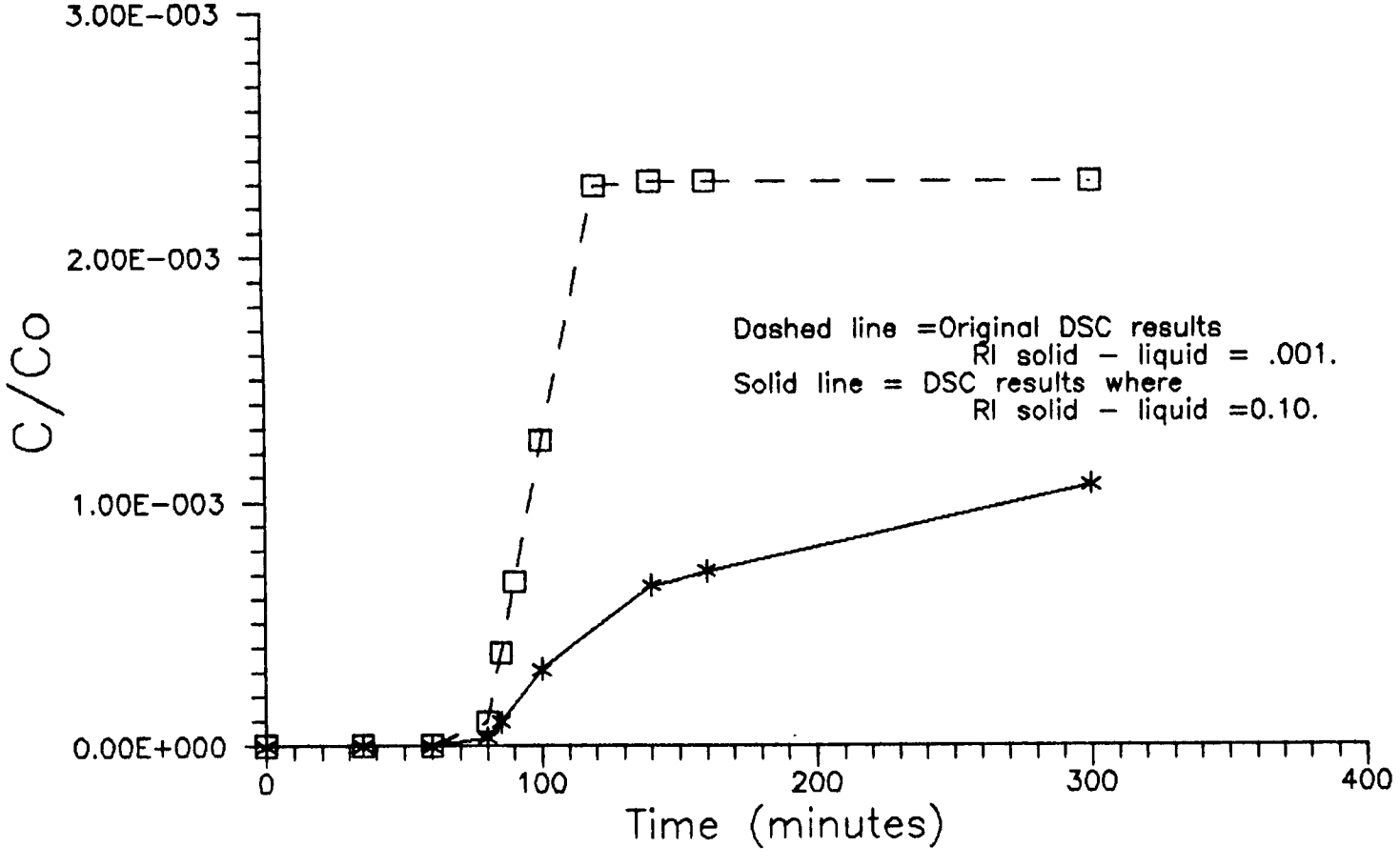

Figure 6.4 Comparison of the original DSC model which simulates the BCF test ran at a water application rate of 5 ml/min to the same DSC model with the RI between the solid and liquid cells increased by a factor of 100 to 0.10.

The RI value governing the process of volatilization is also small but any change in this value, either smaller or larger, results in significant changes in the DSC results (See figures 6.5 and 6.6). For this reason the RI value between liquid and gas is a crucial parameter when modeling tracer tests using the DSC model.

The process of gas diffusion is represented in the model by the RI value between neighboring gas cells. Figures 6.7 and 6.8 illustrate how the tracer concentration in the gas varies with changes in RI. Very little dependence is noted between the result and the RI value. Therefore, for this test, the diffusion coefficient does not need to be precisely known in order to apply the DSC model.

Partition coefficients dictate the size of the gas and solid cells. The variability of the DSC solution with changes in the partition coefficients is illustrated in figures 6.9 and 6.10. Figure 6.9 illustrates the changes in the tracer concentration with changes in the gas cell volume. When the volume is increased by 1000 the results of the model do not change at all. When the gas-liquid RI value is extremely small decreasing the value for K_W (increasing the gas cell volume) any further does not affect the results. However, if the volume of the gas cell is decreased by 1000 (figure 6.10) the results from the model change drastically. If the gas cell is the same size or significantly smaller than the water cell, the computer model simulates the situation where the tracer will quickly move back into the water phase after the tracer pulse has passed. Unfortunately, this is not what occurs in the soil gas environment. In fact, by making the gas volume smaller than the water volume one is actually saying that the

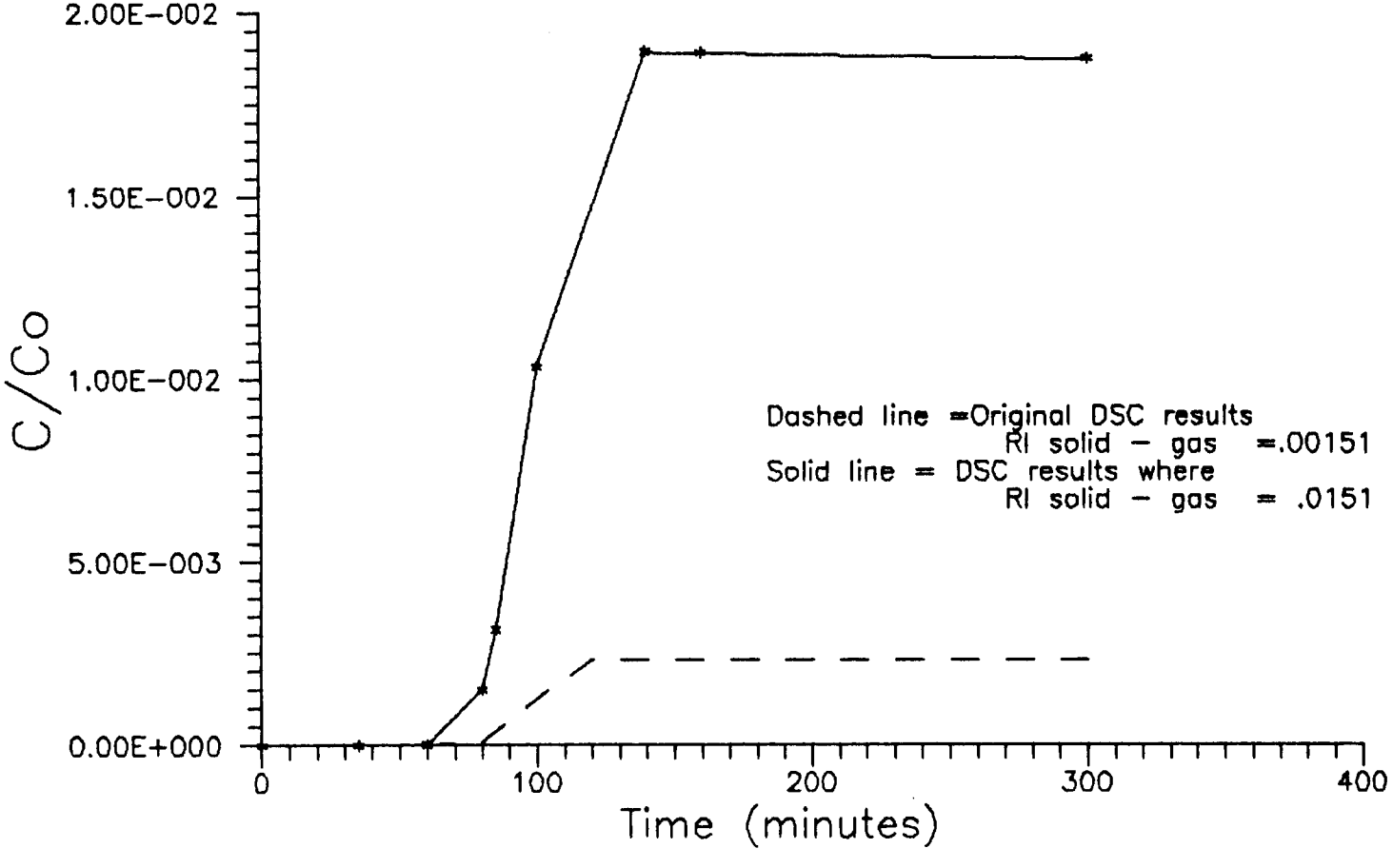

Figure 6.5 Comparison of the original DSC model which simulates the BCF test ran at a water application rate of 5 ml/min to the same DSC model with the RI between the liquid and gas cells increased by a factor of ten to 0.015.

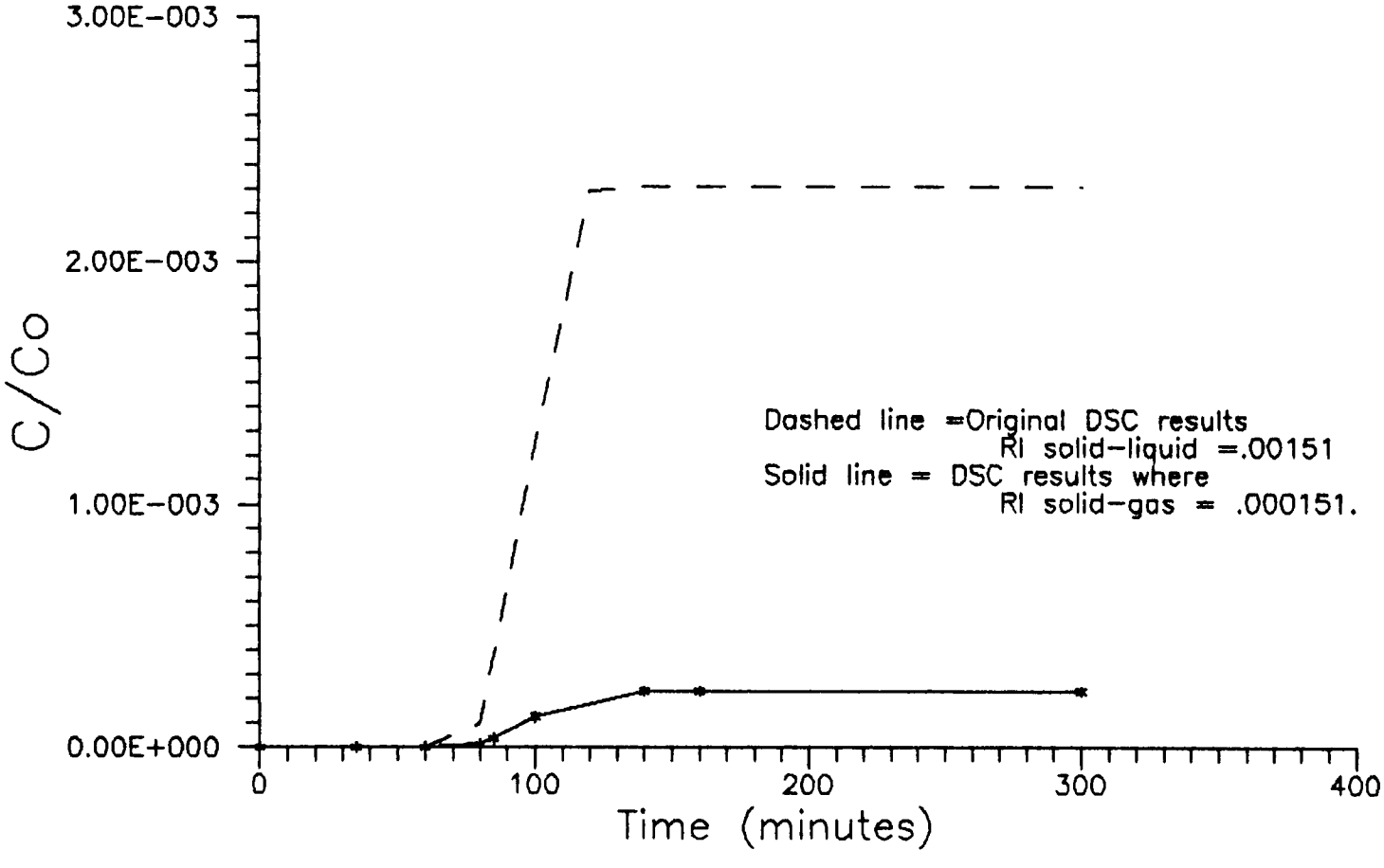

Figure 6.6 Comparison of the original DSC model which simulates the BCF test ran at a water application rate of 5 ml/min to the same DSC model with the RI between the liquid and gas cells decreased by a factor of ten to 0.00015.

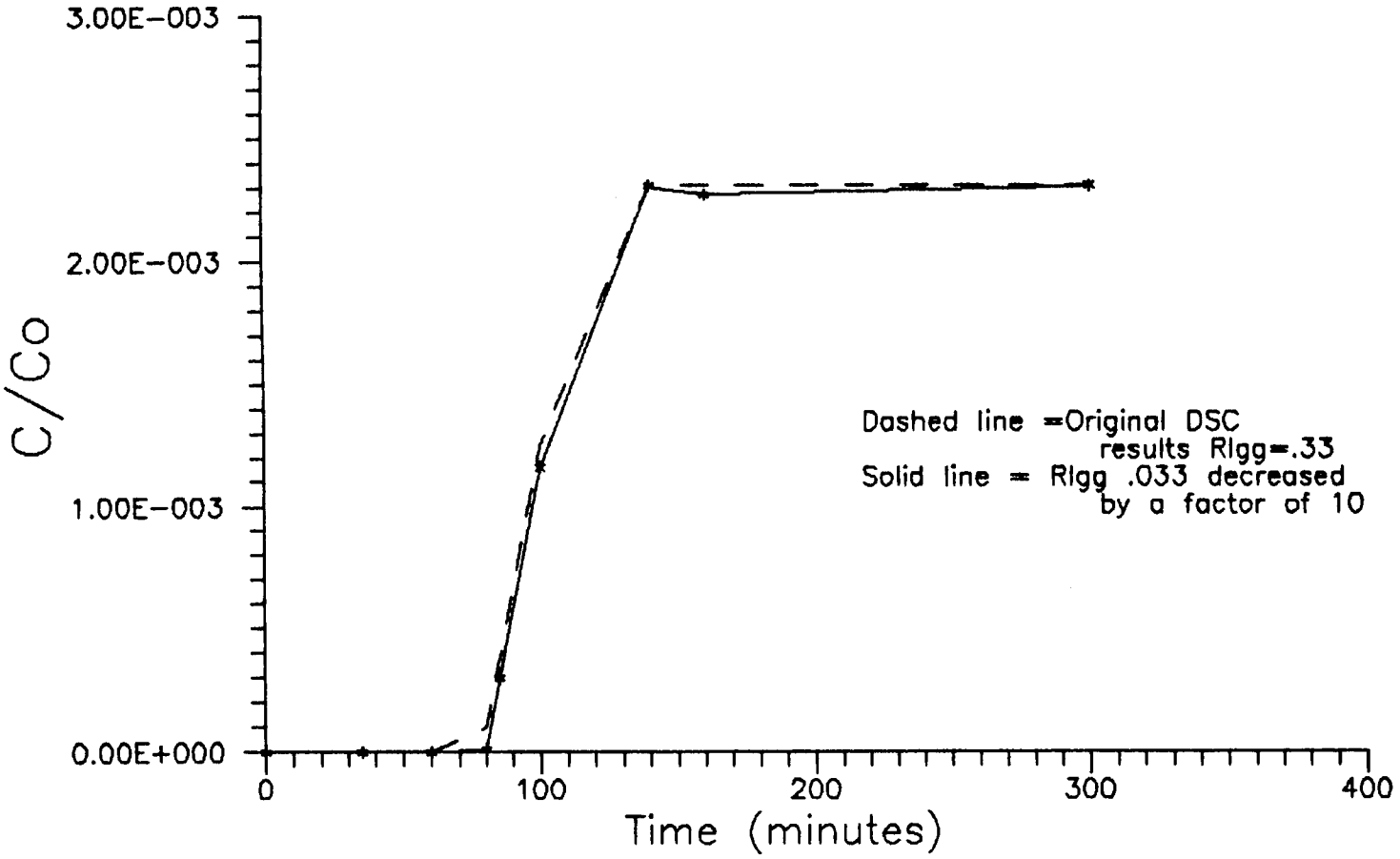

Figure 6.7 Comparison of the original DSC model which simulates the BCF test ran at a water application rate of 5 ml/min to the same DSC model with the RI between neighboring gas cells decreased by a factor of ten to 0.033.

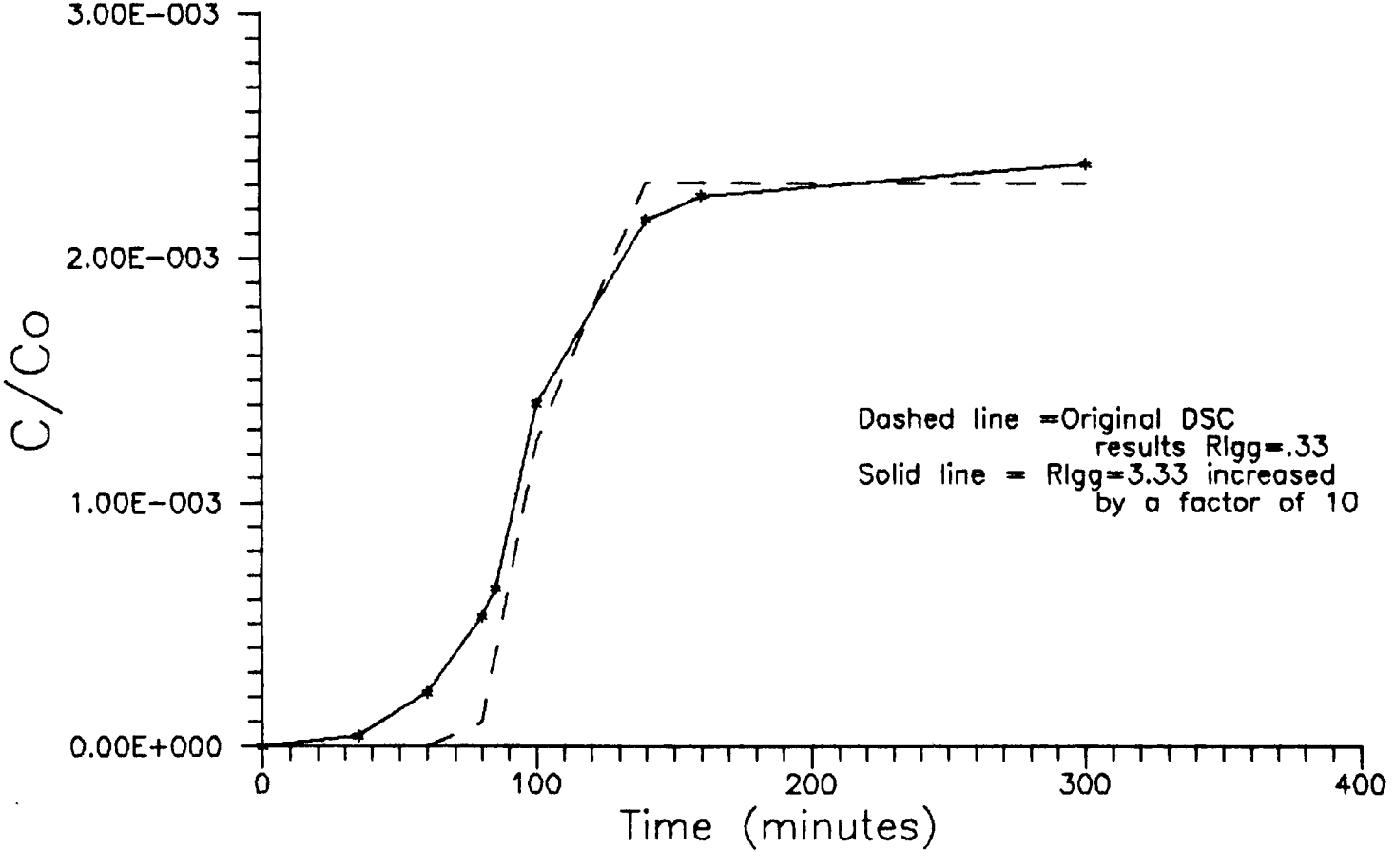

Figure 6.8 Comparison of the original DSC model which simulates the BCF test ran at a water application rate of 5 ml/min to the same DSC model with the RI between neighboring gas cells is increased by a factor of ten to 3.30.

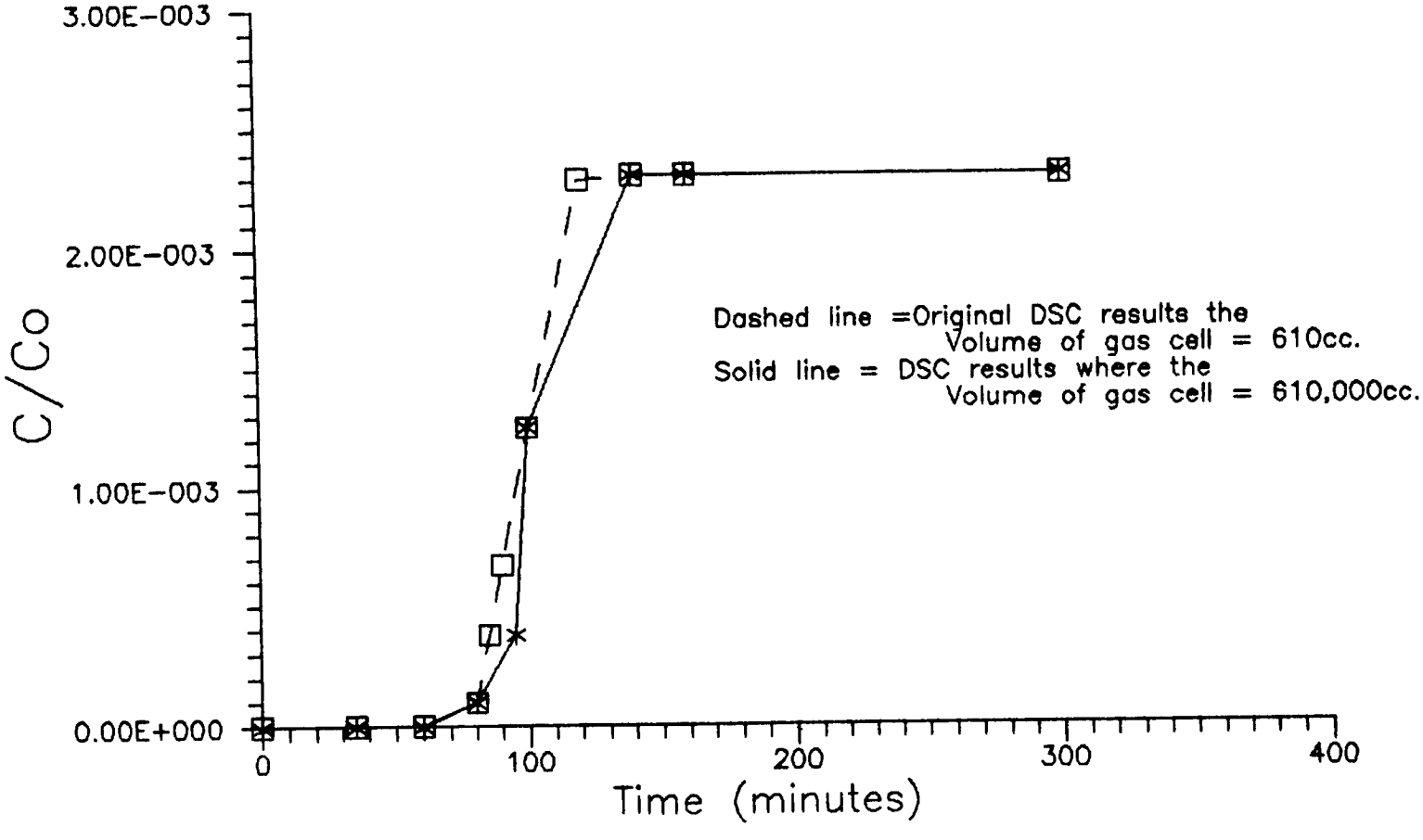

Figure 6.9 Comparison of the original DSC model which simulates the BCF test ran at a water application rate of 5 ml/min to the same DSC model with the gas cell volume is is increased by a factor of 1000 to 610,000 cc.

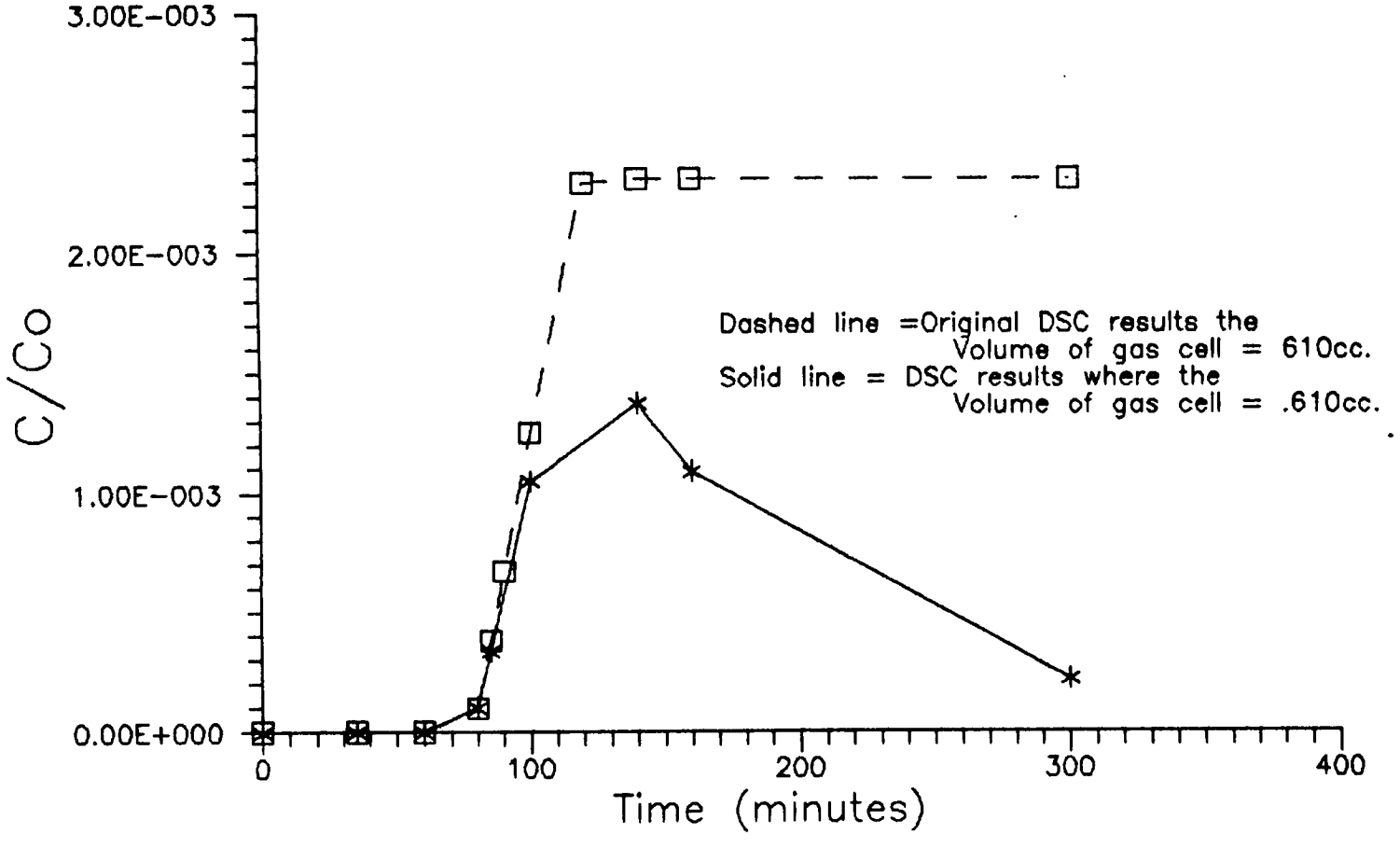

Figure 6.10 Comparison of the original DSC model which simulates the BCF test ran at a water application rate of 5 ml/min to the same DSC model with the gas cell volume is decreased by a factor of 1000 to 0.610 cc.

tracer trends toward dissolution in the liquid state rather than being dissolved in the gaseous state, which is not the case with fluorocarbons at room temperature.

Sorption is incorporated into the DSC model by variations in the solid cell volume. For this BCF test, the RI between the solid and liquid cells was so small that neither increasing nor decreasing the solid cell volume by a factor of 100 changed the model results.

The volume of the water cell used in the model relates to the water application rate and therefore is one of the parameters that is measured during a tracer test. This parameter is quite sensitive to error as seen in figures 6.11 and 6.12. When the volume of water is increased by a factor of ten, which is the same as increasing the water application rate from 5 to 7 ml/min, the DSC results change by almost on order of magnitude. Therefore, it is important to make sure the water application rate is accurately known.

If this method is applied in the field, the water displacement velocity may not be known, so it is important that the computer model be very sensitive to changes in the water velocity. For this simulation, the DSC results were not extremely sensitive to small changes in the water velocity. Figures 6.13 and 6.14 illustrate the model's sensitivity to increasing and decreasing the water velocity by 12 percent. The differences between the original model and the altered model are not significant enough to differentiate between data from the column tests run at the two different water displacement velocities. The low sensitivity is due to the fact that the steep tracer front seen in the laboratory data could not be simulated precisely enough to

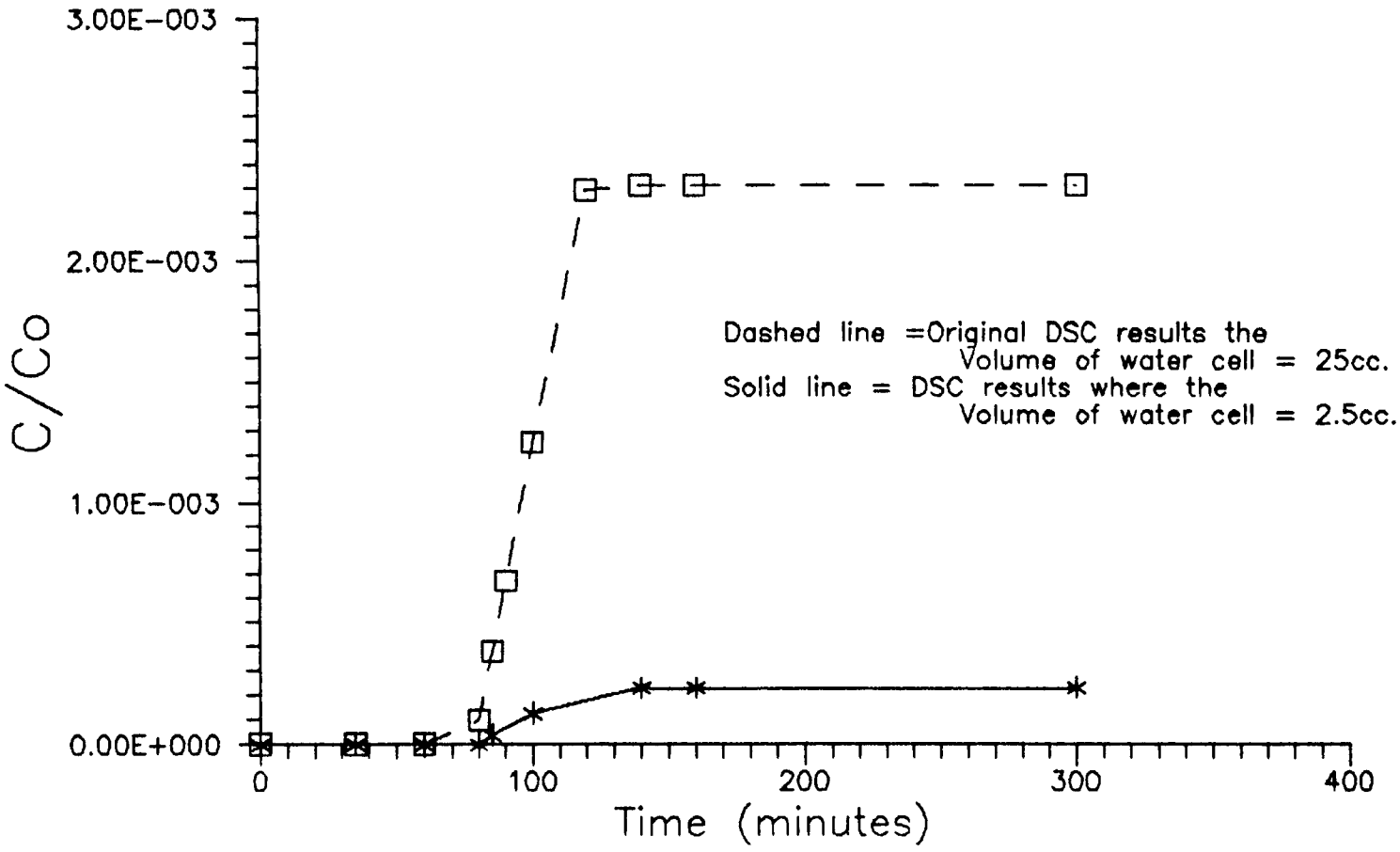

Figure 6.11 Comparison of the original DSC model which simulates the BCF test ran at a water application rate of 5 ml/min to the same DSC model with the water cell volume is decreased by a factor of ten to 2.5 cc.

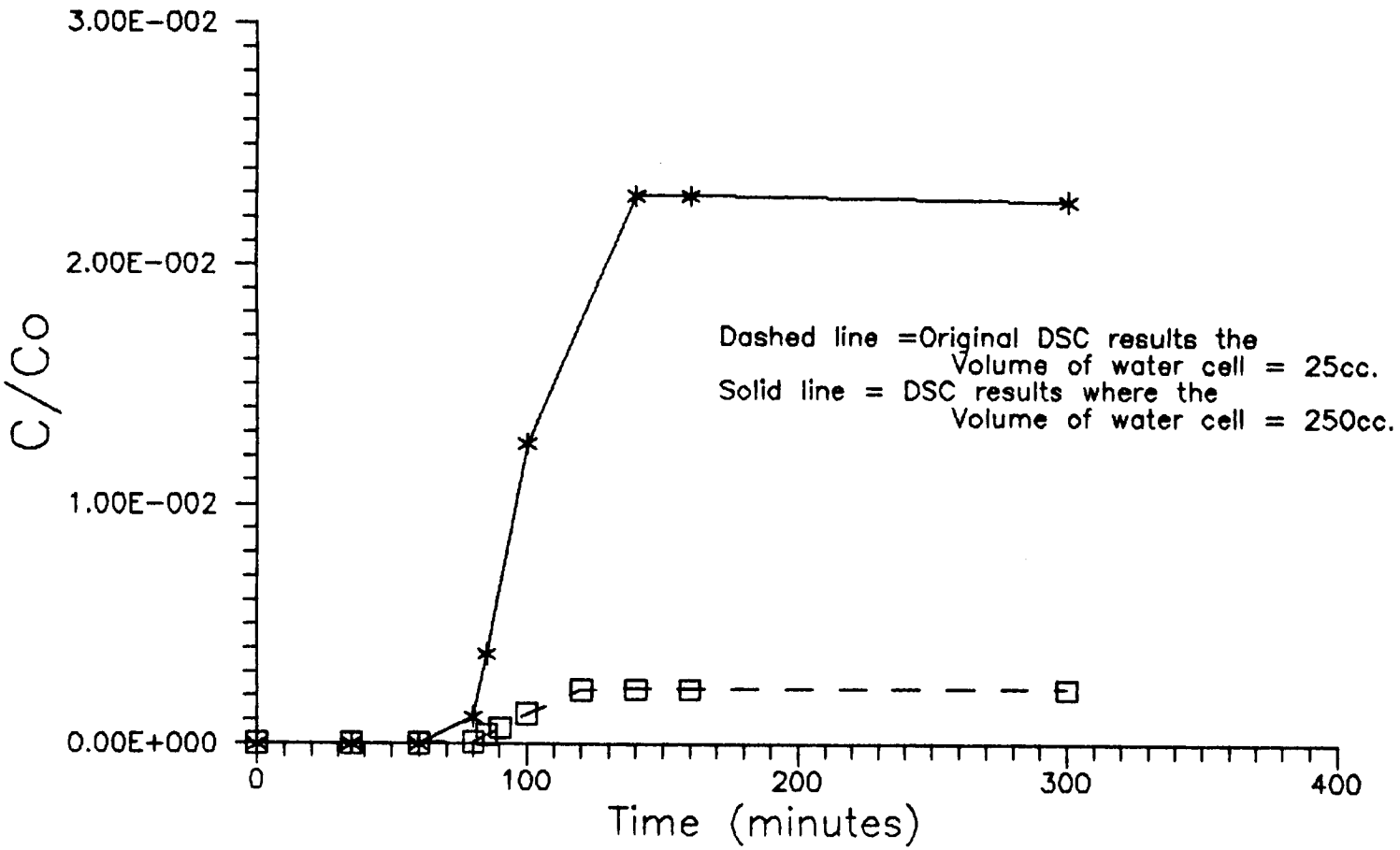

Figure 6.12 Comparison of the original DSC model which simulates the BCF test ran at a water application rate of 5 ml/min to the same DSC model with the water cell volume is increased by a factor of ten to 250 cc.

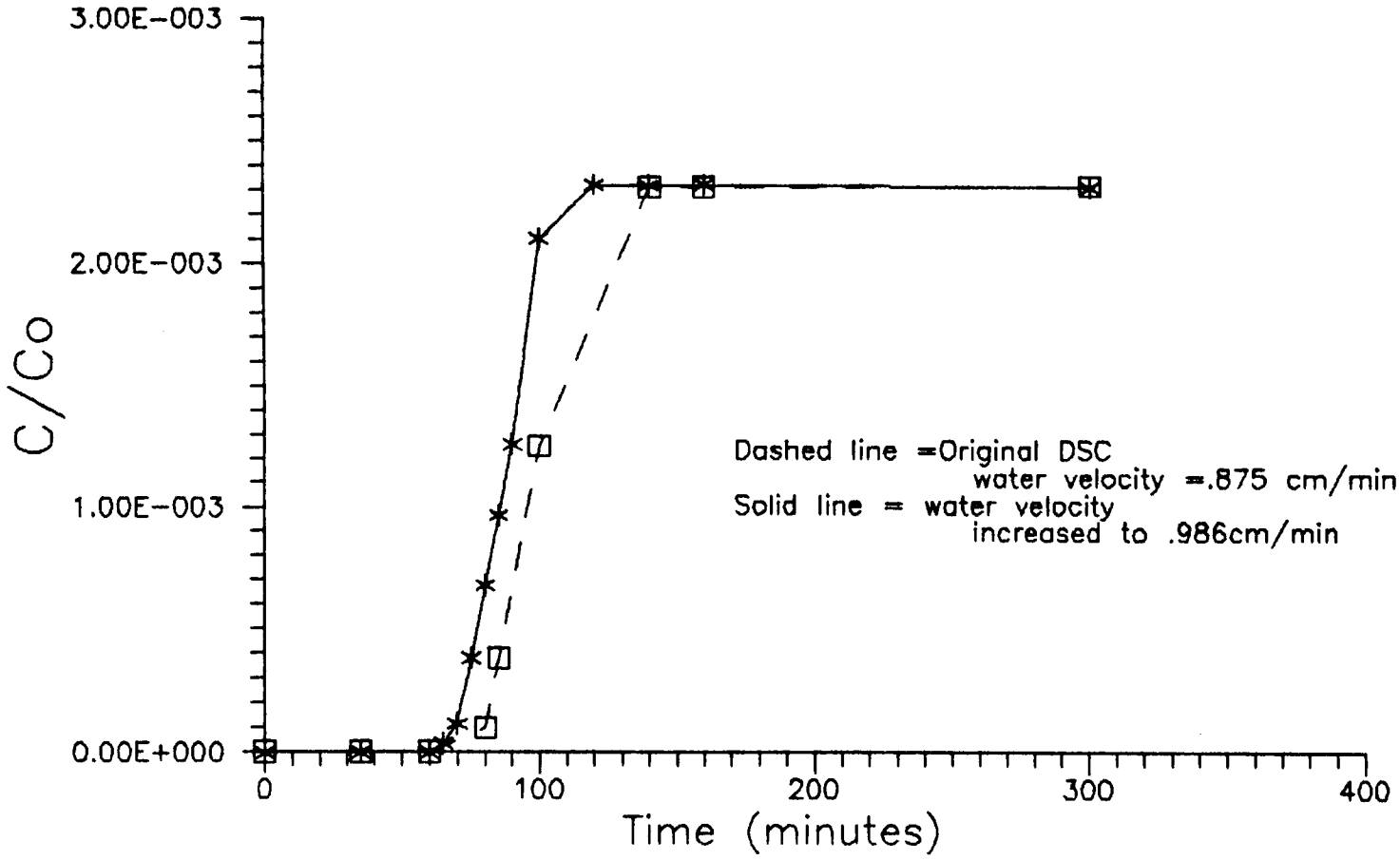

Figure 6.13 Comparison of the original DSC model which simulates the BCF test ran at a water application rate of 5 ml/min to the same DSC model with the water percolation rate increased by 12% to 0.986 cm/min.

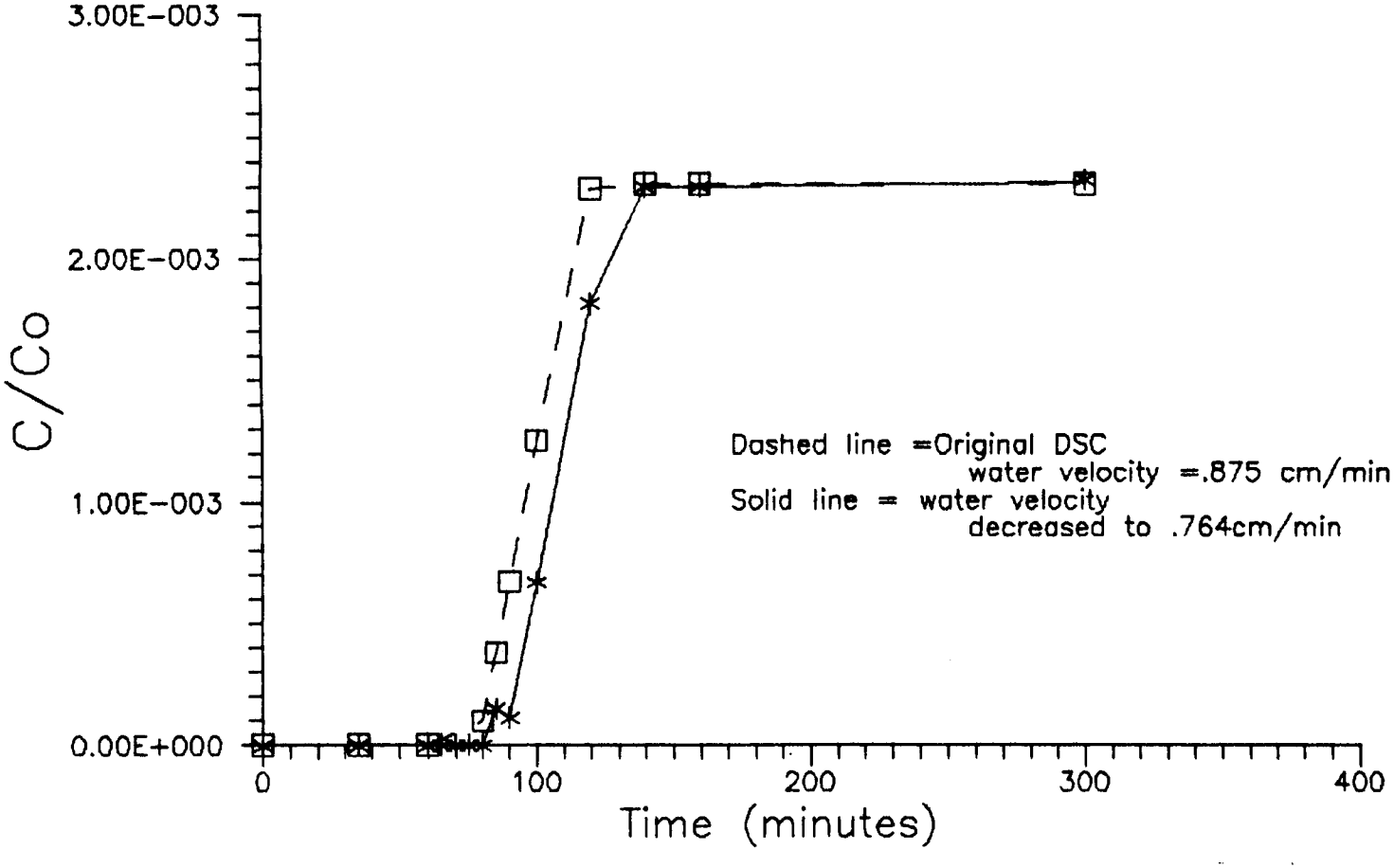

Figure 6.14 Comparison of the original DSC model which simulates the BCF test ran at a water application rate of 5 ml/min to the same DSC model with the water percolation rate decreased by 12% to 0.764 cm/min.

distinquish water travel times to within 12 percent. Fortunately, the laboratory gas breakthrough curve displays a sharp enough breakthrough front that the computer model is not needed to determine the water travel time.

Simulation Number 2

Test number 2 was run using SF6, the tracer found to be affected the most by diffusion. The results of the DSC simulation for this test are presented in figures 6.15 and 6.16.

The model parameters for this test are similar to those used for the BCF test except for the volume of the gas cell. The K_W for SF6 is more than 20 times smaller than for BCF and F-22. The small value for K_W required that the gas cell volume be extremely large (163000 cm^3). The combination of slow flow rate and high volatilization rate results in a significant decrease of tracer in solution compared with a conservative tracer (figure 6.15).

The DSC simulated data are consistent with the laboratory data as seen in figure 6.16. The tracer breakthrough front for the gas is not too steep to be simulated with accuracy by the DSC model. If this kind of a match were obtained for a field test, a value for water application rate could be confidently estimated.

The DSC results showed that sorption was not an important process involved with the transport of SF6. In fact, decreasing the RI value between liquid and solid cells to zero did not change the computer results.

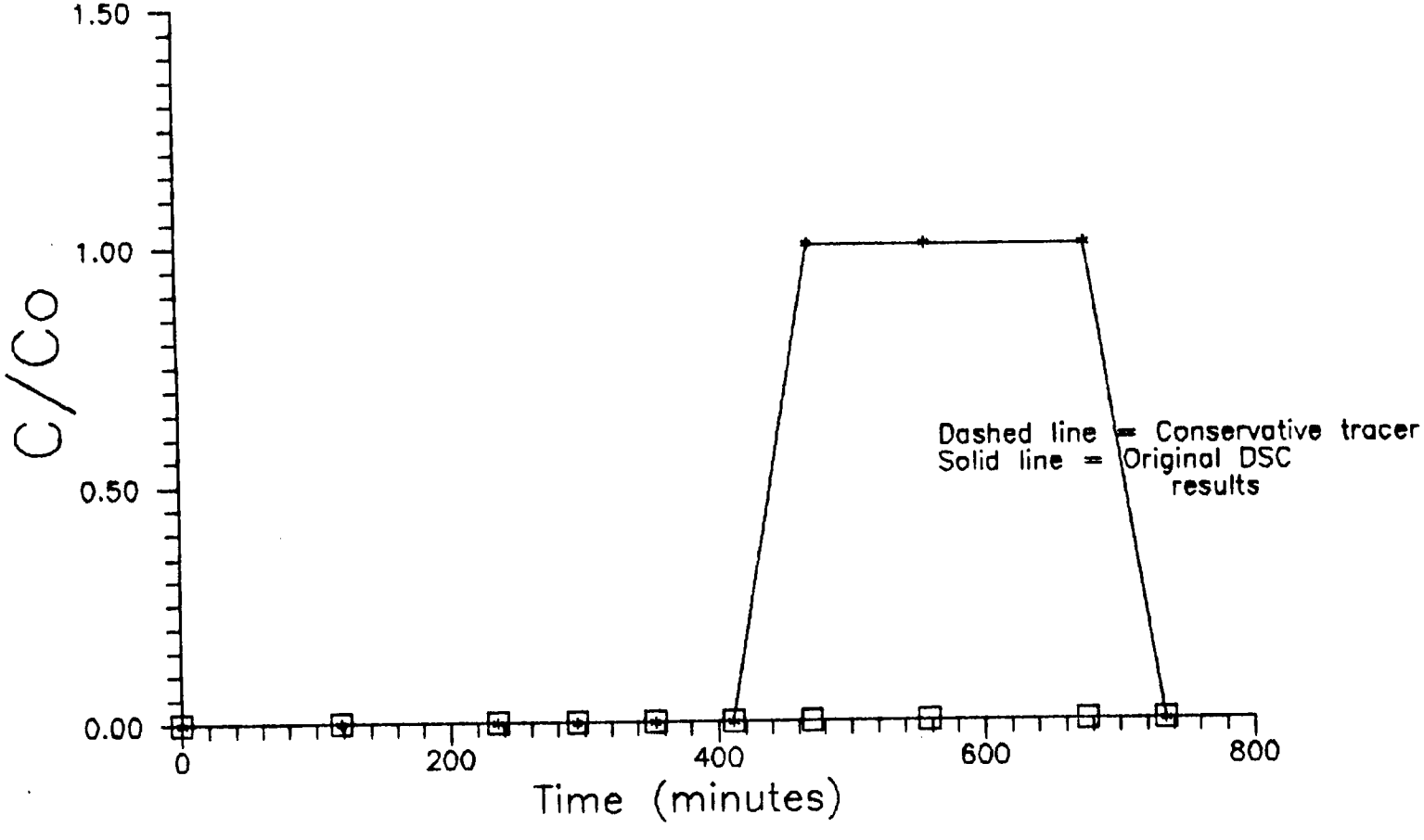

Figure 6.15 Water breakthrough curves comparing the DSC results to that of a conservative tracer for the SF6 test ran at a water application rate of 1ml/min.

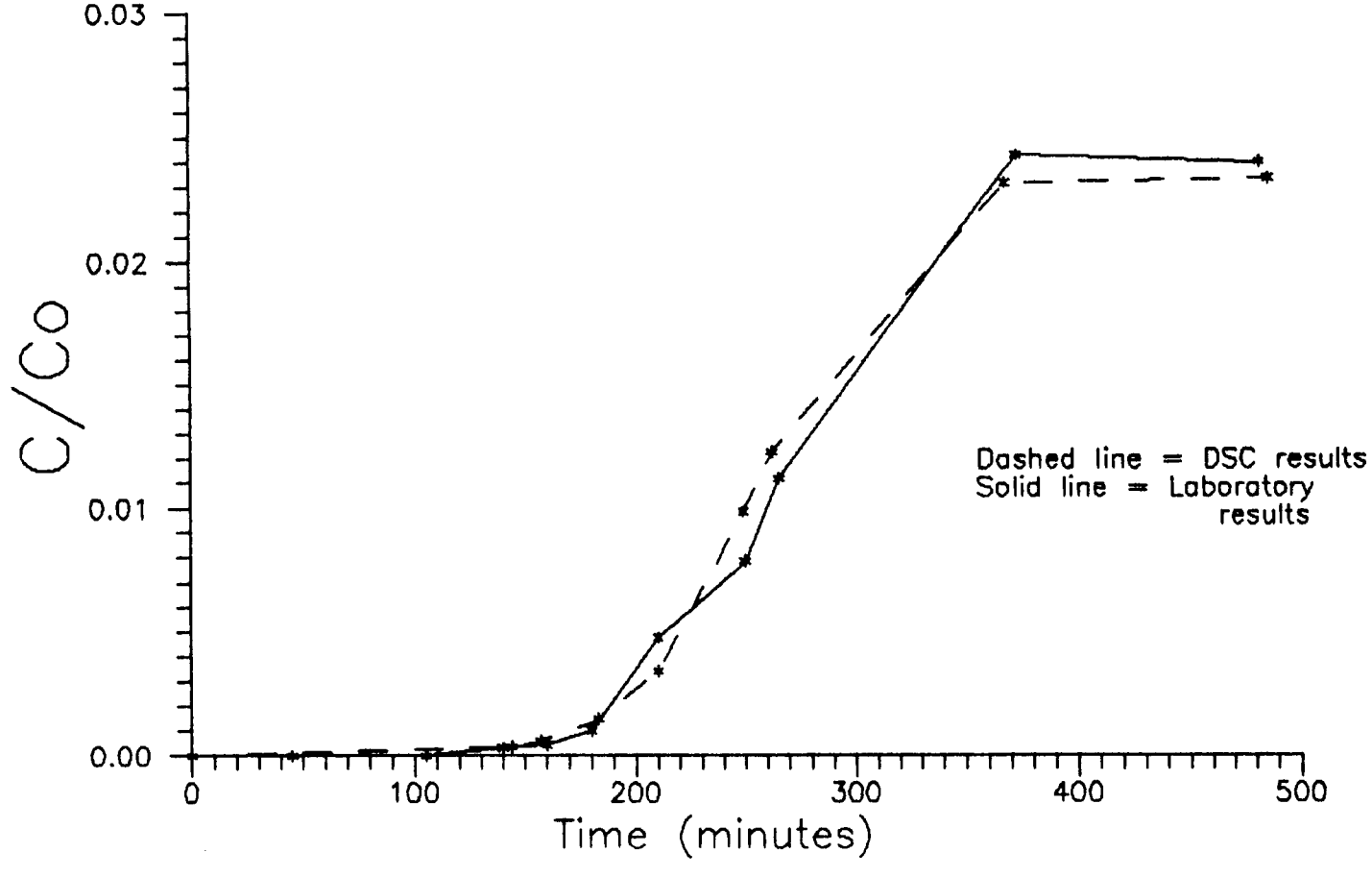

Figure 6.16 Gaseous breakthrough curves comparing the DSC results to the laboratory results for the SF6 test ran at a water application rate of 1 ml/min

The RI value between the liquid and gas cells can be used to calculate a rate constant, K_+, for the volatilization process. K_+ was determined to be 220 minutes.

Simulation Number 3

The water application rate for this simulation was 0.286 cm^3/min. The laboratory results of this test show a gradual increase in SF6 concentration and the breakthrough of SF6 occurring well before the breakthrough of chloride. Comparing the concentration of SF6 in the liquid with the concentration of a nonvolatile conservative equivalent shows that the actual SF6 concentration decreases by more than a factor of 10 compared to the ideal equivalent (figure 6.17).

The computer results for the breakthrough of gaseous tracer compare well with the laboratory data (figure 6.18).

Variations in the computer results with changes in input parameters are presented in figures 6.19 through 6.28. Significant changes in the shape of the breakthrough curves occur with small changes in most of the parameters. The values of RI factors are higher for this simulation than were used in the first simulation where we looked at variability of the model parameters.

Increasing the RI value for the liquid to gas partitioning by only a factor of 8 changes the shape of the breakthrough curve figure (6.19). The increase of the RI value to .8 causes an initial increase in gas concentration but the increase in partitioning soon leaves the concentration of the gas in the liquid so dilute that further partitioning is inhibited. Once the tracer has almost completely

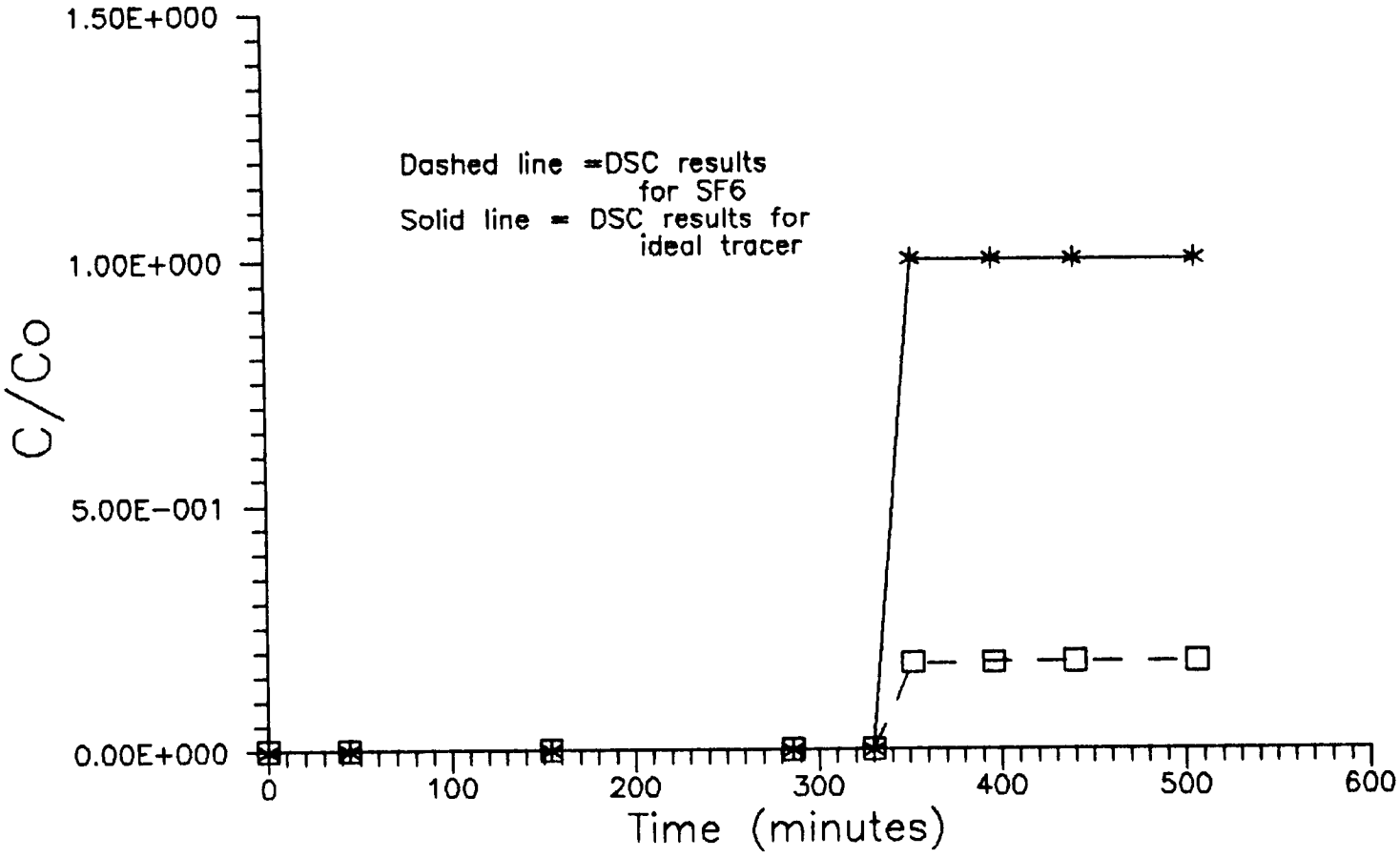

Figure 6.17 DSC water breakthrough curves for the SF6 test ran at 0.285 ml/min compared to water water breakthrough curve simulated for an ideal conservative tracer.

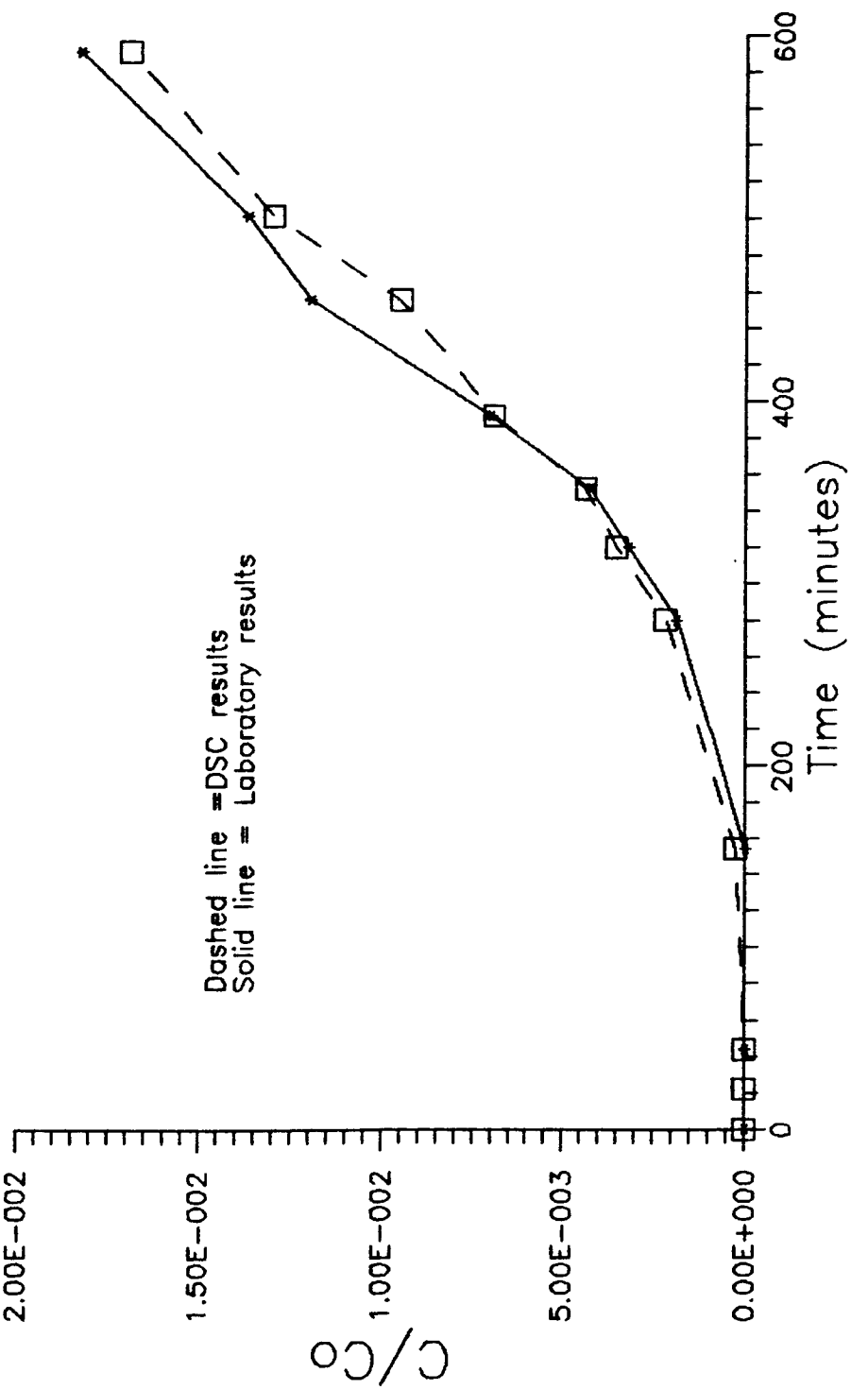

Figure 6.18 Comparison of the original DSC model which simulates the SF6 test ran at a water application rate of 0.285 ml/min to the laboratory results.

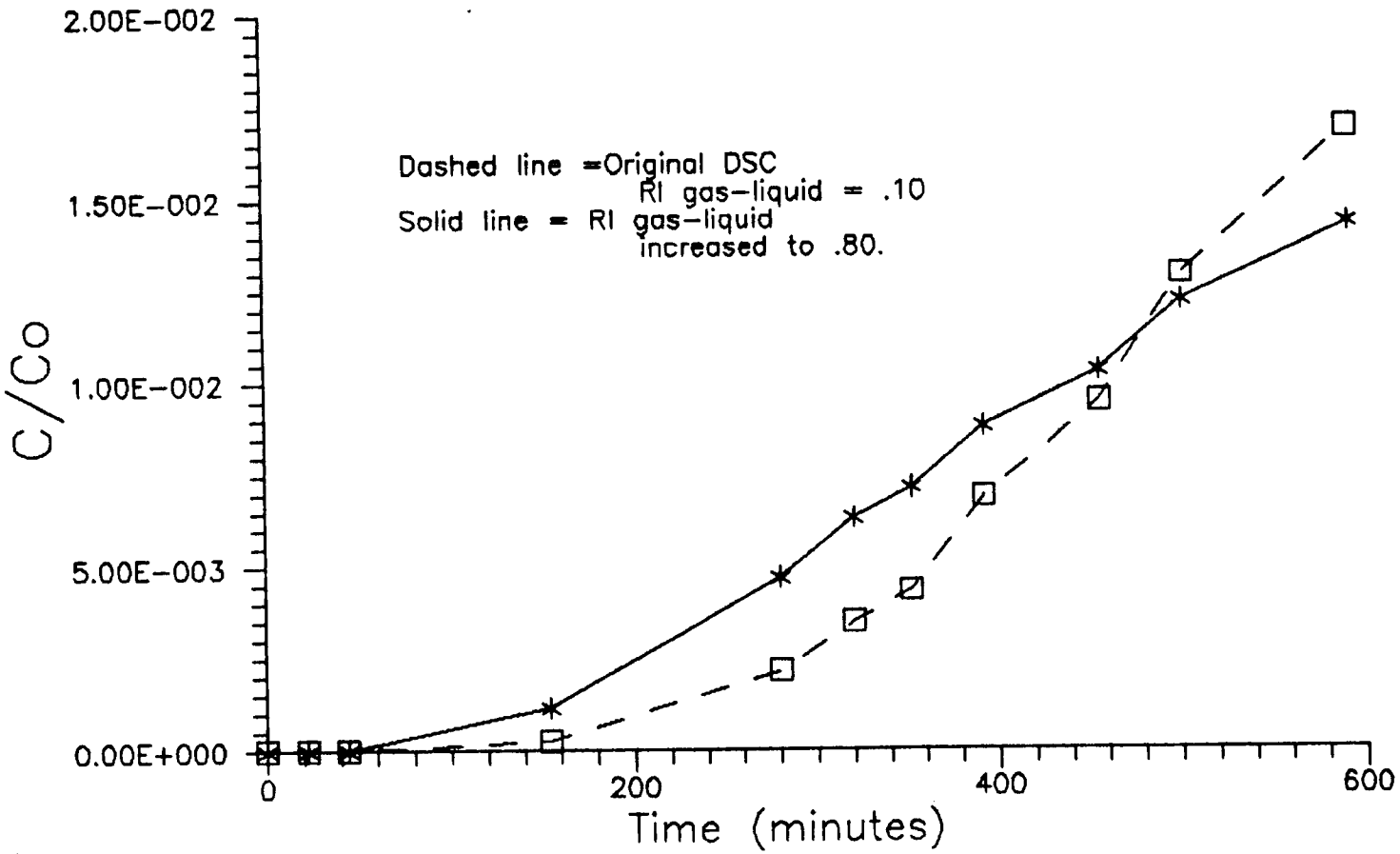

Figure 6.19 Comparison of the original DSC model which simulates the SF6 test ran at a water application rate of 0.285 ml/min to the same DSC model with the RI between the gas and liquid cells increased to 0.8.

volatilized out of solution, the rate of tracer increase in the gas phase slows down and a decrease in slope is observed.

Decreasing the rate of volatilization (decreasing the RI value between the gas and liquid as seen in figure 6.20) decreases the concentration of the tracer in the gas, but the original shape of the breakthrough curve stays the same.

The effect of changing the rate of sorption is shown in figure 6.21. Because SF6 does not exhibit high sorption, decreasing the RI value by 10 does not change the computer results at all. Increasing the sorption rate by the same factor has a more dramatic affect on the results. Figure 6.22 shows how the increase in RI causes an increase in gas concentration. As time increases the sorption effect becomes more important.

The effects of changing the gaseous diffusion coefficient are illustrated in figure 6.23 and 6.24. When the RI value from one gas cell to another gas cell is increased by a factor of two, the breakthrough of tracer in the gas occurs sooner and the concentration of tracer is greater than in the original DSC model. When the RI value is decreased by a factor of 10 from the original value, the breakthrough of tracer is correspondingly retarded. In fact, with small diffusion the breakthrough of the gas almost corresponds with the breakthrough of the simulated ideal tracer. This example illustrated that this technique will work best in estimating water travel times when the diffusion coefficient is very small.

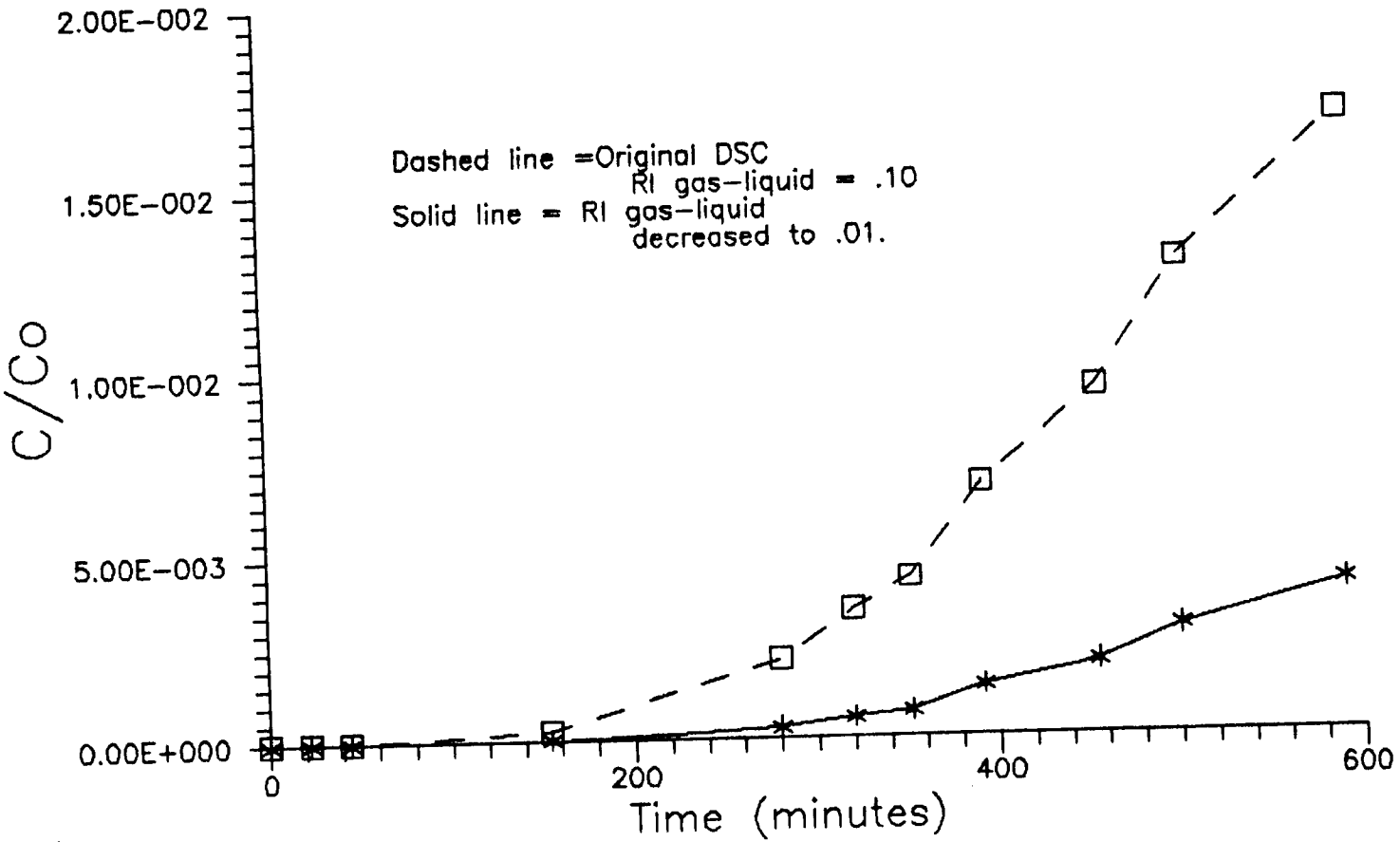

Figure 6.20 Comparison of the original DSC model which simulates the SF6 test ran at a water application rate of 0.285 ml/min to the same DSC model with the RI between the gas and liquid cells decreased to 0.01.

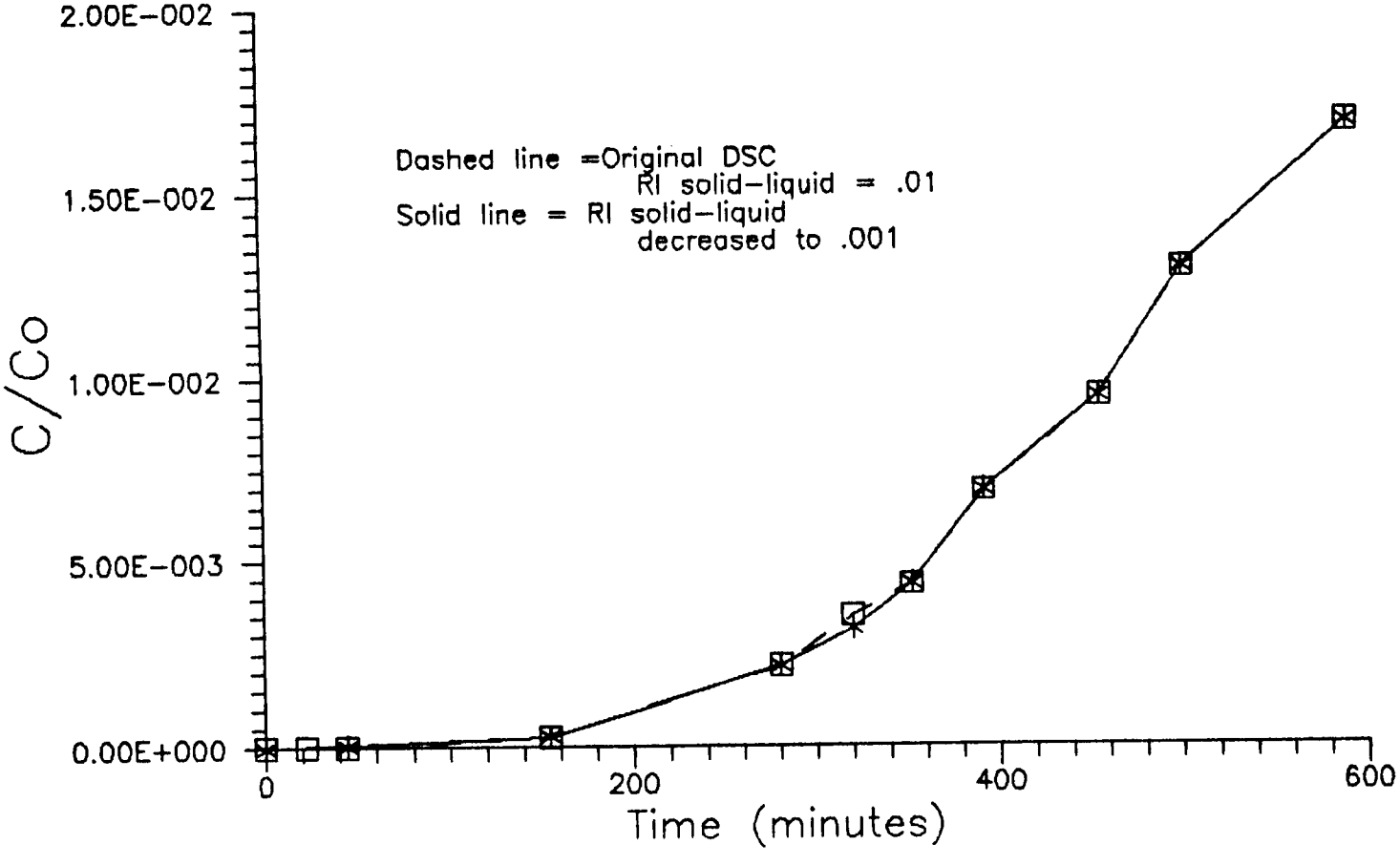

Figure 6.21 Comparison of the original DSC model which simulates the SF6 test ran at a water application rate of 0.285 ml/min to the same DSC model with the RI between the solid and liquid cells decreased by a factor of 10 to 0.001.

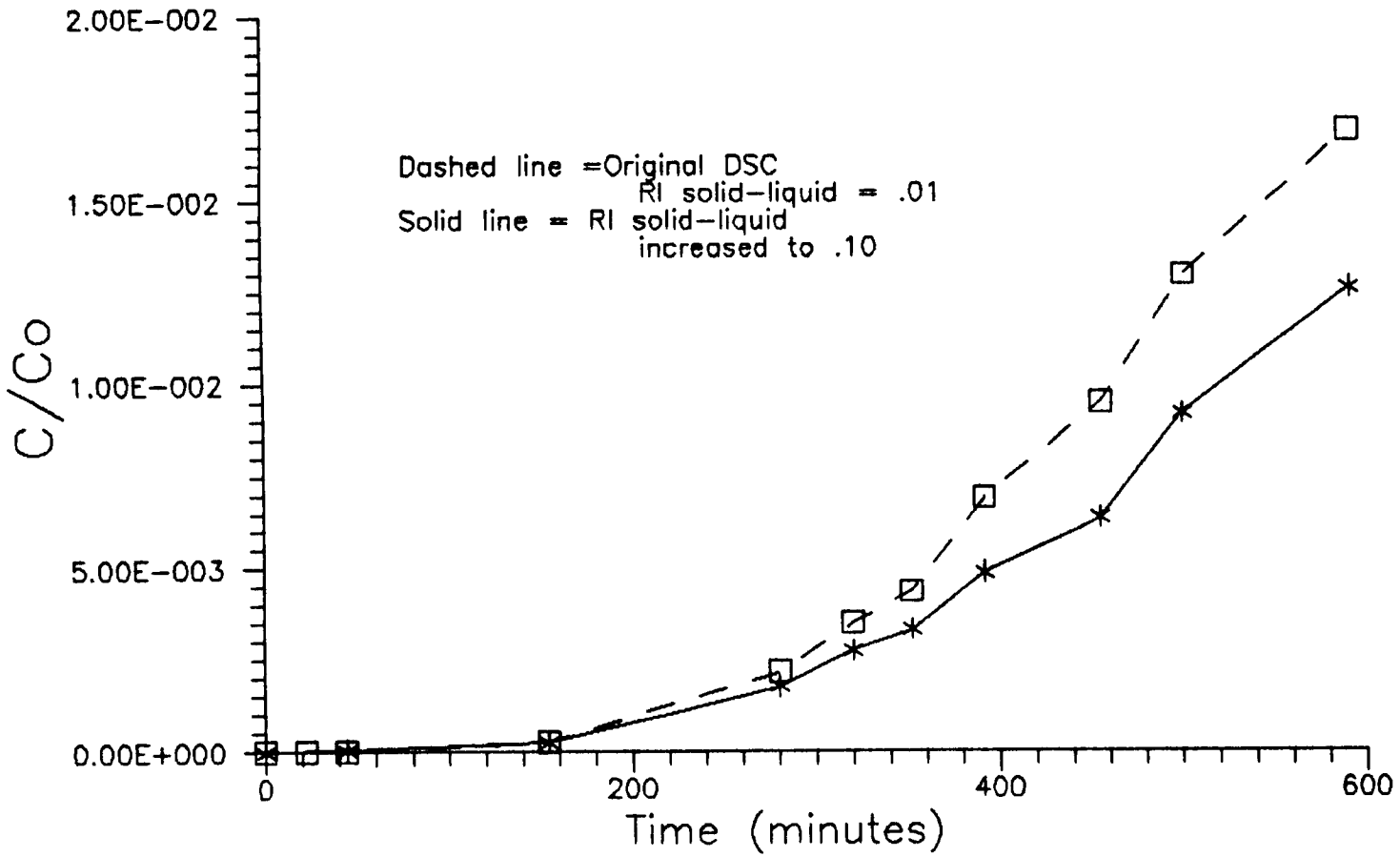

Figure 6.22 Comparison of the original DSC model which simulates the SF6 test ran at a water application rate of 0.285 ml/min to the same DSC model with the RI between the solid and liquid cells increased by a factor of 10 to 0.1.

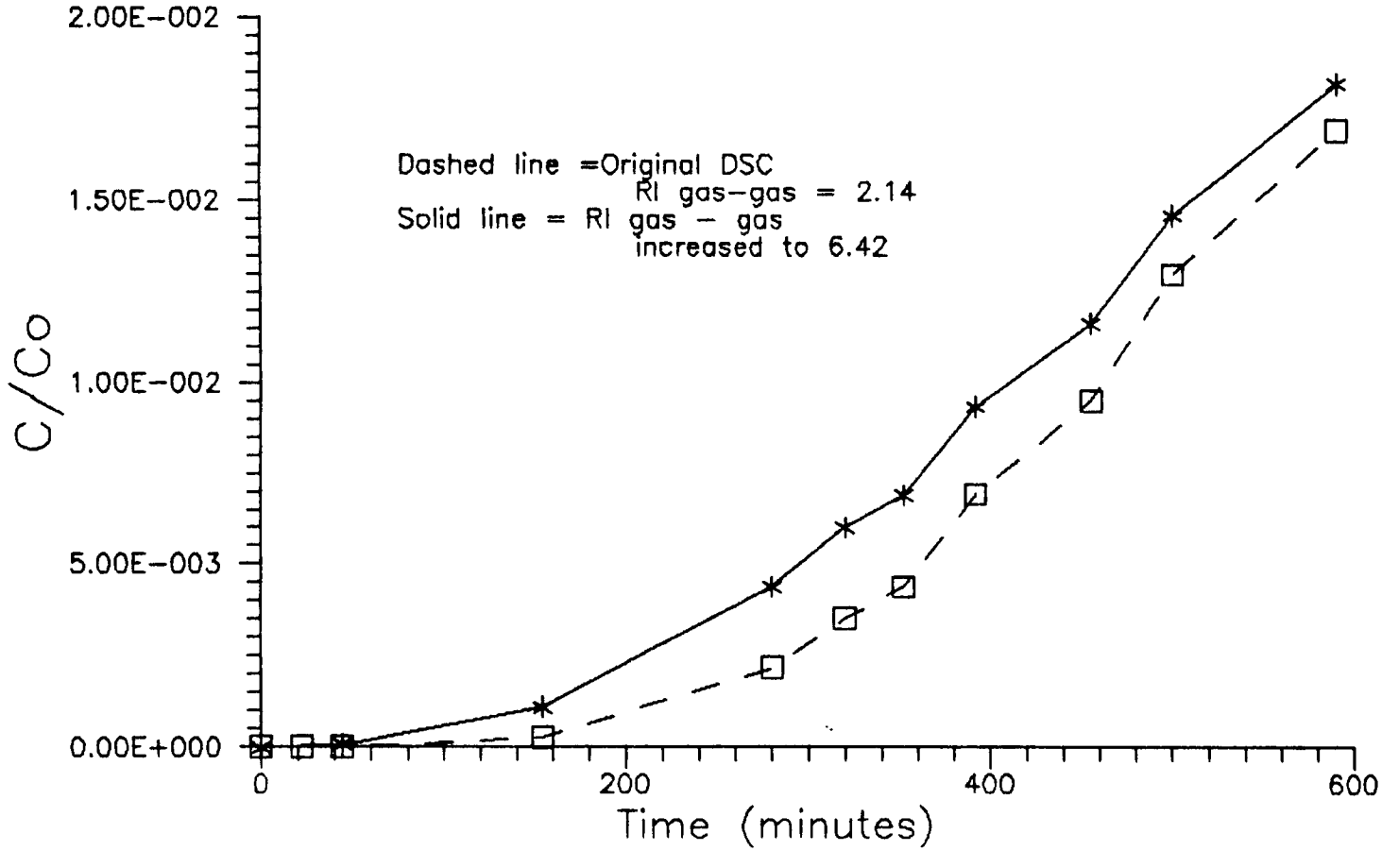

Figure 6.23 Comparison of the original DSC model which simulates the SF6 test ran at a water application rate of 0.285 ml/min to the same DSC model with the RI between neighboring gas cells is increased by a factor of 3 to 6.42.

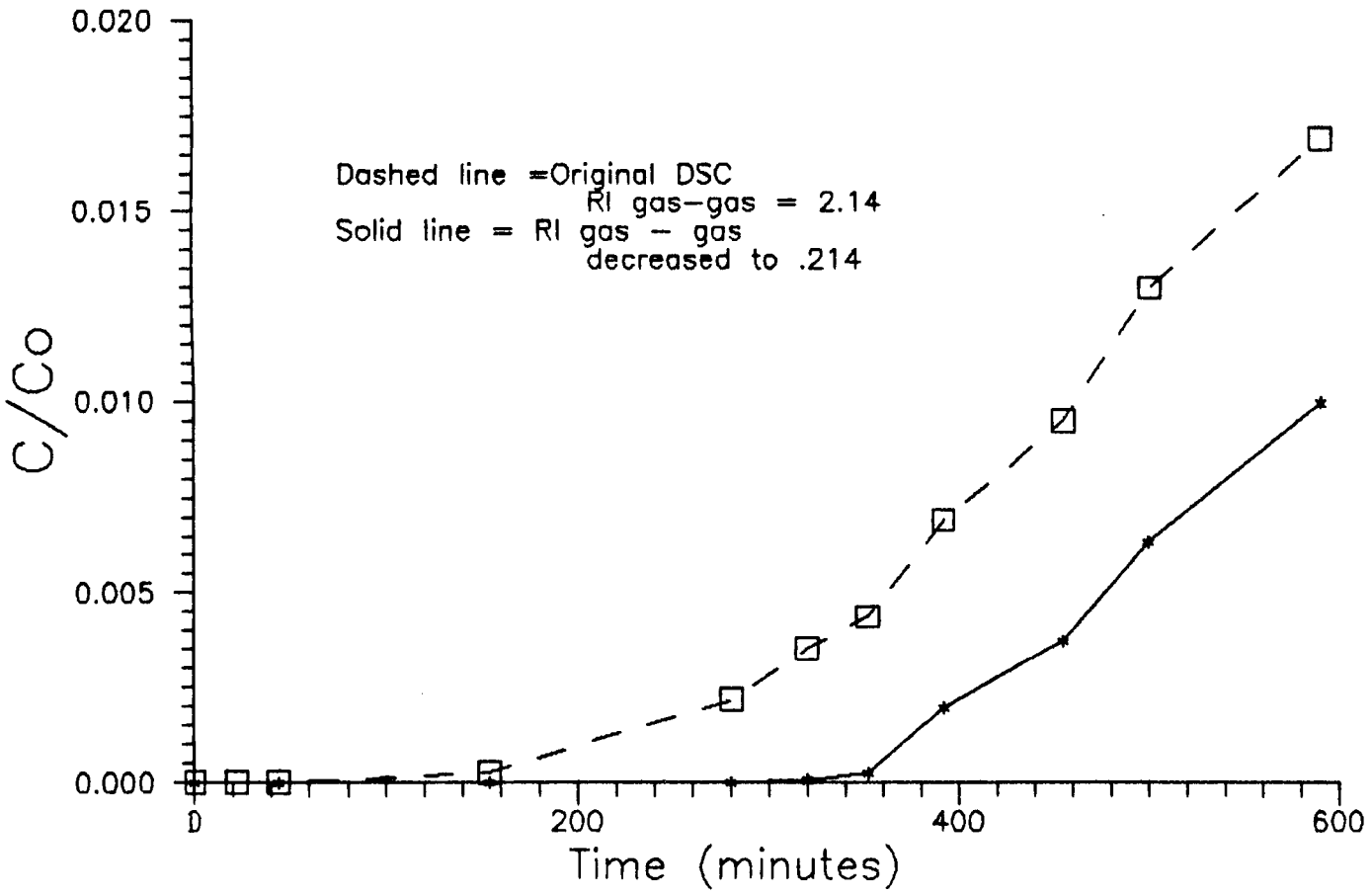

Figure 6.24 Comparison of the original DSC model which simulates the SF6 test ran at a water application rate of 0.285 ml/min to the same DSC model with the RI between neighboring gas cells is decreased by a factor of 10 to 0.214.

Chaging sorption distribution coefficients does not significantly alter the results of the DSC model (See figures 6.25 and 6.26). For this simulation, the sorption rate is slow enough over the period of the test that the size of the distribution coefficient, represented by the size of the solid cell, does not exert much influence on the outcome of the model.

Looking at how changes in the volume of the gas cell affects the results from the DSC model, it is evident that the size of the gas cell ($163000cm^3$) is so large that it dominates the process of volatilization. Figure 6.27 shows that when the volume of the gas cell is increased by a factor of1000 very little change in the concentration of gas occurs. If the gas cell volume is decreased by the same factor the concentration of tracer decreases only slightly, considering the large change in volume (figure 6.28).

Changes in the computer results with changes in water velocity are more pronounced for this lower flow rate than for the higher flow rate simulated in the BCF 5ml/min test. Figures 6.29 and 6.30 illustrate the changes in DSC results when the water velocity is increased or decreased by 12 percent.

When the model parameters used in the third simulation are compared with those used in the SF6 second simulation, an important trend can be observed. As the time step is increased all the RI values, or rate constants increase, implying that as the time frame of the model is expanded the processes of sorption and volatilization become closer to being instantaneous processes. This trend can also be seen in the BCF simulations.

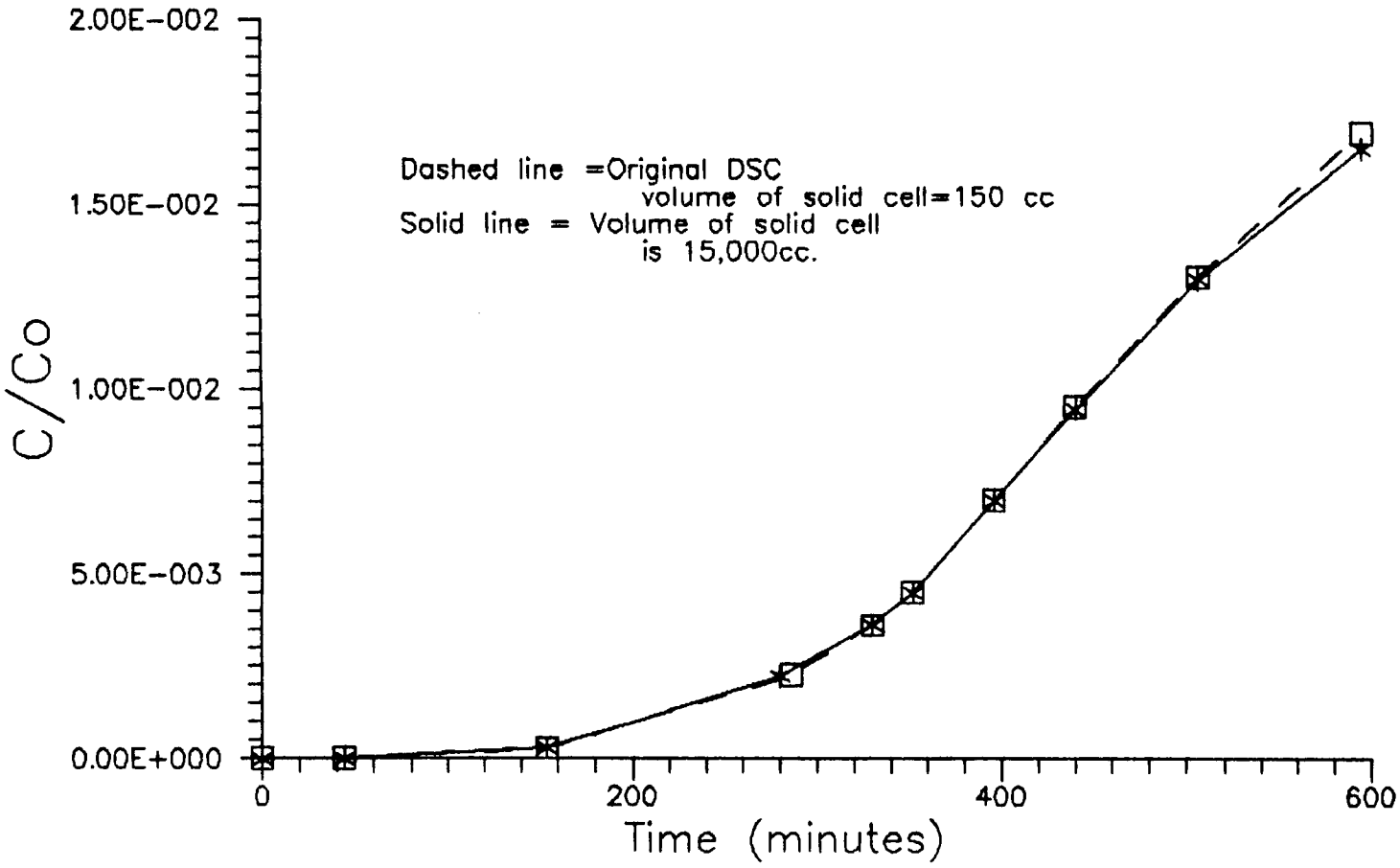

Figure 6.25 Comparison of the original DSC model which simulates the SF6 test ran at a water application rate of 0.285 ml/min to the same DSC model where the solid cell volume is increased by a factor of 100 to 15,000.

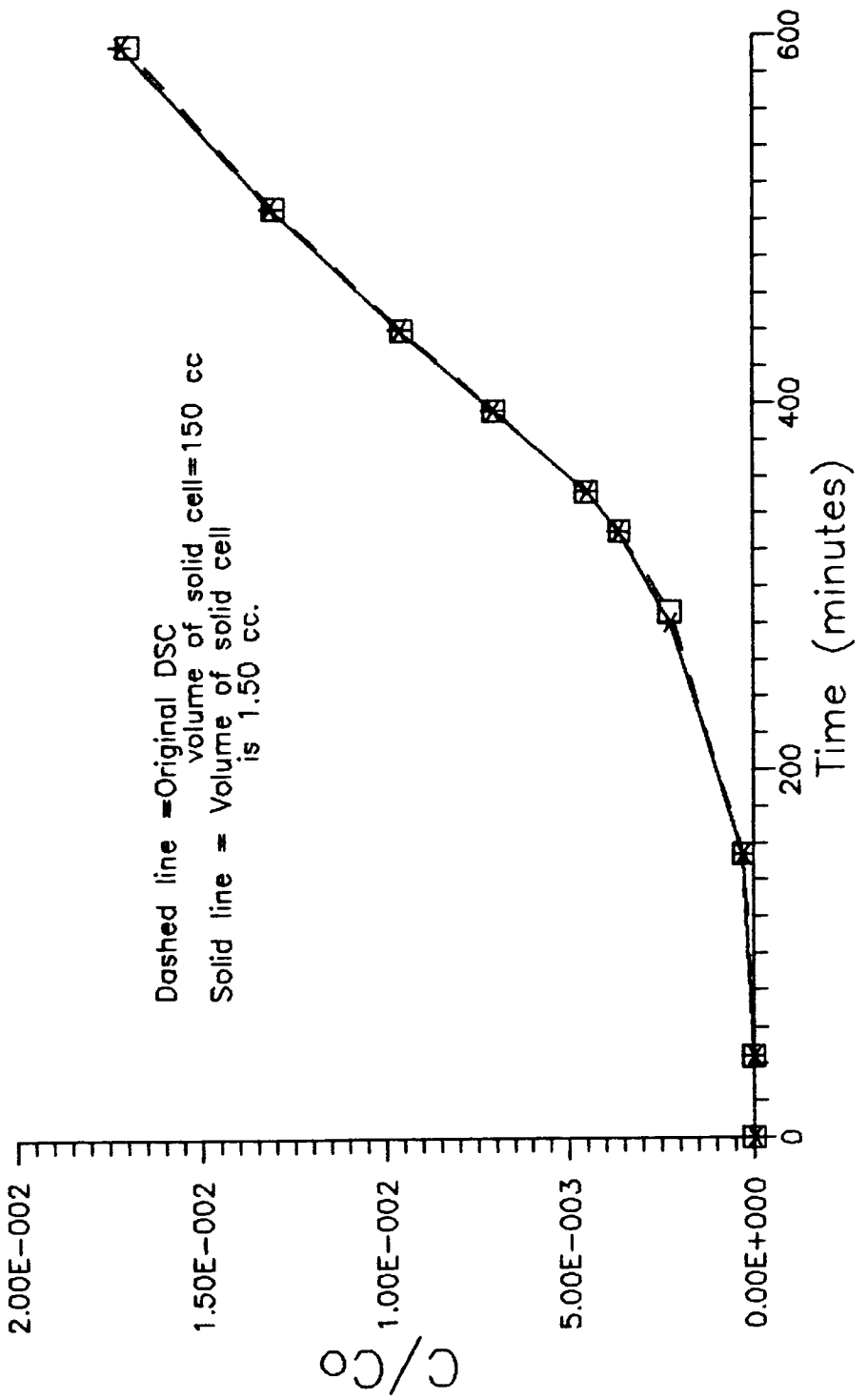

Figure 6.26 Comparison of the original DSC model which simulates the SF6 test ran at a water application rate of 0.285 ml/min to the same DSC model where the solid cell volume is decreased by a factor of 100 to 1.50.

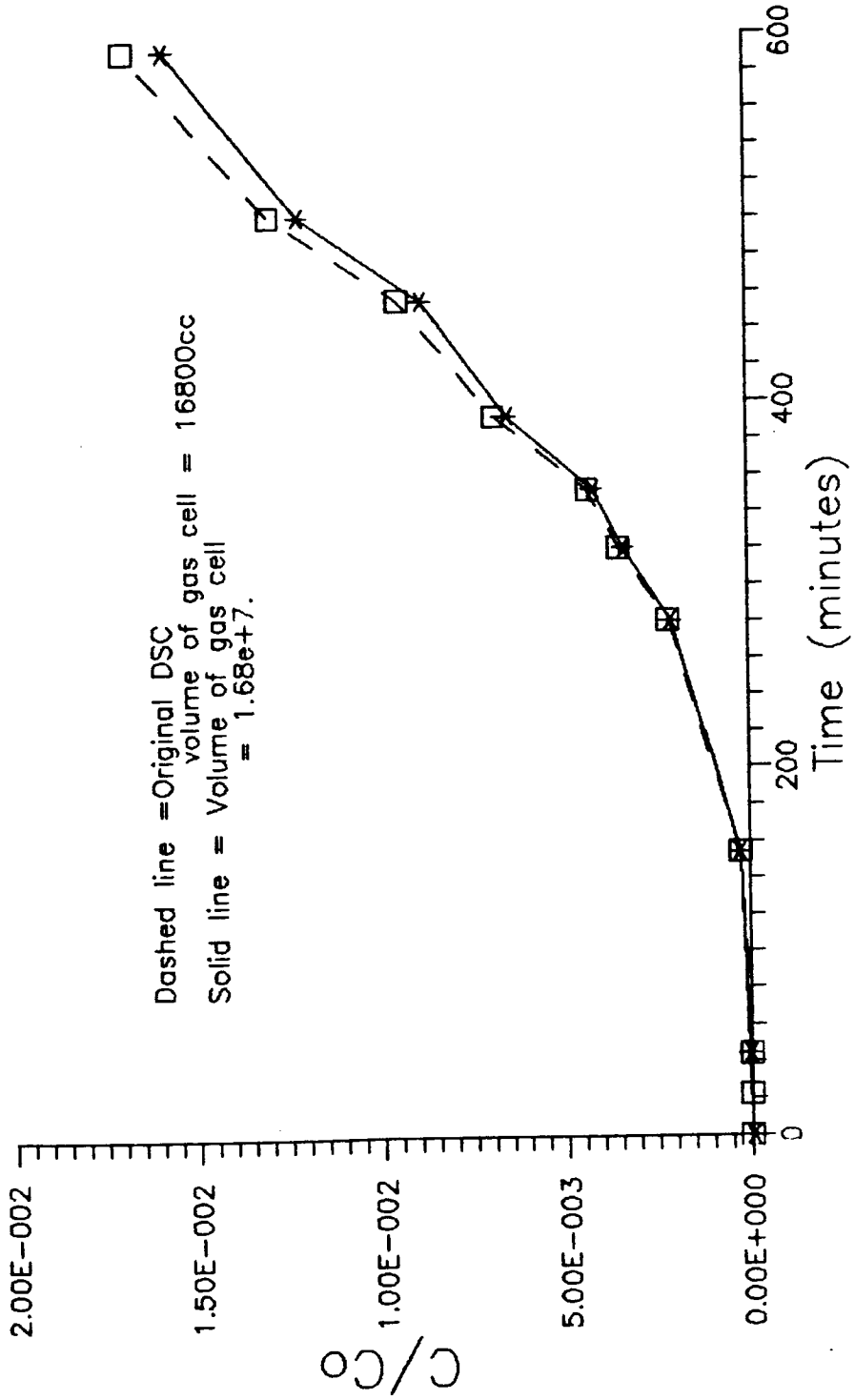

Figure 6.27 Comparison of the original DSC model which simulates the SF6 test ran at a water application rate of 0.285 ml/min to the same DSC model where the gas cell volume is increased by a factor of 1000 to 1.68e+7 cc.

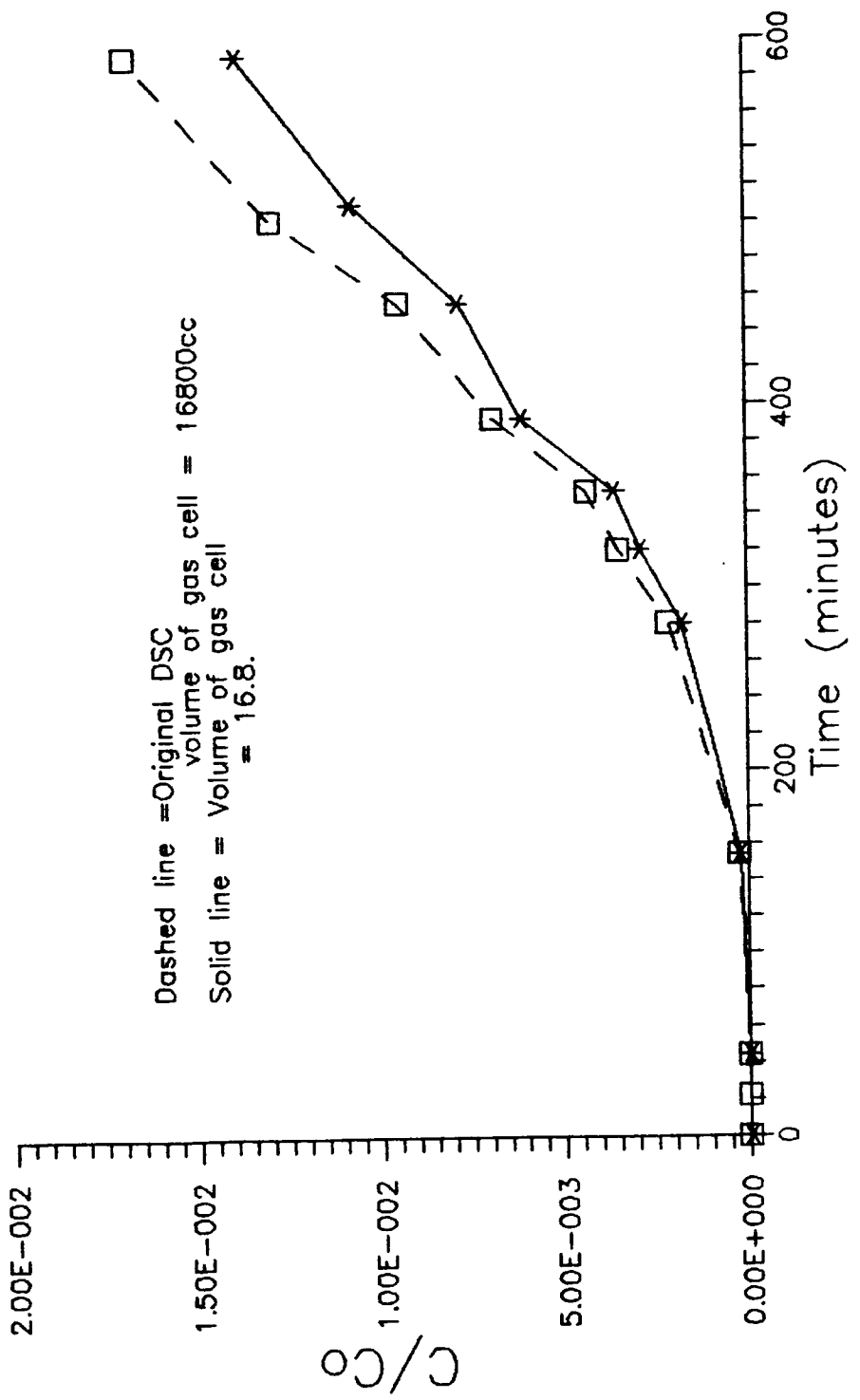

Figure 6.28 Comparison of the original DSC model which simulates the SF6 test ran at a water application rate of 0.285 ml/min to the same DSC model where the gas cell volume is decreased by a factor of 1000 to 16.8 cc.

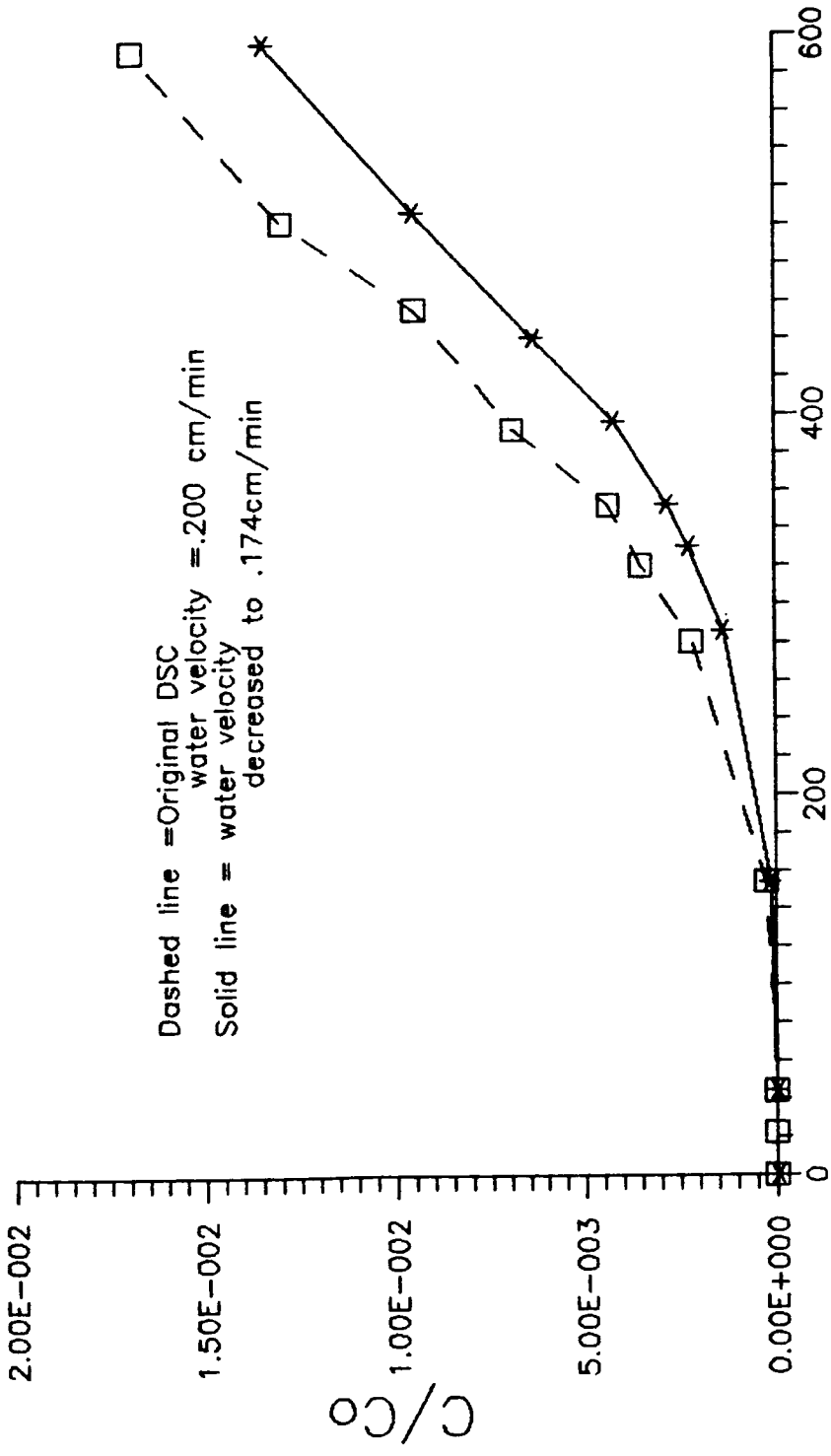

Figure 6.29 Comparison of the original DSC model which simulates the SF6 test ran at a water application rate of 0.285 ml/min to the same DSC model where the water percolation rate is decreased by 12% to 0.174 cm/min.

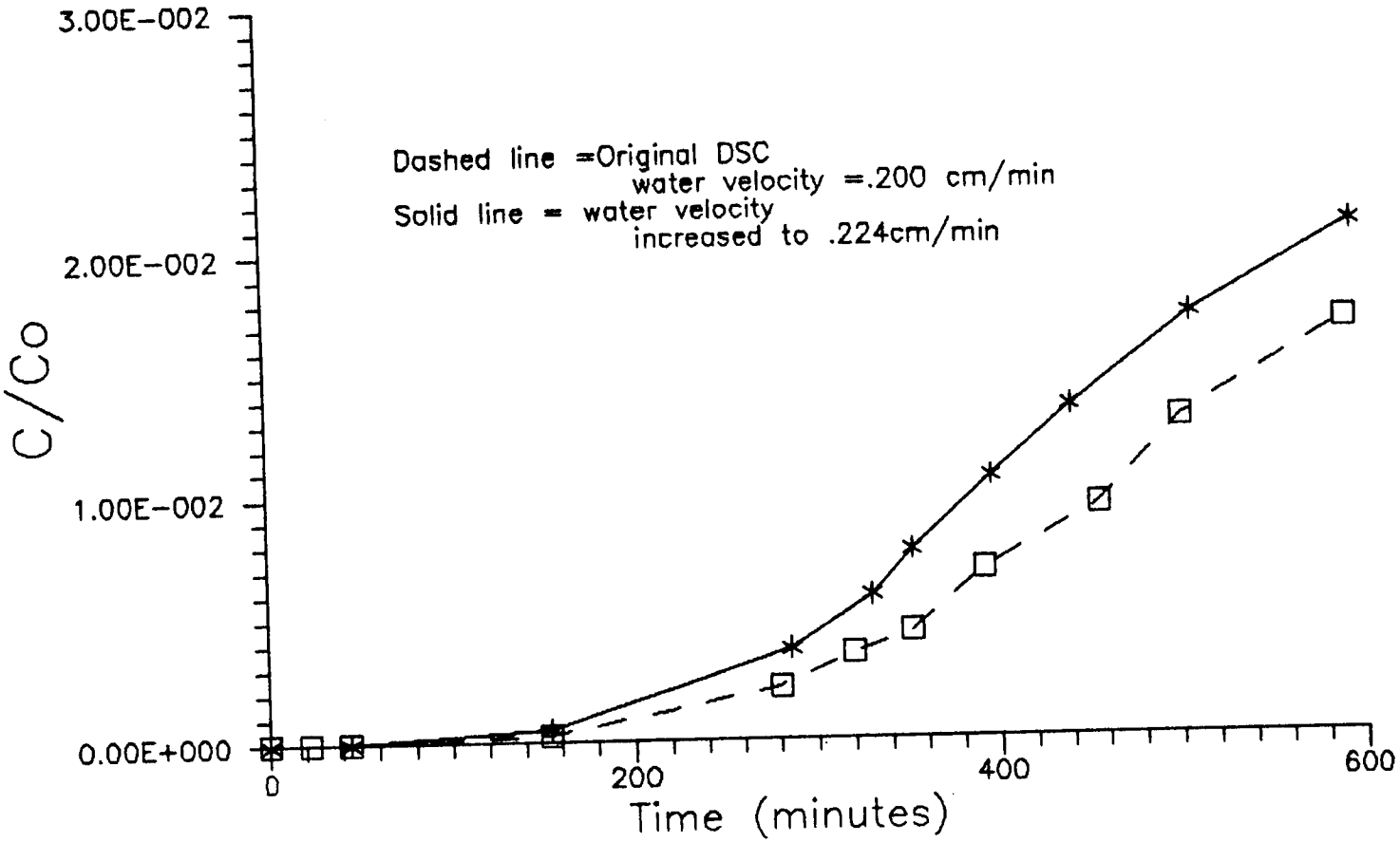

Figure 6.30 Comparison of the original DSC model which simulates the SF6 test ran at a water application rate of 0.285 ml/min to the same DSC model where the water percolation rate is increased by 12% to 0.224 cm/min.

Calculated rate constant for sorption were not meaningful because the computer results showed that sorption does not affect the DSC results. The K_+ for volatilization was calculated to be 319 min, which agrees well with the value calculated for SF6 in Simulation Number 2.

Simulation Number 4

This test was different from all the other tests in that there was only one point from which to infer a breakthrough curve. For most tests run with BCF, the concentration of the tracer in the soil gas was too small to measure because it was impossible to achieve high enough BCF concentrations in the initial tracer solution.

In this test one sample of tracer taken from port number 4 showed the presence of BCF. The same phenomenon occurred later in the test in port number 6, making it seem that the occurrence of tracer in port number 4 was not an isolated occurrence. The concentration found in port number 4 was extremely close to the detection limit for this procedure making it possible that the peak of the breakthrough curve was the only part of the breakthrough curve detectable. Another interesting characteristic of this test is that BCF in the soil gas appeared before the chloride breakthrough curve.

Figure 6.31 shows the breakthrough curve for BCF in the water compared to the breakthrough curve of the equivalent ideal tracer. It is evident that the concentration in the water is extremely small, almost nonexistent. The graph in figure 6.32 shows the computer generated gas breakthrough curve where the peak of the curve coincides

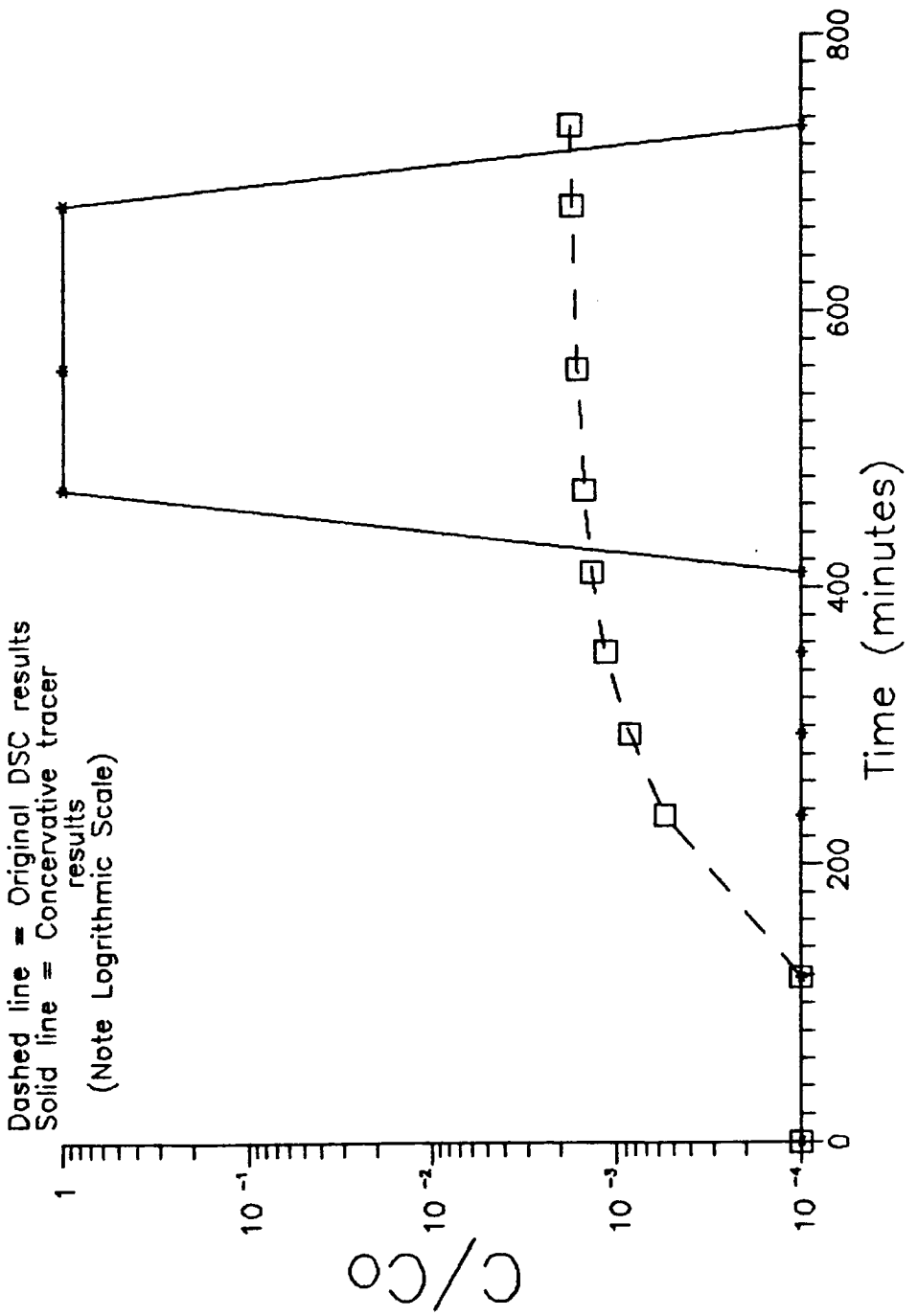

Figure 6.31 Water breakthrough curves comparing the DSC results to that of a conservative tracer for the BCF test ran at a water application rate of 0.083 ml/min.

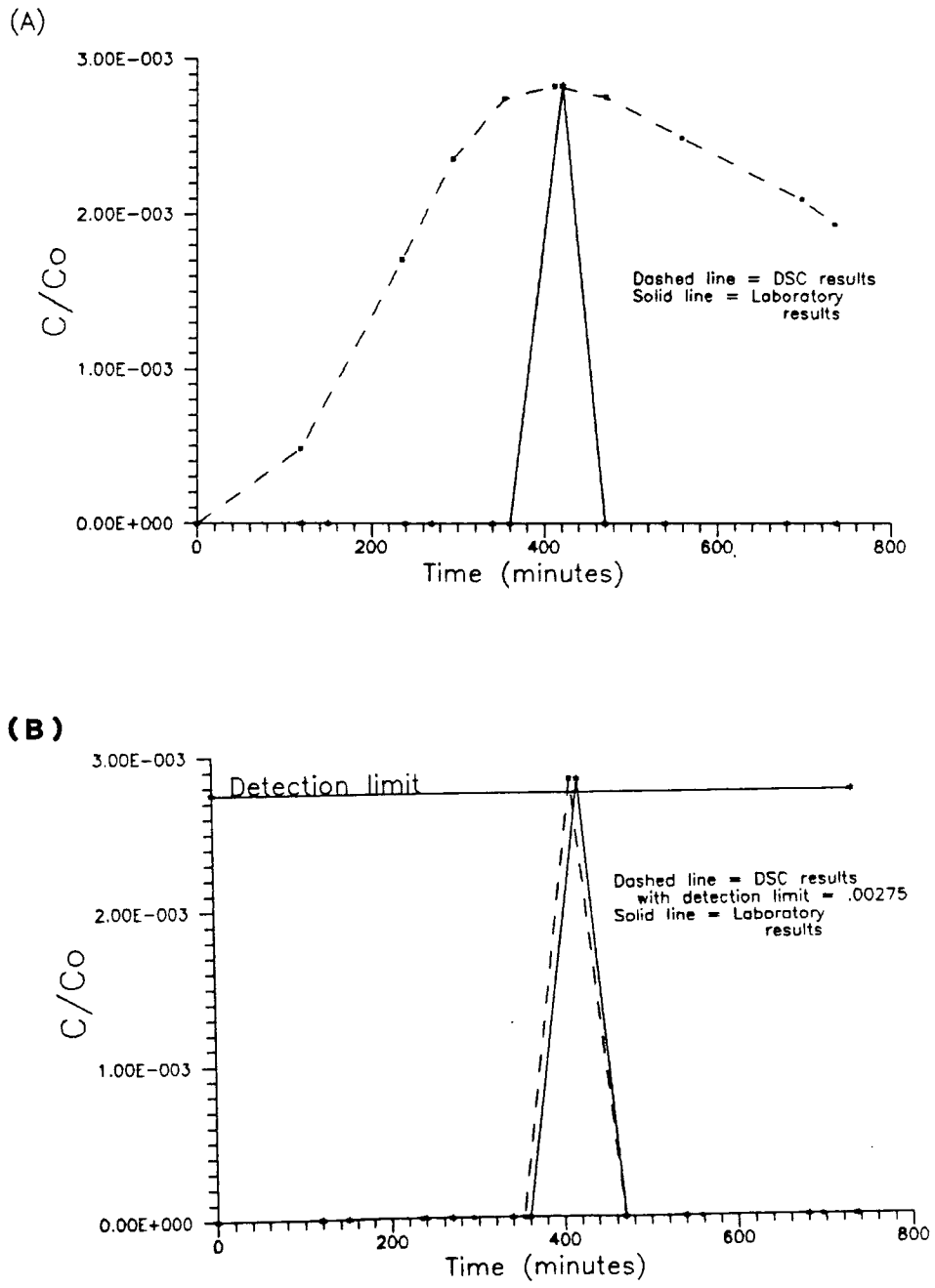

Figure 6.32 Gaseous breakthrough curves comparing the DSC results to the laboratory results for the BCF test ran at a water application rate of 0.083 ml/min, a) original DSC model, b) DSC model with the detection limit equal to 0.00275.

with the peak of the laboratory gas breakthrough curve. If it is assumed that any value less than the sampled data point is below the detection limit than the computer generated curve would correspond to the laboratory curve.

Rate constants calculated from the exchange volumes between the solid and the liquid cells and between the liquid and the gas cells do not agree with the rate constants calculated from the other BCF test. These two tests were run at highly different flow rates with large concentration differences. Considering the large differences between these two tests, the assumption that partitioning between phases is first order linear may be invalid. A more complicated kinetic model such as one summarized in Table 2.2 or another sorption equilibrium model such as the Langmuir of Freundlich models might better simulate the behavior of BCF.

Simulation Number 5

Simulation of F-22 required special considerations because of the presence of F-22 in the column at the beginning of the test. Initial gas concentrations had to be read into the model. Results of the F-22 liquid breakthrough compared to the breakthrough if F-22 was an ideal tracer are shown in figure 6.33. Once again the tracer has almost completely volatilized out of solution by the time it reached the sampling port.

The breakthrough curves for gaseous F-22 using laboratory and DSC results are presented in figure 6.34. At this low flow rate a water displacement velocity could not be estimated using just a gaseous

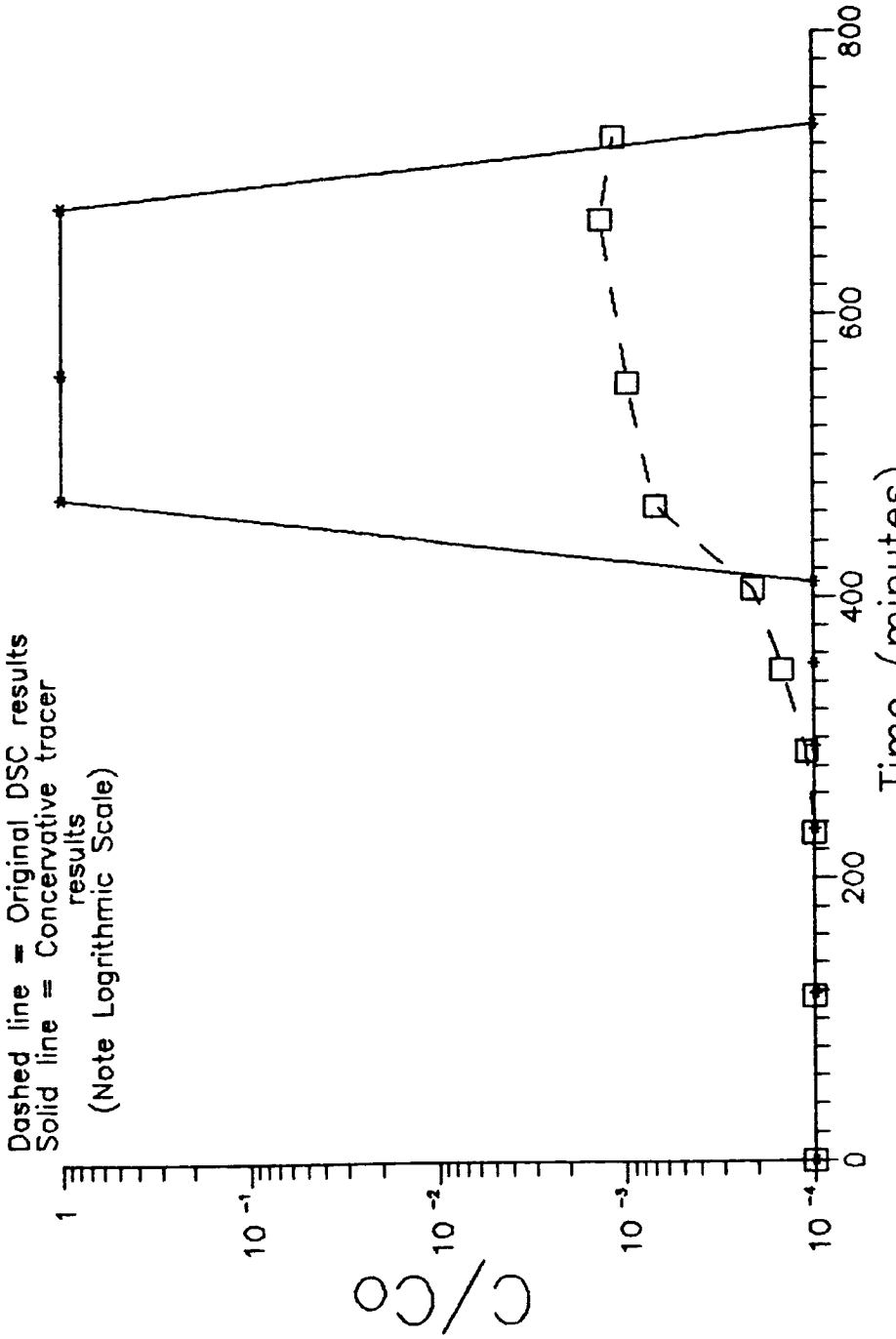

Figure 6.33 Water breakthrough curves comparing the DSC results to that of a conservative tracer for the F-22 test ran at a water application rate of 0.083 ml/min

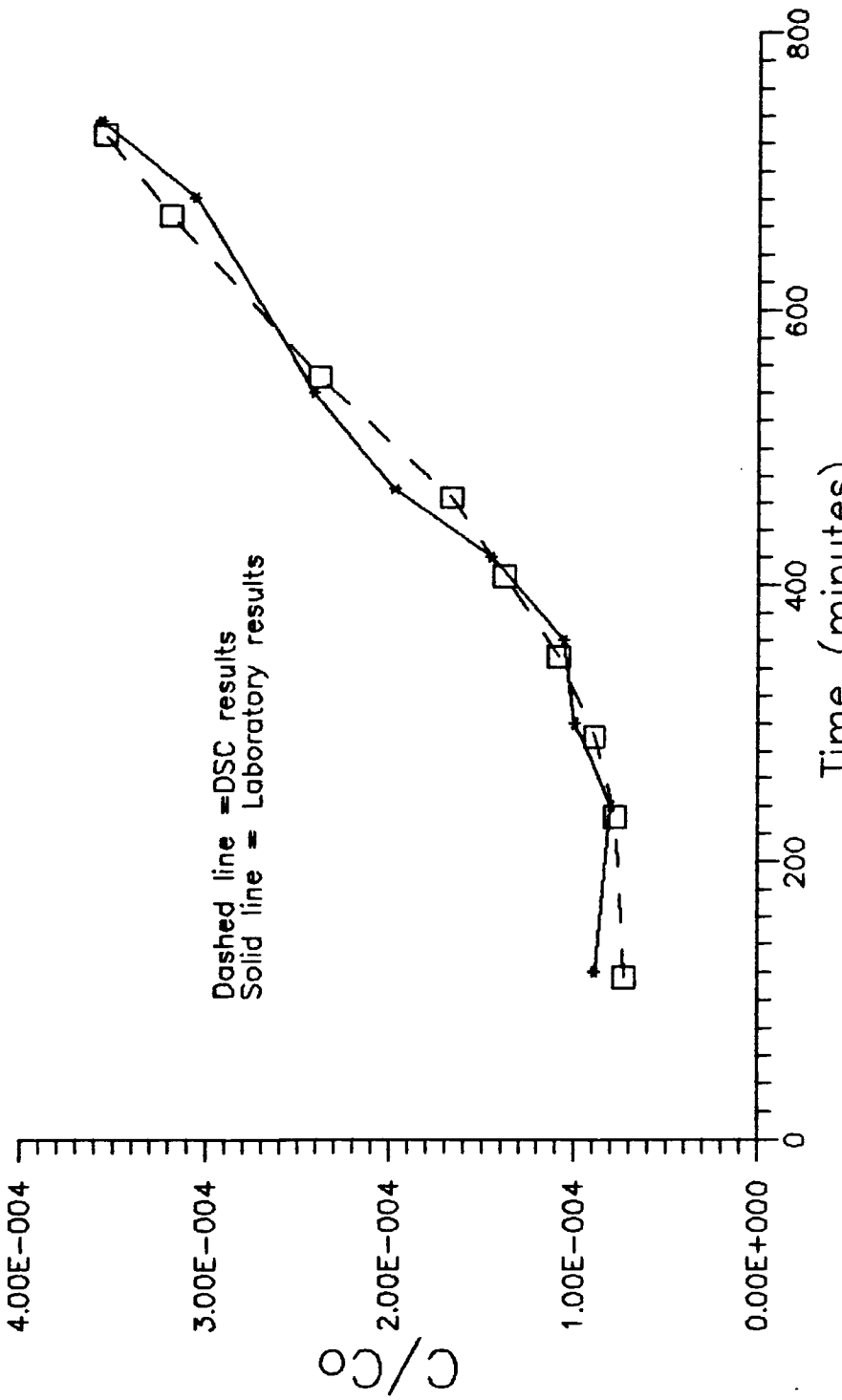

Figure 6.34 Gaseous breakthrough curves comparing the DSC results to the laboratory results for the F-22 test ran at a water application rate of 0.083 ml/min.

breakthrough curve, but if by trial and error analysis a match between the computer and laboratory data could be made, then the travel time of water could be estimated.

Summary of Parameter Sensitivity

In order to apply the volatile tracer technique to the field the DSC model must be highly sensitive to changes in the water displacement velocity. At high flow rates, the DSC results are not highly sensitive to these changes. The major problem is that extremely steep tracer fronts are hard to simulate using the DSC due to numerical limitations. This inability to simulate the tracer front increases the error in estimating water travel times. However, the sensitivity of the model to changes in water displacement velocity increases as the steepness of the tracer front decreases. The SF6 test with a water displacement velocity of 0.200 cm/min was much more sensitive to variations in water displacement velocity.

The parameters used in the model to estimate sorption, volatilization and diffusion are interrelated in such a way that the effect of changing an RI value can not be estimated without knowing the gas, liquid and soil cell volumes. The sensitivity of the DSC results to changes in distribution coefficients relies heavily on the magnitude of the coefficients and on the rate at which the process procedes. For example, if the sorption distribution coefficient is small than an error in estimating that parameter would not significantly alter the the DSC results. But if the sorption coefficient is large than a small error in estimating the sorption

coefficient would significantly alter the results. The same situation is true for the RI factor. When the RI value is large, than the partition coefficient must be known accurately. If the RI value is small any error in the partition coefficient will not significantly affect the DSC results.

Generally, changing the different RI values produced the following results:

- o The exchange volume (RI) between the gas and liquid cells is one of the most important parameters used in the model. It is the only RI value that could cause changes in the actual shape of the breakthrough curve.
- o The RI value between the liquid and solid controlled the magnitude of the gas concentration along with the slope of the breakthrough front.
- o The RI value between neighboring gas cells is a function of the gaseous diffusion coefficient. Changes in this value resulted in changes in the magnitude of the gas concentration and sometimes it altered the arrival time of the gas tracer.

The DSC results were not sensitive to the value of the liquid - solid distribution coefficient, as represented by the solid cell volume. The model was more sensitive to the volume of the gas cell used. The volume of the gas cell controls the process of volatilization and is defined by the value of K_w. If the K_w was decreased (volume of gas cell increased), two effects on the breakthrough curve were noticed. In one example the shape of the breakthrough curve was changed and in the other example the magnitude of the gas concentration was decreased.
When the gas cell volume was increased, little change in the DSC results occured. The reason the increase did not affect the computer results is that fluorocarbon tracers have high K_w values to begin with and any

increase in the already high value can not significantly affect the DSC results.

Changes in the volume of the water cell caused large changes in the magnitude of the breakthrough curve. Therefore, the water application rate which is used to calculate the volume of the water cell must be known accurately.

An attempt was made to simulate the SF6 test run at a water application rate of 0.083 ml/min, but it was impossible to match the computer and the laboratory data. The system boundary recharge concentration (also called the initial concentration of tracer in the water, C_0) was too small to produce the large tracer concentration seen in the gas phase. Computer modeling of the lab data showed that one of the variables measured in the test, the initial tracer concentration, was inaccurate. The error in this test would not have been noticed if modeling had not been done. This shows that if there is something wrong with the test, the computer model will not erroneously match the laboratory data if those data are in error.

The main problem with the computer approach is that there may be more than one solution to the problem. It is possible that more than one water application rate can produce the same gaseous breakthrough curve depending on the partition coefficients, rate constants, and diffusion coefficients used. Therefore, the better the input parameters are known, the more precisely water travel times can be estimated.

The laboratory tests and subsequent computer simulations show that the partition and diffusion coefficients used to model the lab data

were adequately known and did produce breakthrough curves that matched the laboratory data very well.

The major unknowns were the rate constants, which were calculated from the RI values used in the computer model results. The rate constant for BCF volatilization changed depending on flow rate, indicating that the first-order linear model used to calculate K_+ was not appropriate. The rate constant for SF6 volatilization was consistent between tests and can be useful if this technique is adapted to the field. In the field the only unknown parameter left would be the water velocity, and hopefully with a trial and error procedure the water displacement velocity could be estimated.

CHAPTER 7

CONCLUSIONS

Soil columns studies indicate that soil gas concentrations of the fluorocarbon tracers BCF, F-22 and SF6 can estimate water travel times under certain conditions. SF6 is the most mobile tracer and appears to be the most suitable for applying the volatile tracer method to the field. F-22 also appears suitable except it is difficult to purge from the hydrologic system . BCF may be applicable if a method for concentrating the compound in water could be developed.

Gaseous breakthrough curves with steep breakthrough fronts can be used directly, without computer modeling, to estimate water travel time. The first appearance of the fluorocarbon tracer in the soil gas signifies the breakthrough of the liquid. However, if the concentration of tracer gas gradually increases with no discernable breakthrough front, then computer simulation of the results, using the DSC model, is necessary to separate out the effects of gaseous diffusion.

Conditions best suited for this method are those where water displacement velocities rates are not extremely slow and/or the medium is close to saturation. The high saturation of the medium would reduce the processes of volatilization and diffusion, thereby minimizing the importance of most of the parameters needed in modeling.

To accurately apply the computer model, the partition coefficients, diffusion coefficients, rate constants, equilibrium conditions and the degree of saturation must be known. The major difficulty with applying the volatile tracer technique is that values for these parameters are rarely available.

Fractured rock is an example of a hydrologic system where this method could be applied. In this example, the rock matrix is commonly near saturation. Even though flow rate through the rock is extremely slow the tracer would not have a chance to volatilize out of solution until it reaches a sampling point, such as a borehole, where breakthrough curves could be obtained. Flow through the fractures themselves could be much faster than through the matrix, allowing the two different travel times to be distinguished. If the traced water traveled as a slug through the fracture, volatilization and diffusion of the tracer would be reduced, increasing the possibility of a successful tracer test.

Results from this study indicate that a field test of the volatile tracer technique may be successful. However, this technique is not an easily applied technique to estimate the travel time of water. The method requires considerable time and effort be put into characterizing the field parameters and interpreting any results.

APPENDIX A

COLUMN TEST DATA

Presented in this appendix are the data acquired from the 5 column tests reviewed in this thesis.

Table A.1 Test #1 gas chromatography data for the F-22 test ran at a water application rate of 4 ml/min.

Port	Time minutes	Counts on GC	Injection size (cc)	Concentration ng/ml	C/Co
6	0	0			
	45	0			
	70	0			
	90	0			
	105	trace(shoulder peak no counts)			
	120	17646	.5	260.6	.00127
	135	13566	.2	465.9	.00228
	150	20849	.2	796.7	.00389
	210	78532	.3	3404.8	.01663
	345	91727	.2	4006.4	.01956
	375	96309	.2	4224.0	.02063
	405	106266	.2	4639.2	.02265
5	0	0			
	125	0			
	165	0			
	180	trace (shoulder peak not calibrated correctly by GC)			
	195	11779	.3	256.0	.00125
	225	14348	.2	501.8	.00245
	300	136460	.3	3741.0	.01827
	410	89225	.2	38912.0	.01900
4	0	0			
	125	0			
	255	trace not calibrated			
	285	8653	.3	162.8	.000792
	435	36926	.2	663.0	.00324

Table A.2 Test #2 gas chromatography data for the BCF test ran at a water application rate of 5 ml/min.

Port	Time minutes	Counts on GC	Injection size (cc)	Concentration ng/ml	C/Co
6	35	0	.5	0	0
	45	0	.5	0	0
	60	0	.5	0	0
	80	646	.6	slight trace	0
	100	2827	.6	.04867	.00196
	120	4796	.6	.0515	.00208
	142	2769	.5	.0584	.00236
	160	1506	.5	.0563	.00227
	300	3099	.5	.0590	.00238
4	120	0			
	165	0			
	190	0			
	205	0			
	240	0			
	255	0			
	285	0			

Table A.3 Test #3 gas chromatography data for the column test ran at 1 ml/min.

Tracer	Port	Time minutes	Counts on GC	Injection size (cc)	Concentration ng/ml	C/Co
F-22	6	45	3189	.3	7.65	.000458
		105	1632	.2	2.77	.000165
		140	3214	.3	7.74	.000463
		160	7374	.3	23.2	.00139
		180	59967	.4	164.4	.00984
		210	130174	.4	284.0	.0170
		250	136425	.5	302.6	.0181
		265	252038	.5	561.1	.0599
		372	481031	.5	1073.4	.0643
		481	26562	.5	56.8	.00340
6	SF6	45	0			
		105	0			
		140	5272	.3	.06716	.000324
		160	13457	.3	.0831	.000450
		180	124650	.4	.21	.00101
		210	281977	.4	.958	.00471
		250	509676	.5	1.63	.00787
		265	689444	.5	2.315	.0112
		372	1401441	.5	5.021	.0242
		481	1386920	.5	4.97	.0240

Table A.4 Test #4 gas chromatography data for the SF6 test ran at a water application rate of .286 ml/min.

Port	Tracer	Time minutes	Counts on GC	Injection Size (cc)	Concentration ng/ml	C/Co
6	SF6	0				
		20	0			
		50	0			
		80	0			
		110	0			
		140	0			
		170	0			
		210	0			
		230	0			
		270	0			
		280	10947	.5	.3263	.00186
		303	235267	.5	.5425	.00310
		320	246999	.5	.5538	.00316
		352	444992	.5	.744	.00425
		392	947874	.5	1.226	.00701
		455	1849096	.5	2.092	.01195
		500	2159584	.5	2.39	.01366
		590	2962526	.5	3.161	.01806

Table A.5 Test #4 gas chromatography data for the SF6 column test ran with a water application rate of 0.083 ml/min.

Port	Tracer	Time minutes	Counts on GC	Injection Size (cc)	Concentration ng/ml	C/Co
6	SF6	0	0			
		30	0			
		60	0			
		120	0			
		150	0			
		180	0			
		210	0			
		240	0			
		270	250799	.5	.648	.0797
		300	272977	.5	.7325	.0901
		320	304110	.5	.8369	.1047
		340	307616	.5	.8643	.1063
		360	442070	.5	1.375	.1692
		370	365487	.5	1.084	.1333
		420	381686	.5	1.146	.1409
		455	376918	.5	1.128	.1387
		470	400396	.5	1.217	.1497
		510	385253	.5	1.160	.1426
		540	418658	.5	1.286	.1582
		680	488880	.5	1.554	.1911
		735	500149	.5	1.596	.1964
6	F-22	30	6366	.5	11.70	.0000898
		60	7293	.5	13.77	.000106
		120	6272	.5	11.49	.0000888
		150	5334	.5	9.39	.0000721
		180	5894	.5	10.64	.0000817
		210	6067	.5	11.02	.0000846
		240	5811	.5	10.46	.0000802
		270	6135	.5	11.81	.0000858
		300	6937	.5	12.68	.0000995
		320	7304	.5	13.80	.0001059
		340	7255	.5	13.69	.0001050
		360	7336	.5	13.87	.0001064
		370	8884	.5	17.32	.0001330
		420	9625	.5	18.99	.000145
		450	11411	.5	22.98	.000176
		470	12666	.5	25.79	.000198
		510	12821	.5	26.06	.000200
		540	15170	.5	31.90	.000241
		680	18980	.5	39.91	.000306
		735	21910	.5	46.47	.000357

Table A.5 cont'd

Port	Tracer	Time minutes	Counts on GC	Injection Size (cc)	Concentration ng/ml	C/Co
6	BCF	30	0			
		60	0			
		120	0			
		150	0			
		180	0			
		210	0			
		240	0			
		270	0			
		300	0			
		320	0			
		340	0			
		360	0			
		370	0			
		420	1812	.5	.0640	.002834
		450	0			
		470	0			
		510	0			
		540	0			
		680	0			
		735	0			

APPENDIX B

DISCRETE STATE COMPARTMENT MODEL

Appendix B is a listing of the Discrete State Compartment Model used to simulate fluorocarbon movement in the column studies. This version of the program was written to be run on a IBM microcomputer by R.H. Seidemann (1986).

```
*$nofloatcalls
$storage:2
      Program DSC

* Originally called Program FISTMO by M.E. Campana

$include:'common.blk'

* Go to subroutine READS to enter bulk of data.

      CALL reads

* Go to subroutine WRITES to write data entered

      CALL writes

* Start Iterating

      nsbrv = 1
      nsbrc = 1
      nprnt = 1

      WRITE (*,200)

      DO 30 iteration = 1, nit

      WRITE (*,201) iteration

* zero arrays

      CALL zero

* Check to see if new SBRV or SBRC need to be read in:

      IF ((iteration .EQ. ITsbrv(nsbrv)) .OR. (IFsbrv .LT. 0)) THEN
           READ (1,101) (sbrv(j),j=1,icel)
           WRITE(2,101) (sbrv(j),j=1,icel)
           WRITE(3,101) (sbrv(j),j=1,icel)
      ENDIF
      IF  (iteration .EQ. ITsbrv(nsbrv)) nsbrv = nsbrv + 1

      IF ((iteration .EQ. ITsbrc(nsbrc)) .OR. (IFsbrc .LT. 0)) THEN
           READ (1,101) (sbrc(j),j=1,icel)
           WRITE(2,101) (sbrc(j),j=1,icel)
           WRITE(*,101) (sbrc(j),j=1,icel)
      ENDIF
      IF  (iteration .EQ. ITsbrc(nsbrc)) nsbrc = nsbrc + 1

* Go through K-rout table, row by row:

      DO 10 km = 1, kz
```

```
      la = krout(km,1)
      lb = krout(km,2)
      lc = krout(km,3)

      IF (la .EQ. 0) then
           brv(lb) = sbrv(lb)
           totalin(lb) = sbrv(lb) * sbrc(lb)
           ni(lb) = 1
      ELSEIF (lc .EQ. 1) THEN
           CALL xchanj
      ELSE
           CALL flow
      ENDIF

   10 CONTINUE

* Decay states

      IF (rd .NE. 1.) THEN
           DO 20 j = 1, ncel
   20      state(j) = rd * state(j)
      ENDIF

* Impulse response on tracer ages?

      IF (mage .EQ. 1) CALL mageim

* Check to see if printouts desired:

      IF ((iteration .EQ. ITprin(nprnt)) .OR. (IFprnt .LT. 0) .OR.
     .    (iteration .EQ. nit))   CALL write1

   30 IF (iteration .EQ. ITprin(nprnt)) nprnt = nprnt + 1

* Iteration done

           CALL write2

   99 STOP '         Program DSC Completed'

  101 FORMAT (8g10.3e1)
  200 FORMAT (//'               Input Completed'//)
  201 FORMAT (1H+,'     Currently working on iteration:  ',i4)

      END

* * * * * * * * * * * * * * * * * * * * * * * * * * * * * * * * * * * * *

      SUBROUTINE zero

* This subroutine initializes or re-initializes arrays.
```

```
$include:'common.blk'

      DO 10 j = 1, ncel
        t(j) = 0.
        nc(j) = 0.
        ni(j) = 0.
        add(j) = 0.
        age(j) = 0.
        var(j) = 0.
        brv(j) = 0.
        bdv(j) = 0.
        bdc(j) = 0.
        sbdv(j) = 0.
        xchnjin(j) = 0.
        totalin(j) = 0.
        xchnjout(j) = 0.
        totalout(j) = 0.
        exvol(j) = 0.
   10   sumcon(j) = 0.

      RETURN
      END

* * * * * * * * * * * * * * * * * * * * * * * * * * * * * * * * * * * * *

      SUBROUTINE xchanj

* This subroutine exchanges equal volumes of water between two cells.

$include:'common.blk'

      xv = ri(km) * vol(la)

      IF (jtype .EQ. 1) THEN
* MMC
           IF (xv .GT. vol(lb)) xv = vol(lb)
           xvo = xv * state(la) / vol(la)
           extolb = xv * state(lb) / vol(lb)
      ELSE
* SMC
           xvo = xv * state(la) / vol(la)
           extolb = xv * (state(lb) + xvo) / (vol(lb) + xv)
      ENDIF

      xchnjout(la) = xchnjout(la) + xvo
      xchnjin(lb) = xchnjin(lb) + xvo

      xchnjin(la) = xchnjin(la) + extolb
      xchnjout(lb) = xchnjout(lb) + extolb

      exvol(la) = exvol(la) + xv
```

```
      exvol(lb) = exvol(lb) + xv

      ni(la) = ni(la) + 1
      ni(lb) = ni(lb) + 1

      IF(state(la) .GT. state(lb)) THEN


* Adjust States

      state(la) = state(la) - xvo + extolb
      state(lb) = state(lb) + xvo - extolb

      IF (ni(la) .EQ. noin(la)) CALL mix(la)
      IF (ni(lb) .EQ. noin(lb)) CALL mix(lb)

      ENDIF
      RETURN
      END

* * * * * * * * * * * * * * * * * * * * * * * * * * * * * * * * * * * * *

      SUBROUTINE flow

* This subroutine calculates flow changes

$include:'common.blk'

* Check to see whether cell has been mixed and volumetric quantities
*   calculated before allowing it to discharge.

      IF (nc(la) .EQ. 0) CALL mix(la)

* Calculate total amount of material entering cell and brv.

      totalin(lb)  = totalin(lb)  + totalout(la)  * ri(km)
      brv(lb) = brv(lb) + bdv(la) * ri(km)
      ni(lb) = ni(lb) + 1

* Check to see whether all inputs in downstream cell are accounted for.

      IF (ni(lb) .EQ. noin(lb)) CALL mix(lb)

      RETURN
      END

* * * * * * * * * * * * * * * * * * * * * * * * * * * * * * * * * * * * *

      SUBROUTINE mix(ld)

* This subroutine calculates volumes and boundary discharge volumes.
```

```
*    If IVAR = 0, a steady volume regime with BRV = BDV is specified.
*    If IVAR not equal to zero, then a linear reservoir is assumed.

$include:'common.blk'

      IF ( (ivar .NE. 1) .OR. (fac(ld) .EQ. 0.0) ) THEN
           bdv(ld) = brv(ld)
      ELSE
           bdv(ld) = fac(ld) * (vol(ld) + brv(ld) - phi(ld))
           IF (bdv(ld) .LT. 0) bdv(ld) = 0.
           vol(ld) = vol(ld) + brv(ld) - bdv(ld)
      ENDIF

* This part of the subroutine mixes the contents of a cell once it
*   has received all of its inputs.  The cell state is calculated here,
*   as is the total amount of material moving out of the cell, TOTALOUT.

      IF (itype .EQ. 1) THEN
*MMC
        totalout(ld) = state(ld) * bdv(ld) / vol(ld)
      ELSE
*SMC
        totalout(ld) = (state(ld) + totalin(ld)) * bdv(ld)
     .                 / (vol(ld) + brv(ld))
      ENDIF

      state(ld) = state(ld) + totalin(ld) - totalout(ld)

      nc(ld) = nc(ld) + 1

      RETURN
      END

* * * * * * * * * * * * * * * * * * * * * * * * * * * * * * * * * * * * *

      SUBROUTINE mageim

* This subroutine is used only in the case of an impulse-response
*   experiment.  The quantities calculated here will converge to
*   mean (i.e., MEAN AGE NUMBER) and variance of the age number
*   distribution of each cell after a sufficient number of
*   iterations. use only for a steady flow, steady volume fsm.
*   This subroutine requires a constant DELTA.

$include:'common.blk'

      DO 10 j = 1, ncel

      conc = state(j) / vol(j)

      IF (conc .NE. 0.0) THEN
```

```
          sumcon(j) = sumcon(j) + con
              t(j)  =  t(j)  + conc * float(iteration)
             add(j) = add(j) + conc * float(iteration**2)

             age(j) = t(j) * delta / sumcon(j)
             var(j) = add(j) * delta**2 / sumcon(j) - age(j)**2
        ENDIF

     10 CONTINUE

        RETURN
        END

* * * * * * * * * * * * * * * * * * * * * * * * * * * * * * * * * * * * * * * *

        SUBROUTINE reads

* This subroutine reads in most of the data

$include:'common.blk'

        OPEN (1, FILE = 'dsc.dat')

        WRITE (*,100)
        READ (*,200) item
        IF (item .EQ. 0) THEN
              OPEN (3)
        ELSE
              OPEN (3, File = 'CON', status = 'new')
        ENDIF

* Card type 1a - Format 8i10

        READ (1,104) ncel, icel, nit, kz, IFsbrv, IFsbrc
        WRITE (3,104) ncel, icel, nit, kz, IFsbrv, IFsbrc

* Card type 1b - Format 8i10

        READ (1,104) mage, itype, jtype, ivar, massin, massout, IFprnt
        WRITE (3,104) mage, itype, jtype, ivar, massin, massout, IFprnt

* Optional card type 2a - Format 10i8

        IF (IFprnt .GT. 0) THEN
             READ (1,103) (ITprin(i),i=1,IFprnt)
             WRITE (3,103) (ITprin(i),i=1,IFprnt)
        ENDIF

* Optional card type 2b - Format 10i8

        IF (IFsbrv .GT. 0) THEN
```

```
          READ (1,103) (ITsbrv(i),i=1,IFsbrv)
          WRITE (3,103) (ITsbrv(i),i=1,IFsbrv)
     ENDIF

* Optional card type 2c - Format 10i8

     IF (IFsbrc .GT. 0) THEN
          READ (1,103) (ITsbrc(i),i=1,IFsbrc)
          WRITE (3,103) (ITsbrc(i),i=1,IFsbrc)
     ENDIF

* Optional card type 2d - Format 8f10.3

     IF (IVAR .EQ. 1) THEN
          READ (1,105) (fac(i),i=1,ncel)
          WRITE (3,105) (fac(i),i=1,ncel)

          READ (1,105) (phi(i),i=1,ncel)
          WRITE (3,105) (phi(i),i=1,ncel)
     ENDIF

* Card type 3 - Format 8f10.3

     READ (1,105) half, delta, date
     WRITE (3,105) half, delta, date

     IF (half .LE. 0.0) THEN
          rd = 1.0
     ELSE
          rd = 2.0 ** (- delta / half)
     ENDIF

* Card type 4a - 8f10.3

     READ  (1,105) (state(j),j=1,ncel)
     WRITE (3,105) (state(j),j=1,ncel)

* Card type 4b - 8f10.3

     READ  (1,105) (vol(j),j=1,ncel)
     WRITE (3,105) (vol(j),j=1,ncel)

* Card type 5a - 8f10.3
     READ  (1,105) (sbrv(j),j=1,icel)
     WRITE (3,105) (sbrv(j),j=1,icel)

* Card type 5b - 8f10.3

     READ  (1,105) (sbrc(j),j=1,icel)
     WRITE (3,105) (sbrc(j),j=1,icel)
```

```
* Card type 6 - 40i2

      READ  (1,101) (noin(j),j=1,ncel)
      WRITE (3,101) (noin(j),j=1,ncel)

* Card type 7a - 20i4

      DO 10 k = 1,3
      READ  (1,102) (krout(i,k),i=1,kz)
   10 WRITE (3,102) (krout(i,k),i=1,kz)

* Card type 7b - 8f10.3

      READ  (1,105) (ri(j),j=1,kz)
      WRITE (3,105) (ri(j),j=1,kz)

* Card type 7c - 8f10.3

      READ  (1,105) (ro(j),j=1,ncel)
      WRITE (3,105) (ro(j),j=1,ncel)

      RETURN

  100 FORMAT (//
     . '                        Program DSC - Mixing Cell Model'//
     . '                     Last Modification: November 10, 1985'////
     . '                  Do you wish to see unformatted input data ?'//
     . '                        1 = yes        0 = no'//
     . '                     (P

  103 FORMAT (10I
  104 FORMAT (8I10)
  105 FORMAT (8g10.3e1)
  200 FORMAT (i1)

      END

* * * * * * * * * * * * * * * * * * * * * * * * * * * * * * * * * * * * * *

      SUBROUTINE writes

* This subroutine writes out the input data

$include:'common.blk'

* Write out to file DSC.out

      OPEN (2, FILE = 'dsc.out', STATUS = 'new')
      CLOSE (3)
```

```
      WRITE (*,100)
      READ (*,200) item
      IF (item .EQ. 0) THEN
            OPEN (3)
      ELSE
            OPEN (3, File = 'CON', status = 'new')
      ENDIF

* Write out initial info

      WRITE (2,201) ncel, icel, nit, date, delta, massin, itype, jtype,
     .              ivar, IFsbrv, IFsbrc, half, rd
      WRITE (*,201) ncel, icel, nit, date, delta, massin, itype, jtype,
     .              ivar, IFsbrv, IFsbrc, half, rd

* Write out K-rout table

      WRITE(2,202)
      WRITE(3,202)

      DO 10 km = 1, kz
        WRITE(2,203) (krout(km,n),n=1,3),ri(km)
   10   WRITE(3,203) (krout(km,n),n=1,3),ri(km)

* Write out system boundary info

      WRITE(2,204)
      WRITE(3,204)

      WRITE(2,205) (k,sbrv(k),sbrc(k),k=1,icel)
      WRITE(3,205) (k,sbrv(k),sbrc(k),k=1,icel)

* Initial states printed out exactly as they were read in.
*   If necessary, convert initial states given with concentration
*   dimensions to mass dimensions, i.e. (concentration * unit ref-
*   erence volume dimensions).


      WRITE(2,206)
      WRITE(3,206)

      DO 20 j = 1,ncel
        WRITE (2,207) j,state(j),vol(j),noin(j),ro(j)
        WRITE (3,207) j,state(j),vol(j),noin(j),ro(j)

   20   IF (massin .NE. 1) state(j) = state(j) * vol(j)

* Print out non-steady volume info

      IF(ivar .EQ. 1) THEN
           WRITE (2,208)
```

```
          WRITE (2,209) (j, fac(j), phi(j), j = 1, ncel)

          WRITE (3,208)
          WRITE (3,209) (j, fac(j), phi(j), j = 1, ncel)
      ENDIF

      RETURN

  100 FORMAT (//
     . '                  Do you wish to see formatted input data ?'//
     . '                          1 = yes        0 = no'//
     . '                       (Press RETURN key to continue)')
  200 FORMAT (i1)
  201 FORMAT (//////
     . '    Number of cells: ',i5/
     . '    Number of cells receiving inputs from outside system: ',i5//
     . '    Number of interations: ',i7/
     . '    Starting time: ',g10.3/
     . '    One iteration: ',g10.3,'  time units'//
     . '    Massin:',i3,'    (1 = state dimensions)'/
     . '    Itype: ',i3,'    (1 = modified mixing cell for flows)'/
     . '    Jtype: ',i3,'    (1 = modified mixing cell for exchanges)'/
     . '    Ivar:  ',i3,'    (1 = variable volumes)'//
     . '    Number of changes in SBRV: ',i4/
     . '    Number of changes in SBRC: ',i4//
     . '    Half-life: ',g10.3,'  time units'/
     . '    Decay per iteration: ',g10.3//)
  202 FORMAT (//'           KROUT                RI'/)
  203 FORMAT (3(4x,i3),8x,g10.3)
  204 FORMAT (//'   ICEL     Initial SBRV    Initial SBRC')
  205 FORMAT (2x,i5,2(6x,g10.3))
  206 FORMAT (//'  Cell #    Initial Conc.  Initial Vol.  # Inputs'
     .  '        RO')
  207 FORMAT (5x,i4,2(5x,g10.3),5x,i4,5x,g10.3)
  208 FORMAT (//'  Cell #      FAC      Threshold')
  209 FORMAT (5x,i4,3x,2g10.3)

      END
* * * * * * * * * * * * * * * * * * * * * * * * * * * * * * * * * * * * *

      SUBROUTINE write1

* This subroutine writes out information for selected iterations

$include:'common.blk'

      WRITE(2,201) iteration, date + delta * float(iteration)
      WRITE(*,201) iteration, date + delta * float(iteration)

      WRITE(2,202)
      WRITE(*,202)
```

```
      DO 10 j = 1,ncel
        totalin(j) = totalin(j) + xchnjin(j)
        totalout(j) = totalout(j) + xchnjout(j)
        sbdv(j) = ro(j) * bdv(j)
        bdc(j) = state(j) / vol(j)

        WRITE (2,203) j, bdc(j), state(j), totalin(j), totalout(j),
     .                vol(j), brv(j), bdv(j)
   10   WRITE (*,203) j, bdc(j), state(j), totalin(j), totalout(j),
     .                vol(j), brv(j), bdv(j)

      IF (mage .EQ. 1) THEN
           WRITE (2,204)
           WRITE (2,205) (j, age(j), var(j), j=1,ncel)

           WRITE (*,204)
           WRITE (*,205) (j, age(j), var(j), j=1,ncel)
      ENDIF

      WRITE (*,206)

      RETURN

  201 FORMAT (//'  Iteration # ',i6,'     Time: ',g10.3)
  202 FORMAT (/' Cell  BDC     State  Total in  Total out',
     . '       Volume     BRV       BDV')
  203 FORMAT (i4,7g10.3)
  204 FORMAT (/' Cell   Mean    Variance')
  205 FORMAT (i4,2g10.3)
  206 FORMAT (//)

      END

* * * * * * * * * * * * * * * * * * * * * * * * * * * * * * * * * * * * * *

      SUBROUTINE write2

* The subroutine writes the final output tableau

$include:'common.blk'

* This section calculates the cell mean age numbers using
*   the volume method.  It should not be used when exchanges
*   occur, else erroneous answers will result.

      IF (ivar .EQ. 0 .AND. IFsbrv .EQ. 0) THEN

           DO 1 j = 1, ncel
    1      ni(j) = 0
```

```
      DO 10 j = 1, kz
        la = krout(j,1)
        lb = krout(j,2)
        lc = krout(j,3)

        IF (la .EQ. 0) THEN
             IF (itype .EQ. 1) THEN
                  age(lb) = vol(lb) / brv(lb)
             ELSE
                  age(lb) = (vol(lb) + sbrv(lb)) / brv(lb)
             ENDIF
        ELSEIF (lc .NE. 1) THEN
             age(lb) = age(lb) + (age(la) * bdv(la) * ri(j))
     .                  / brv(lb)
             ni(lb) = ni(lb) + 1
             IF ((lb .GT. icel) .AND. (ni(lb) .EQ. noin(lb)))
     .             age(lb) = age(lb) + delta * vol(lb) / brv(lb)
        ENDIF

10    CONTINUE

   ENDIF

   WRITE(2,201)
   WRITE(*,201)
   DO 20 j = 1, ncel
     WRITE(2,202) j, vol(j), brv(j), bdv(j), exvol(j),
    .     sbdv(j), age(j)
20   WRITE(*,202) j, vol(j), brv(j), bdv(j), exvol(j),
    .     sbdv(j), age(j)

   CLOSE (1)
   CLOSE (2)

   RETURN

201 FORMAT (// ' Cell  Volume    BRV       BDV      EXVOL',
   . '     SBDV    Mean Age')
202 FORMAT (i4,6g10.3)

   END
```

APPENDIX C

BATCH TEST PROCEDURES

To quantify the tracer sorptive behavior of a particular soil, Ks values must be known. BCF and SF6 tracers have been studied and partition coefficients have been published (Kreamer, 1982). Distribution products for F-22 had to be determined for this study. To accomplish this, stainless-steel canisters with injection ports for tracer introduction were used. These canisters were filled with a known amount of soil so that the exact amount of air space within the air tight canister was known. Tracer gas was introduced into the soil canisters and allowed to equilibrate.

After equilibration, syringe samples of gas were removed and injected into the gas chromatograph. Ks values can be calculated because the amount of tracer gas injected is known and concentration of the tracer in the soil gas measured .

Presented in the next few pages is the detailed procedures and calculations needed to obtain a value for Ks.

Two batch tests were performed to determine Ks values for F-22, using two different canisters. One canister was used to determine the Ks for F-22 under dry conditions and the other canister had a water content of close to 10%.

Before a test could be run the volumes of the canisters and the amount of soil in each canister must be known. The simplest method for calculating canister volumes is to measure the amount of water water

needed to fill the container. Top and bottom sections of the canisters were determined separately (Table C.1).

Table C.1 Volume of empty canisters.

Container	Volume Bottom (ml)	Volume Top (ml)
A	50.19	5.04
B	50.04	6.33
C	50.30	4.98

Standardization tests were run on the empty canisters to test for leakage and to quantify adsorption of tracer on to canisters. The canisters were found to leak/adsorb 8.5% of the tracer placed inside.

Soil samples were weighed and packed into the canisters. The volume of any empty air spaces are calculated and recorded in Table C.2.

Table C.2 Soil weight and void volume in soil canisters.

Can	wt (g)	Bulk Density (g/cc)	Volume Soil (cc)	Volume Total (cc)	Volume Air (cc)	Volume Voids (cc)	Grain Density (g/cc)
B	73.85	1.50	49.07	56.37	7.30	27.91	2.53
C	51.22	1.42	51.22	55.28	4.60	21.38	2.53

The canisters are now ready to be used in the tracer adsorption test. Details of the test procedure are summarized below:

- o Weigh and pack soil into air tight canisters.
- o Remove volatile organics from soil by purging canisters with nitrogen a 150^{o}C for three days.
- o Leave nitrogen gas in containers at atmospheric pressure to simulate subsurface conditions.

- o Syringe inject water into canister. Water should be purified by purging with helium for 24 hours.
- o Let water equilibrate for 24 hours in canisters
- o Inject tracer into canister through foil septums to avoid adsorption on the teflon septums, making sure that the injection syringes are clean by heating in an oven at $50^{o}C$.
- o Let canisters equilibrate for 8 hours.
- o Syringe inject a portion of the soil gas into the gas chromatograph using a clean syringe.
- o Calculate Ks value.
- o Replace foil septums on canister, purge with nitrogen and restart.

Calculations performed to determine Ks are summarized below.

$$Ks = \frac{\text{Amount sorbed on soil/weight of soil in canister}}{\text{Amount of tracer in the air/volume of air in soil}}$$

The two quantities that must be calculated in this equation are the amount of tracer sorbed onto the soil and the amount of tracer in the air.

*Amount of tracer in air is equal to:

$$\frac{\text{(Amount of tracer in sample(cc))}}{\text{(Amount of tracer injected into GC(cc))}} \times \text{Conc of std. (g/cc)} \times \text{Vol of air in can (cc)}$$

Amount of tracer injected into the can is equal to:

(volume injected into can) x (conc. of std.)

Volume injected must be adjusted for adsorption onto the can and leakage:

Volume injected = (1-%adsorbed) x (volume injected)

*Amount adsorbed onto the soil is equal to:

Amount injected into can - Amount of tracer in air

A Ks value determined for the F-22 using Highland Wash sand with 10 percent water content was 0.358 cc gas/gm solid. Dry Highland Wash sand had a Ks of 0.659 cc gas/gm solid.

APPENDIX D

GAMMA-RAY ATTENUATION PROCEDURE FOR MEASURING WATER CONTENT OF SOIL COLUMN

Water content measurements had to be taken after the tracer tests were finished because the gamma-ray appartatus and the gas chromatograph were located on opposite sides of town. Unfortunately, on transport of the soil column across town the glass shattered, destroying the soil column. A new column was made using the same techniques and type of sand to fill the column. PVC was used to construct the new column to avoid another accident with glass.

The instrumentation used in this study to measure the attenuation of gamma radiation is the same as that used by Thames and Evans (1968). Figure D.1 illustrates the gamma-ray apparatus used in the study. The radiation source and detector travel up and down the instrument frame so that water content measurements can be taken any place along the soil column. The gamma ray source used was 200 mc of Cs^{137}.

The attenuation of gamma radiation as the radiation passes through a soil is a function of the bulk density and the water content of the soil. The equation governing the attenuation is:

$$I = I_0\{\exp\,[-(u_s p + u_w \theta)x - u_{PVC} p_{PVC} x_{PVC}]\} \qquad (D.1)$$

(From Davidson et al., 1963)

where

I = radiation intensity after being attenuated.
I_0 = radiation intensity with no interference.
u_s = mass adsorption coefficient for soil (cm^2/g).
p = bulk density of the soil (g/cc).

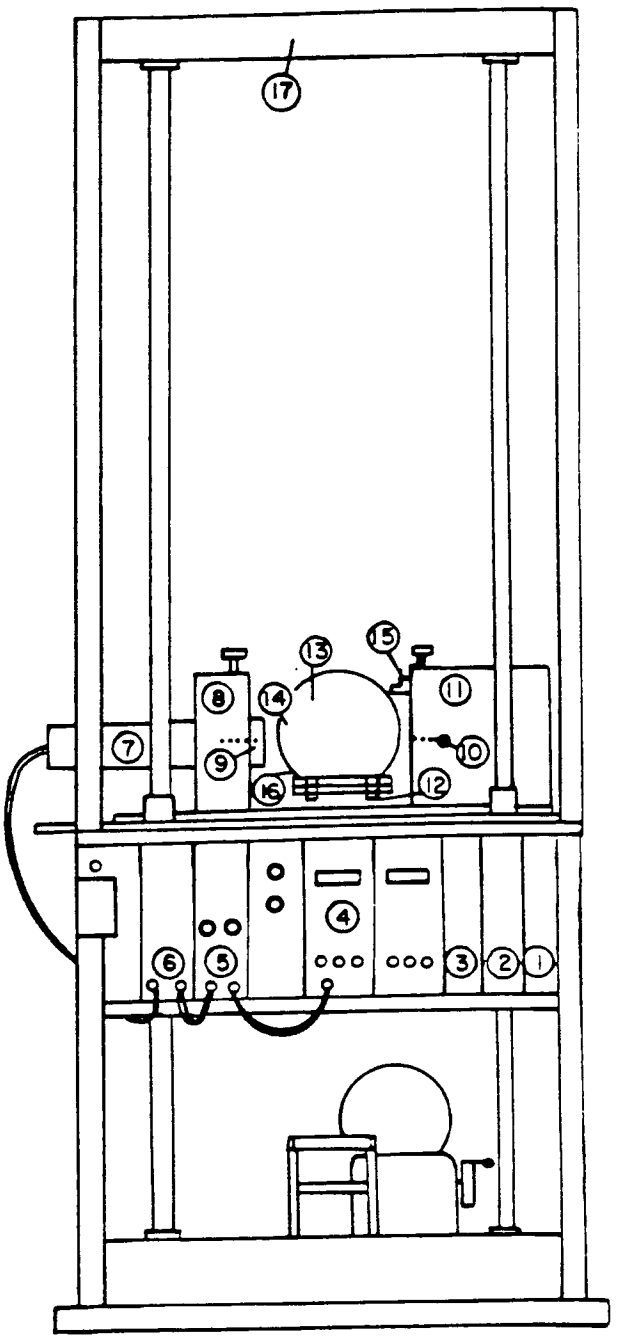

1 Power Supply
2 High Voltage Power Supply
3 Timer
4 Six Digit Counter
5 AGC Amplifier
6 Linear Amplifier
7 Gamma Detector
8 Lead Detector Shield
9 Gamma Beam Collimater
10 Cs-137 Gamma Source
11 Lead Source Shield
12 Aluminum Track
13 Endplate Reservoir
14 Insulation
15 Precooled Water Inlet Port
16 Precooled Water Outlet Port
17 Steel Frame

Figure D.1 Gammaray instruement used to measure water content of sand column.

u_w = mass adsorption coefficient for water (cm^2/g)
0 = water content (g/cc).
x = thickness of soil (cm).
u_{PVC} = mass adsorption coefficient for PVC (cm^2/g).
p_{PVC} = density of PVC (g/cc).
x_{PVC} = thickness of PVC in the column (cm).

Because only one radiation source was available each component of the equation had to evaluated separately before the water content could be measured. First the mass adsorption coefficient of the PVC had to be evaluated. The density of the PVC was determined by measuring the weight and dimensions of a sample piece. The density was found to be 1.462 g/cc.

Equation D.1 is modified to determine u_{PVC}

$$u_{PVC} = \frac{\ln(I/I_o)}{p_{PVC}} \qquad (D.2)$$

Using Equation D.2 and the data from Table D.1 u_{PVC} was determined to be 0.07448 cm^2/g.

Table D.1 Summary of gamma ray data taken to determine u_{PVC}.

I (5 minute counts through PVC and air)	I_o (5 minute counts in air alone)
4728196	5217329
4732444	5218102
4730142	
4732056	
4732538	
4728306	
Average 4730614	Average 5217715

The next parameter needed to solve Equation D.1 for water content is the mass adsorption coefficient of the soil. Gamma-ray attenuation measurements were taken through the dry soil column. Using the dry column the parameters for 0 and p_s were not needed and Equation D.1 reduces to Equation D.3.

$$u_s = \frac{-\ln(I/I_o) - u_{PVC}p_{PVC}x_{PVC}}{p_s x_s} \qquad (D.3)$$

Bulk density was calculated at 5 spots along the column. Thus, requiring that gamma-ray attenuation through the dry soil column and through the air (I_o) be measured at five spots. Counts were taken for five minutes for all measurements. Table D.2 summarizes the data taken for the dry column.

Table D.2 Gamma ray attenuation data for dry soil.

Location	I(counts/5 minutes)	I_o(counts/5 minutes)
62 cm	1444092 1446597	5203982
70 cm	1374183 1373927	5211180
80 cm	1340344 1340957	5206698
90 cm	1342251 1344840	5200434
100 cm	1365360	5201175

All the I and I_0 reading were averaged for the dry soil and the average I and I_0 were found to be 1373901 and 5204694 counts respectively. Using the Equation D.3 and using the known density of the soil as 1.53 g/cc, the average u_s was found to be equal to 0.0778245 cm^2/g.

The average u_s is used to go back and recalculate the exact bulk density of the soil at the measured locations. These were the bulk densities which were used to determine water content at each measuring points. The water contents were averaged to determine the average water content for the column.

Three application rates were used to determine the relationship between the water application rate and water content. Water was dripped onto the column at rates of 5ml/min, 1ml/min, and .333ml/min. After the water was introduced the column was allowed to equilibrate just as in the tracer experiments. Using Equation D.1 water content for the 5ml/min rate was found to be .1360 g/cc or 8.9% volume wettness. The 1ml/min application rate had a water content of .113g/cc or 7.5% volume wettness. The last measurements taken for the .33 ml/min test had a water content of .10417 g/cc or a volume wettness of 6.8%. Data for these tests are presented in Tables D.3, D.4, and D.5.

Table D.3 Gamma ray results for a water application rate of 5 ml/min.

Location	I(counts/ 5minutes)	I_o (counts/5 minutes)
62 cm	1354050	5211913
	1358354	5210207
70 cm	1224863	5207401
	1224469	5218797
80 cm	1216698	5211653
	1218551	5209676
	1217901	
90 cm	1182859	5219003
	1183507	5208716
100 cm	1207191	5201042
	1205023	5204120

Table D.4 Gamma ray attenuation measurements for a water application rate of 1 ml/min.

Location	I(counts/5 minutes)	I_o(counts/5 minutes)
62 cm	1289025	5220660
	1287249	5224656
		5225385
		5229753
		5323131
		5229526
70 cm	1268346	5230550
	1267615	5226868
80 cm	1234339	5226241
	1236033	5228061
90 cm	1219056	5227261
	1221082	5223560
100 cm	1221435	5228721
	1223320	5231232

Table D.5 Gamma-ray measurements for a water application rate of 0.33 ml/min.

Location	I(counts/5 minutes)	I_o(counts/ 5 minutes)
62 cm	1256403	5213932
	1258228	5215072
70 cm	1244559	5218457
	1245442	5222090
		5217042
80 cm	1229750	5221787
	1226196	5223586
90 cm	1222917	5220727
	1223115	5224387
100 cm	1246683	5226958
	1248831	5226279

References

Anderson, M. P., 1984. Movement of Contaminants In Groundwater: Groundwater Transport -- Advection and Dispersion. Groundwater Contamination Studies in Geophysics, Nuclear Regulatory Commission. National Academy Press, Washington D.C.

Bassett. R.L., E.P. Weeks, M.L. Ceazan, S.G. Perkins, D.C. Signor, D.L. Redinger, R.L. Malcolm, G.R. Aiken, E.M. Thurman. P.A. Avery, W.W Wood, G.M. Thompson, and G.K. Stiles, 1981. Preliminary Data From a Series of Artificial Recharge Experiments at Stanton, Texas. United States Geological Survey, Open File Report 81-149.

Bowman, R.S., 1984. Evaluation of Some New Tracers For Soil WAter Studies. Soil Sci. Soc. Am. J. 48:987-993.

Brown, J.D., 1980. Evaluation of Fluorocarbon Compounds as Ground Water Tracers: Soil Column Studies. Unpublished Ms. Thesis, University of Arizona, Tucson, Arizona.

Cameron, D.R., and A. Klute, 1977. Convective-Dispersive Solute Transport With a Combined Equilibrium and Kinetic Adsorption Model. Water Resources Research, 13(1):183-188.

Campana, M.E., 1975, Finite State Models of Transport Phenomena in Hydrologic Systems. Unpublished Ph.D Dissertation, University of Arizona, Tucson, Arizona.

Corey, J.C., S.F. Peterson, and M.A. Wakat, 1971. Measurement of Attenuation of Cs(137) and Am(241) Gamma Rays for Soil Density and Water Content Determinations. Soil Sci. Soc. Amer. Proc., 35:212-219.

Davidson, J.M., J.W. Biggar, and D.R. Nielsen, 1963. Gamma-Radiation Attenuation for Measuring Bulk Density and Transient Water Flow in Porous Materials. Jour. Geophy. Res., 68(16):4777-4783.

Davis, S.N., G.M. Thompson, H.W. Bentley and G. Stiles, 1980. Ground-water tracers -- A Short Review. Ground water. 18(1):14-23.

E.I. Du Pont De Nemours & Company. Solubility Relationships Between Fluorocarbons and water. Freon Product Information, "Freon" P

Earp, D.E, 1981. Factors A
Fluorocarbons into Unsaturated Porous Materials. Unpublished Ms. Thesis, University of Arizona, Tucson, Arizona.

Environmental Protection Agency, July 1982. Test Method, Purgeable Halocarbons -- Method 601. Environmental Monitoring and Support Laboratory, Cincinnati, Ohio.

Evans, D.D., 1965. Gas Movement in Methods of Soil Physics edited by C.A. Black. American Society of Agronomy Monograph #9. 319-330 p.

Freeze, R.A., and J.A. Cherry, 1979. Groundwater. Prentice Hall, Inc., Englewood Cliffs, N.J. 604p.

Fritton, D.D., 1969. Resolving Time, Mass Adsorption Coefficient and Water Content with Gamma-ray Attenuation. Soil Sci. Soc. Amer. Proc., 33:651-654.

Green, R.T., 1985. Transport of Radionuclides as Vapor in Unsaturated Fractured Rock. Unpublished PH.D Dissertation, University of Arizona, Tucson, Arizona.

Hillel, D., 1982. Introduction to Soil Physics. Academic Press,Inc., London, 364 p.

Jaynes, D.B., and A.S. Rogowski, 1983. Applicability of Fick's Law to Gas Diffusion. Soil Sci. Soc. Am. J. 47:425-430.

Karickhoff, S.W., 1980. Sorption Kinetics of Hydrophobic Pollutants in Natural Sediments. In: Contaminants and Sediments, Vol. 2 (Edited by R. A. Baked.) Ann Arbor Science, Ann Arbor, MI. 314-322 p.

Kreamer, D.K., 1982. In Situ Measurement of Gas Diffusion Characteristics in Unsaturated Porous Media by Means of Experiments. Unpublished Ph.D Dissertation, University of Arizona, Tucson, Arizona.

Kreamer, D.K., 1983. Proposed Greater Confinement Disposal Tracer Test Plan for Reynolds Electrical and Engineering Company, Las Vegas, Nevada. Unpublished report.

Mansell, R.S., L.C. Hammond, and R.M. McCurdy, 1973. Coincidence and Interference Corrections for Dual-Energy Gamma Ray Measurements of Soil Density and Water Content. Soil Sci. Soc. Amer. Proc., 35: 500-504.

Marrin, D.L., 1984. Remote Detection and Preliminary Hazard Evaluation of Volatile Organic Contaminants in Groundwater. Unpublished Ph.D Dissertation, University of Arizona, Tucson, Arizona.

Marshall, T.J., 1959. The Diffusion of Gases Through Porous Media. J. Soil Sci., 10:79-82.

Miller, C.T. and W.J. Weber, Jr., 1983. Kinetic Models for Adsorption of Organic Solutes by Granular Soils. Presented at the 1983 Annual Meeting of the American Chemical Society, Washington, D.C.

Miller. C.T., W.J. Weber, 1984. Modeling Organic Contaminant Partioning in Ground-Water Systems. Groundwater, 22(5):584- 592.

Millington, R.J., 1959. Gas Diffusion in Porous Media. Science, 130:100-102

O'Connor, D.J., J.P. Connolly, 1980. The Effect of Concentration of Adsorbing Solids on the Partition Coefficient. Water Research, 14:1517-1523.

Oddson, J.K., J. Letey, and L.V. Weeks, Jr., 1983. Predicted Distribution of Organic Chemical in Solution and Adsorbed as a Function of Position and Time for Various Chemical and Soil Properties. Soil Sci. Soc. Amer. Proc., 34:412-417.

Penman, H.L., 1940. Gas and Vapour Movements in the Soil, 1, The Diffusion of Vapours Through Porous Solids. J. Agric. Sci. 30:437-462.

Rasmussen, T.C., and D.D. Evans, 1986. Unsaturated Flow and Transport Through Fractured Rock -- Related to High-Level Waste Repositories -- Phase II. Report prepared for the Division of Radiation Programs and Earth Sciences, U.S. Nuclear Regulatory Commission, Washington D.C., under contract no. NRC-04-81-224 (in progress).

Rasmussen, T.C.,1982. Solute Transportin Saturated Fractured Media. Unpublished Ms. Thesis, University of Arizona, Tucon, Arizona.

Russell, A.D., 1981. Sorption and Desorption Processes Affecting the Enrichment of the Fluorocarbons CCl_2F_2 and CCl_3F in Ground Water. Unpublished Masters Thesis, University of Arizona, Tucson, Arizona.

Russell, A.D., and G.M. Thompson, 1983. Mechanisms Leading to Enrichment of the Atmospheric Fluorocarbons CCl_3F and CCl_2F_2 in Groundwater, Water Resources Research, 19(1):57-60.

Silliman, S.E., 1981. Laboratory Evidence of the Scale Effect in Solute Transport Through Saturated Porous Media. Unpublished Masters Thesis, University of Arizona, Tucson, Arizona.

Sallam, A., W.A. Jury, and J. Letey, 1984. Measurement of Gas Diffusion Coefficient Under Relatively Low Air-Filled Porosity. Soil Sci. Soc. Am. J. 48:3-6.

Shafrin, E.G., and W. A. Zisman, 1960. Constitutive Relations In the Wetting of Low Energy Surfaces and Theory of the Retraction Method of Preparing Monolayers. J. Phys. Chem., 64:519-524.

Slattery, J.C., R.B. Bird, 1958. Calculation of the Diffusion Coefficient of Dilute Gases and of the Self-Diffusion Coefficient of Dense Gases. A.I.Ch.E. Journal, 4(2):137-142.

Stiles, G.K., 1982. Retention Characteristics of Fluorocarbon Tracers in Ground-Water Flow. Unpublished Ms. Thesis, University of Arizona, Tuscon, Arizona.

Thames, J.L., D.D. Evans, 1968. An Analysis of the Vertical Infilration of Water Into Soil Columns. Water Resources Research, 4(4):817-828.

Thompson, G.M., J.M. Hayes, 1979. Trichlorofluoromethane in Groundwater -- A Possible Tracer and Indicator of Groundwater Age. Water Resources Research, 15(3):546-554.

Thompson, G.M., J.M. Hayes, and S.N. Davis, 1974. Fluorocarbon Tracers in Hydrology. Geophys. Res. Lett., 1(4):177-180.

Thompson, G.M., G.K. Stiles, 1981. Final Evaluation of Six Fluorocarbon Compounds for Use as Groundwater Tracers. Report for Environmental Sciences Division, Oak Ridge National Laboratory, 1-11 p.

Van Genuchten, M.Th. and W.J. Alves, 1982. Analytical Solutions of the One-Dimensional Convection-Dispersion Solute Transport Equation. United States Department of Agriculture Technical Bulletin 1661 p. 3.

Weber W.J., 1972. Physico-Chemical Processes For Water Quality Control. Wiley and Sons Inc., 640p.

Weeks, E.P., D.E. Earp and G.M. Thompson, 1982. Use of Atmospheric Flourocarbons F-11andF-12 to Determinethe Diffusion Parameters of the Unsaturated Zone in the Southern High Plains of Texas. Water Resources Research, 18(5):1365-1378.

Weast, R.C., Ed.,1980. Chemical Rubber Company Handbook of Chemistry and Physics. CRC Press Inc., Boca Raton, Florida, E 34-36.